AD-A085 880 DAYTON UNIV OH RESEARCH INST F/G 9/2
ACCURACY OF DIGITIZED PHOTOMETRIC DATA.(U)
APR 80 P A GRAF, H T MOHLMAN F33615-76-C-0525
UNCLASSIFIED AMRL-TR-79-76 NL

LEVEL II

ACCURACY OF DIGITIZED PHOTOMETRIC DATA

P. A. GRAF
R. T. MOHLMAN
UNIVERSITY OF DAYTON
RESEARCH INSTITUTE
300 COLLEGE PARK AVENUE
DAYTON, OHIO 45469

APRIL 1980

Approved for public release; distribution unlimited.

AIR FORCE AEROSPACE MEDICAL RESEARCH LABORATORY
AEROSPACE MEDICAL DIVISION
AIR FORCE SYSTEMS COMMAND
WRIGHT-PATTERSON AIR FORCE BASE, OHIO 45433

[illegible]

[illegible]

[illegible]

Cameron Station
Alexandria, Virginia 22314

TECHNICAL REVIEW AND APPROVAL

AMRL-TR-79-76

This report has been reviewed by the Office of Public Affairs (PA) and is releasable to the National Technical Information Service (NTIS). At NTIS, it will be available to the general public, including foreign nations.

This technical report has been reviewed and is approved for publication.

FOR THE COMMANDER

[illegible]

[illegible]

SECURITY CLASSIFICATION OF THIS PAGE (When Data Entered)

REPORT DOCUMENTATION PAGE	READ INSTRUCTIONS BEFORE COMPLETING FORM
1. REPORT NUMBER: AMRL-TR-79-76	2. GOVT ACCESSION NO.: AD-A085880
	3. RECIPIENT'S CATALOG NUMBER
4. TITLE (and Subtitle): ACCURACY OF DIGITIZED PHOTOMETRIC DATA.	5. TYPE OF REPORT & PERIOD COVERED: Technical Report, 1 Sept 76 — 30 April 79
	6. PERFORMING ORG. REPORT NUMBER
7. AUTHOR(s): P. A. Graf, H. T. Mohlman	8. CONTRACT OR GRANT NUMBER(s): F33615-76-C-0525
9. PERFORMING ORGANIZATION NAME AND ADDRESS: University of Dayton Research Institute, 300 College Park Avenue, Dayton, Ohio 45469	10. PROGRAM ELEMENT, PROJECT, TASK AREA & WORK UNIT NUMBERS: 62202F, 7231-16-08
11. CONTROLLING OFFICE NAME AND ADDRESS: Air Force Aerospace Medical Research Laboratory, Aerospace Medical Division, Air Force Systems Command, Wright-Patterson AFB, Ohio 45433	12. REPORT DATE: April 1980
	13. NUMBER OF PAGES: 139
14. MONITORING AGENCY NAME & ADDRESS (if different from Controlling Office)	15. SECURITY CLASS. (of this report): UNCLASSIFIED
	15a. DECLASSIFICATION/DOWNGRADING SCHEDULE

16. DISTRIBUTION STATEMENT (of this Report)

Approved for public release; distribution unlimited

17. DISTRIBUTION STATEMENT (of the abstract entered in Block 20, if different from Report)

18. SUPPLEMENTARY NOTES

19. KEY WORDS (Continue on reverse side if necessary and identify by block number)

Biodynamic Data Analysis
Photometric Data Reduction
Estimate of Error
Digitizing
Data Acquisition
Digital Data Processing

20. ABSTRACT (Continue on reverse side if necessary and identify by block number)

This report documents the error analysis of the photometric data acquisition and analysis system used to process impact data collected on various AMRL impact facilities by the Biomechanical Protection Branch of the AMRL. Sources of error are identified in the data acquisition, digitizing, calibration, and digital processing phases of the total analysis system. The estimates of total error accrued in the coordinate solutions to the data from the

DD FORM 1 JAN 73 1473

SECURITY CLASSIFICATION OF THIS PAGE (When Data Entered)

105400

Block 20. (Continued)

Restraint System Dynamics (Nylon/Operational/Rigid) Comparison, the Upper Torso Retraction Study, and the -50G_x Injury Protection Comparison tests are derived and presented. In the digital processing phase of the report, a frequency response function was developed for the 11-point quadratic least square smoothing technique used to compute the velocity and acceleration data. This frequency response was confirmed by applying the 11-point smoothing technique to time displacement data with known velocity and acceleration characteristics.

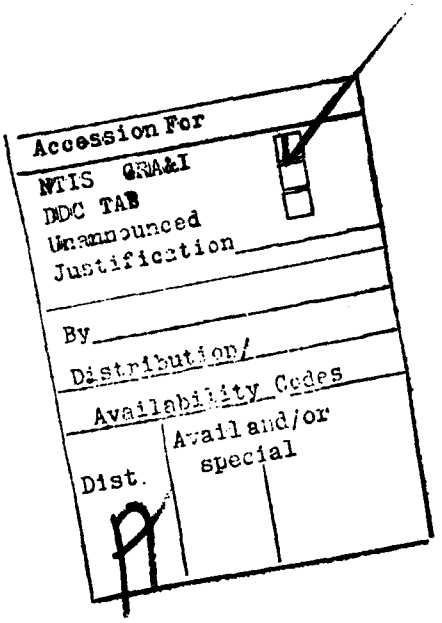

SUMMARY

This report documents the error analysis of the photometric data acquisition and analysis system used to process impact data collected on various AMRL impact facilities by the Biomechanical Protection Branch of the AMRL. The accuracy with which a photometric system can be used to predict time displacement data is influenced by inaccuracies experienced in data acquisition, digitizing the recorded data, and processing the digitized data. Each of these areas is discussed in considerable detail in this report.

In the data acquisition phase, the accuracy with which data were acquired depended upon the ability to precisely apply fiducials to anthropometric points on each subject, the precision with which the distances between the fiducials could be measured, the ability of the test subjects to maintain the positions of their body segments from the time of measurement to the time of event initiation, and the distortion introduced to the film image by the recording lens. The ability to consistently apply fiducials and measure the breadth between them is difficult to evaluate; nevertheless, some tabular data are presented and the error in the trageon to trageon breadth was estimated to be 0.1167 inches. The distortions introduced by the recording and projection lenses were negligible for the Milliken camera but quite substantial for the Photosonics camera with the 5 millimeter lens. The algorithm derived to adjust the Photosonics data is presented in this report.

In the digitizing phase, this report presents the criterion used to evaluate the quality of the digitized data, the calibration function for the Milliken and Photosonics camera, and an estimate of the total error accrued to the coordinate solutions from the data acquisition, digitizing, and calibration errors. Data which failed to meet the quality control criteria were partially or completely redigitized. As part of this criteria, the overall random error in digitizing was calculated to have a two sigma value of 20 counts. The errors estimated to have accrued to coordinate solutions to the data from the

Restraint System Dynamics (Nylon/Operational/Rigid) Comparison, the Upper Torso Retraction Study, and the $-50G_x$ Injury Protection Comparison tests ranged from less than 0.1 inches to just over 0.15 inches except where lateral components of motion contributed significantly to the error, in which cases the estimated error approached 0.25 inches.

In the data processing phase, this report presents comparisons of coordinate solutions, and the velocity and acceleration data derived from them, with data reduced from other sources, and analyses the error introduced to the derived velocity and acceleration data. These coordinate solutions (displacement from photo data) and their derived velocity and acceleration data were computed using the 11-point quadratic least square smoothing technique used in the Hyge Impact Facility Photo Data Analysis Program (HIFPD). These displacement data show very good agreement with the corresponding data recorded with a displacement transducer. We were unable to make a valid comparison between velocity and acceleration data derived from these photo displacement data and the corresponding electronically recorded velocity and acceleration data. However, acceleration data derived from both the photo displacement and the transducer displacement data using the 11-point fit technique did agree reasonably well except for the amplitude of the acceleration spikes. The poor agreement between the acceleration spikes is explained by the frequency response of the 11-point fit technique.

The frequency response function derived for the 11-point fit technique shows that for the 500 frames per second photo data the acceleration can be determined within 5 percent only for frequencies of approximately 7 Hz or less. The corresponding frequencies for displacement and velocity are 29 Hz and 10 Hz, respectively. This frequency response for the electronically recorded data where the sampling rate was 1024 samples per second was approximately double the above frequencies. Thus one way to improve the accuracy of the displacement, velocity, and acceleration data is to sample the data at a much higher rate.

Additional comparison tests where known displacement, velocity, and acceleration data were compared with the corresponding displacement, velocity, and acceleration derived using the 11-point fit technique confirms the results of the frequency response function at both the 500 and 1024 sample per second digitizing rates.

PREFACE

This report documents the error analysis of the photometric data acquisition system and the evaluation of the 11-point quadratic least square smoothing routine used to analyze these photo data in the Hyge Impact Facility Photometric Data (HIFPD) analysis program. The work was performed by personnel of the University of Dayton Research Institute (UDRI) under USAF Contract F33615-76-C-0525 with the Biomechanical Protection Branch of the Biodynamics and Bioengineering Division, Air Force Aerospace Medical Research Laboratory (AMRL/BBP) at Wright-Patterson Air Force Base. The contract monitors were Major John P. Kilian and CMSgt. Joseph M. Powers.

Special thanks are due to Dr. Thomas R. Schori and Dr. Alan P. Berens for their guidance and assistance in compiling these analyses.

TABLE OF CONTENTS

LIST OF ILLUSTRATIONS

LIST OF TABLES

INTRODUCTION

The accuracy with which a photometric system can be used to predict time displacement data is influenced by inaccuracies experienced in:

- Data acquisition
- Digitizing the recorded data
- Processing the digitized data.

In each of these areas several factors contribute to the total error. The significance of the error introduced by any given source varies according to the system design and application, however, we shall consider the sources and attempt to assess the contribution of each.

DATA ACQUISITION ACCURACY

The accuracy with which data were acquired depends upon the ability to precisely apply fiducials to anthropometric points on each subject, the precision with which the distances between these fiducials could be measured, the ability of the test subjects to maintain the positions of their body segments from the time of measurement to the time of event initiation, and the distortion introduced to the film image by the recording lens. The later was not observable until the recorded images were projected, thus the recording lens distortion and projection lens distortion will be treated later as a common source of error.

The ability to repeatedly apply fiducials to anthropometric points and the precision with which their relative locations can be measured have been difficult to isolate. Table 1 presents the standard deviations of the pretest measurements acquired during the Restraint System Dynamics (Nylon-Operational-Rigid) comparison program. These data do not necessarily reflect the accuracy of the individual measurements taken, but rather they indicate the inaccuracies in repetitive placement of fiducials and repetitive posturing of the subjects. The relatively high standard deviations in hip-knee distances reflect the difficulty encountered in repeatedly locating the same point on the greater femoral trochanter and accurately applying a fiducial on the garment over this point. The high standard deviations in measurements of breadths across the knees and ankles are indicative of the difficulty encountered in replicating the posture of each subject.

Measurements were taken with an aluminum caliper rule graduated in centimeters and millimeters, the reading being recorded to the nearest millimeter. Two scales were available, one referenced to the flat base, the other referenced to the fixed jaw on the opposite end. The jaw-jaw scale was used for measuring body segment lengths and breadths, while the base-jaw scale was used for measuring heights.

TABLE 1

STANDARD DEVIATIONS OF PRETEST MEASUREMENTS (IN) RSD(N/O/R) SUBJECTS

	A1	A22	A3	B4	B22	B3	C1	C2	C3
Head Band Fiducial Height	.33	.31	.54	.64	.21	.32	.44	.63	.26
Shoulder Fiducial Height	.43	.46	.68	.39	.17	.33	.53	.26	.56
Iliac Crest Fiducial Height	.32	.65	.20	.37	.22	.41	.33	.21	.26
Trageon to 9-TAP Origin	.17	.16	.19	.22	.22	.33	.17	.21	.13
Trageon to Head Band Fiducial	.46	.35	.24	.56	.23	.22	.39	.42	.25
Shoulder to Elbow	.31	.17	.39	.31	.25	.30	.22	.26	.34
Elbow to Wrist	.14	.09	.19	.34	.32	.45	.19	.20	.30
Hip to Iliac Crest	.47	.31	.26	.30	.39	.58	.17	.24	.35
Hip to Knee	.38	.52	.72	.49	.50	.77	.65	.34	.65
Mid-Thigh to Knee	.34	.10	.11	.05	.07	.00	.19	.35	.20
Knee to Ankle	.26	.29	.15	.17	.18	.25	.28	.22	.20
Breadth at Trageons	.11	.17	.15	.11	.09	.08	.07	.15	.08
Breadth at Shoulders	.24	.23	.24	.21	.13	.55	.13	.53	.23
Breadth at Elbows	.56	.46	.81	.44	.59	.94	.43	.85	.77
Breadth at Hips	.39	.20	.67	.20	.41	.25	.19	.24	.28
Breadth at Knees	1.30	1.02	.65	.96	.41	1.48	1.37	.82	.98
Breadth at Ankles	2.49	.61	.82	1.84	1.18	1.05	1.26	.62	1.07
Mid-Shoulder Height	.25	.31	.39	.33	.19	.22	.18	.25	.41

Breadth measurements were used to calculate conversion factors which were used to convert projected image coordinates to seat coordinate values. The only reliable indicator of the accuracy of these measurements was the variations in Trageon-Trageon breadth. Other breadth measurements were subject to change due to weight gain/loss, posturing variations, etc. The greatest standard deviation for an individual subject trageon-trageon dimension was .15 in., the least being .07 in. The mean of the differences from the means for the subject population was .0026 inches and the standard deviation from the mean of the differences was 0.1167 inches.

The equation used to calculate the standard deviations was

$$S = \sqrt{\frac{\Sigma\Delta^2 - \frac{(\Sigma\Delta)^2}{n}}{n-1}}$$

Since the time lapse between measurements and event initiation usually exceeded three minutes it is not unreasonable to assume that slight changes in subject posture probably occurred during these periods. Such changes in subject posture would have resulted in changes of breadths across fiducials at the elbows, wrists, knees and ankles.

DIGITIZING ACCURACY

In an initial study conducted in November 1977, the overall random error in digitizing was calculated to have a two sigma value of twenty counts (≈ .020 inch projected image). Two approaches were taken in this study. The first approach was to have each of two operators digitize the same fiducial displayed on the screen one hundred times. The standard deviations from the mean were 9.53 counts for operator A and 9.99 counts for operator B. The second approach was to have each of the operators digitize eight fiducials from each of 150 frames. The differences between readings were taken and the standard deviation overall was 10.01 counts.

During these procedures the coordinate displays on the A-D converter were covered to prevent the operator from seeing the values until they were recorded on hard copy.

From the results of this study a quality monitoring program was initiated on a "go-nogo" basis. For a given test the film data were digitized according to the procedure established for the test program. An alternate operator then digitized the same data from ten percent of the frames selected at random. Differences between the original readings and "check" readings were taken. If ninety-five percent of the differences fell within the $\pm$ 20 counts limits the data were accepted for processing. If less than ninety-five percent of the differences fell within the limits they were reviewed to determine whether some trend was indicated, i.e., were the differences outside the limits obtained from a frame or frames during a specific time period in the test, or did they tend to be readings from a specific point or points tracked, or were they scattered at random among the tracked points and frames?

If a trend was indicated, the data were redigitized and rechecked accordingly. If the unacceptable readings were at random throughout the test the film was totally redigitized. It is well to note at this point that data digitized from the Injury Protection Comparison Program could not be digitized to the prescribed limits. After

redigitizing several tests it became obvious that the standard deviation was slightly less than twenty counts. Since the fiducials tracked were the intersections of two lines approximately 1/8 inch wide, the "go-nogo" criterion was reduced to seventy percent of the readings.

These procedures provided a statistical indication of the general quality of the digitized data from each test. They could in no way guarantee that errors of greater magnitude could not be passed through to Electronic Data Processing. Methods employed to detect such errors are discussed in the section "Processing the Digitized Data".

DIGITIZER SCALING ACCURACY

The accuracy with which the projected image coordinates were scaled depended upon

- Relationship between X and Y sensitivities
- Distortions introduced by recording and projection lenses.

The system employed to digitize data was a Producers Service Corporation model PVR film analyzer (PVR), Serial Number 1017, which was interfaced to a teletype terminal (TTY) equipped with paper tape punch and read stations.

Figure 1 presents a schematic view of the film projection and reading crosshairs system. The recorded image was projected onto the first surface of the glass viewing screen. The light from the projected image cast shadows of the crosshairs onto the same surface. This rendered negligible any effect of diffraction through the projection screen since the observed images were coplanar.

The fact that the crosshairs were not in the same plane suggested the possibility of a difference in scaling sensitivities between the two axes of the Projected Image Coordinate System (PCS). A cursory functional check, accomplished periodically, indicated the mean slopes of both scales were 1000 $\pm$ 2 counts per inch. The procedure for this check consisted of taping a clear mylar film containing a 1/2 inch x 1/2 inch grid to the second surface of the projection screen. The crosshairs were positioned over the origin of the grid and the scales were set to zero. The X crosshair was placed over the intersections of the X-axis and the vertical gridlines from X= -4 inches to X=4 inches. The vertical crosshair was returned to X=0 and the intersections of the horizontal lines and Y-axis were read from Y= -2.5 to Y=2.5 inches. During this procedure the crosshairs were positioned over the intersection by viewing with only one eye. With the reflection of the pupil being centered on the intersection being digitized, the sight line was considered to be normal to both the projected image plane and the grid plane.

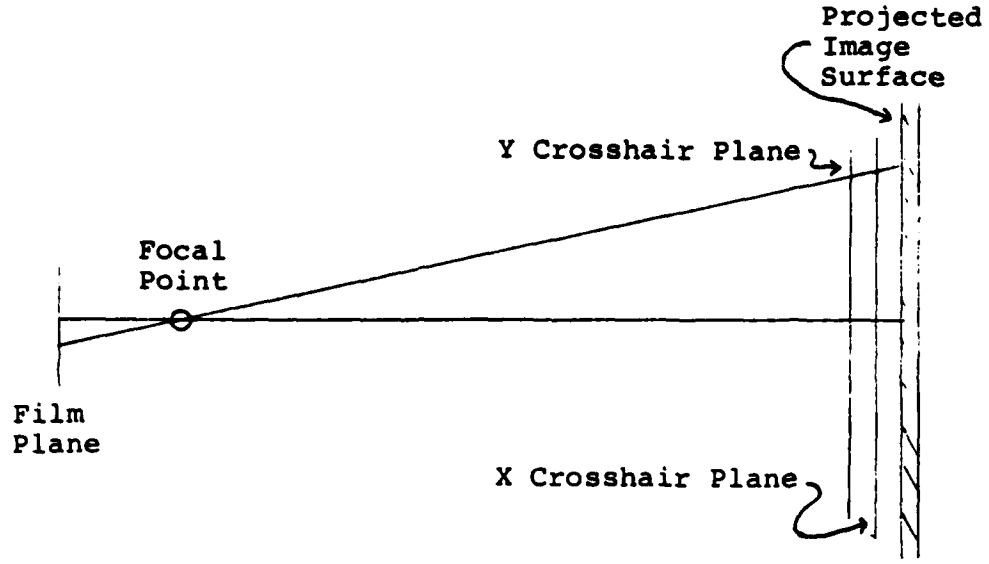

Figure 1. Schematic of Film Projection and Reading Crosshairs System.

Distortions introduced by recording and projection lenses were found to be negligible in the area of the frame being evaluated for data recorded on the Milliken cameras with lenses of 8 mm, 10 mm, 15 mm and 1 inch focal lengths, but quite severe for data recorded on the Photosonics cameras with 5 mm lenses which were used onboard during the $-50G_x$ Injury Protection Comparison Study.

Table 2 presents the data derived from a photo recording of a grid board located at the centerline (Seat Coordinate System (SCS) Y=0) of the seat of the Body Positioning Retraction Device observed by the Milliken primary data camera (side view) fitted with a 10 mm lens. The mean conversion factor was calculated to be 114.463 counts per inch using

$$\text{Conversion Factor} = \frac{\Sigma \text{ IMAGE DISPLACEMENTS}}{\Sigma \text{ GRID DISPLACEMENTS}}$$

Dividing each of the image displacements by this conversion factor yielded the values of Calculated Grid Displacement. The mean of the differences between the calculated and actual grid displacements was .0007 inches and the standard deviation about the mean was .0772 inches. A linear regression analysis of the image displacements and grid board displacements yielded a conversion factor of 114.36 counts per inch. The coefficient of determination (r^2) was .99986 and the correlation coefficient (r) was .99993.

Review of the first films recorded on the Photosonics cameras equipped with 5 mm lenses demonstrated severe barrel distortion (magnification decreased as distance from the optical axis increased). A photorecording of a grid board (1 in. x 1 in. grid) placed at the centerline of the Injury Protection Comparison seat was evaluated on the PVR. A plot of projected image displacement versus grid displacement is presented in Figure 2.

From readings of grid lines in the relatively undistorted central portion of the image frame ($\cos \gamma \geq .99$) and the fiducials on the seat frame structure, the apparent distance from the focal point of the camera to the grid board was calcualted to be 60.63 inches. Using an arc of radius 60.63 inches each reading was modified by dividing by

TABLE 2

SCALE CALIBRATION DATA PRIMARY DATA CAMERA
(STATION A) BODY POSITIONING RETRACTION DEVICE

Grid Displacement (inches)	Image Displacement (counts)	Conversion Factor (counts/inch)	Calculated Grid Displacement	Difference Between Calculated and Actual	[Difference Between Calculated and Actual]^2
0	0				
1	117	117.0	1.022	.022	.000484
2	226	113.0	1.974	-.026	.000676
3	341	113.67	2.979	-.021	.000441
4	456	114.0	3.984	-.016	.000256
5	572	114.40	4.997	-.003	.000009
6	680	113.33	5.941	-.059	.003481
7	785	112.14	6.858	-.142	.020164
8	918	114.75	8.020	.020	.000400
9	1041	115.67	9.095	.095	.009025
10	1144	114.40	9.994	-.006	.000036
11	1263	114.82	11.034	.034	.001156
12	1382	115.17	12.074	.074	.005476
13	1500	115.38	13.105	.105	.011025
14	1609	114.93	14.057	.057	.003249
15	1737	115.80	15.175	.175	.030625
16	1838	114.87	16.058	.058	.003364
17	1948	114.59	17.019	.019	.000361
18	2059	114.39	17.988	-.012	.000144
19	2169	114.16	18.949	-.051	.002601
20	2276	113.80	19.884	-.116	.013456
21	2391	113.86	20.889	-.111	.012321
22	2509	114.05	21.920	-.080	.000640

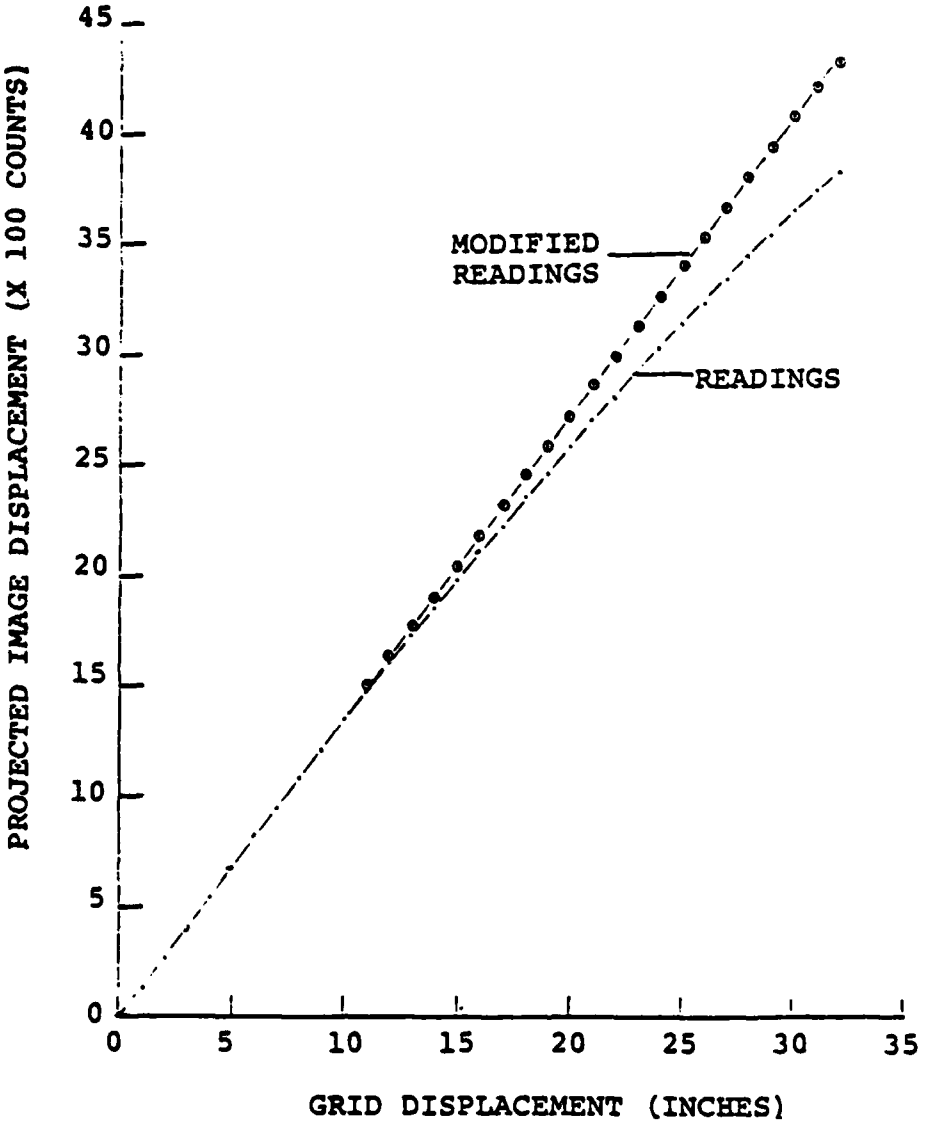

Figure 2. Average and Modified Readings vs. Grid Displacement.

the cosine of the angle between the optical axis and the ray from the observed point. A conversion factor was calculated in terms of counts read per inch grid displacement for each point. The best straight line fit to the resulting conversion factors was calculated to be 136.1 counts per inch (1633.2 counts per foot). The coefficient of determination (r^2) and correlation coefficient (r) each exceeded .9999. Application of this conversion constant to the modified readings resulted in solutions within $\pm$ .10 inch. These results are tabulated in Table 3 and plotted in Figure 2. The mean of the errors was .0206 inch and the standard deviation was .0345 inch.

From the preceeding discussion the contribution to error due to the digitizing process was comprised of errors induced in the conversion factor slope determination and the data point digitizing. We can compute the standard deviation of the combined error introduced into the time-displacement solutions by the digitizing process with the following equation[1]:

$$S = \sqrt{X^2\sigma_B^2 + B^2\sigma_X^2}$$

where

S = the standard deviation of the combined error in inches

B = the regression coefficient in inches per count (reciprocal of calibration factor which is in counts/inch)

σ_B = the standard deviation of the estimate of the regression coefficient B in inches per count

X = digitized reading in counts

σ_X = the standard deviation of the overall random error in the digitized data in counts.

[1] Ryan, J. P., A. P. Berens, A. C. Robertson, R. J. Dominic, and K. C. Rolle, July 1971, Medium Altitude CRITICAL Atmospheric Turbulence (MEDCAT) Data Processing and Analysis, AFFDL-TR-71-82, Air Force Flight Dynamics Laboratory, Air Force Systems Command, Wright-Patterson Air Force Base, Ohio.

TABLE 3

DATA FOR MODIFICATION OF FILM READINGS
TO COMPENSATE FOR IMAGE DISTORTION

Grid Displacement (inches)	Average Image Displacement (counts)	Angular Displacement from Optical Axis (Y) (degrees)	Reading cosY	f (count/inch)	Calculated Displacement (inches)
1	134.3	.9449	134.3	134.3	.98
2	272.7	1.889	272.8	136.4	2.00
3	407.5	2.833	408.0	136.0	3.00
4	541.6	3.775	542.8	135.7	3.99
5	680.5	4.714	682.8	136.6	5.02
6	813.5	5.652	817.5	136.2	6.00
7	947.5	6.586	953.8	136.3	7.01
8	1086.0	7.517	1095.4	136.9	8.05
9	1215.0	8.443	1228.3	136.5	9.02
10	1349.5	9.366	1367.7	136.8	10.05
11	1478.7	10.283	1502.8	136.6	11.04
12	1603.3	11.195	1634.4	136.2	12.01
13	1737.0	12.102	1776.5	136.7	13.05
14	1857.0	13.002	1905.9	136.1	14.00
15	1986.7	13.896	2046.6	136.4	15.04
16	2113.0	14.783	2185.3	136.6	16.05
17	2233.0	15.663	2319.1	136.4	17.04
18	2360.0	16.535	2461.8	136.8	18.09
19	2472.3	17.400	2590.9	136.4	19.04
20	2588.0	18.256	2725.2	136.3	20.02
21	2709.0	19.104	2866.9	136.5	21.07
22	2812.3	19.944	2991.7	136.0	22.98
23	2925.7	20.774	3129.1	136.0	22.99
24	3040.0	21.596	3269.5	136.2	24.02
25	3149.3	22.408	3406.5	136.3	25.03
26	3256.0	23.211	3542.8	136.1	26.03
27	3357.0	24.005	3674.8	136.1	27.00
28	3463.7	24.788	3815.2	136.3	28.03
29	3562.6	25.562	3949.2	136.2	29.02
30	3668.5	26.326	4093.0	136.4	30.07
31	3759.3	27.081	4222.2	136.2	31.02
32	3840.0	27.825	4342.0	135.7	31.90

For data acquired with the Milliken camera with a 10 millimeter lens, the standard deviation of the combined error S from the above equation ranges from 0.087 to 0.102 inches for the full range of X (X=0 to 2500 counts). The computed values of the remaining variables used to compute S are:

$\sigma_B = 2.0647 \times 10^{-5}$ inches/count

$B = 0.008744$ inches/count

$\sigma_X = 10$ counts.

For data acquired with the Photosonics camera with the 5 millimeter lens, the standard deviation S is approximately 0.15 inches over the entire range of corrected X (X=0 to 4342 counts). The values of the remaining variables for this camera and lens are:

$\sigma_B = 4.74717 \times 10^{-6}$ inches/count

$B = 0.0073472$ inches/count

$\sigma_X = 20$ counts.

For this camera the value of S is determined by the $B^2\sigma_X^2$ term and is independent of the $X^2\sigma_B$ term.

PROPAGATION OF ERRORS IN DISPLACEMENT SOLUTIONS

Having discussed the sources of error in acquisition and digitizing of data it is now possible to estimate the cumulative error induced in the solutions of seat coordinate positions of points on test subjects. In these analyses the following assumptions have been made:

- The standard deviations of the measurements of breadths of subjects at fiducials were 0.12 inch (the standard deviation at the trageons during the RSD-N/O/R tests).
- Lateral motion of tracked points was negligible except at the elbows which demonstrated obvious inward lateral motion as the upper extremities extended.
- Reference dimensions were accurate to $\pm$ 1/16 inch (.06).

As was cited above, the elbows of all subjects demonstrated obvious lateral motion toward the centerline of the seat as the hands extended forward. They all appeared to approach, but not exceed, the planes in which the shoulder fiducials lay.

The mean of the pretest lateral displacements of the elbows was 10.84 inches and the means of the pretest lateral displacements of the shoulders was 8.88 inches. Therefore the mean of the maximum lateral motion demonstrated by the elbows, 1.96 inches at maximum extension of the upper extremities, was used to estimate the error in elbow coordinate solutions.

The coordinate solutions were calculated by

$$Q = \frac{d_1}{d} f_c X$$

in which:

d_1 = distance in inches from the focal point of camera to the plane, normal to the optical axis, in which the observed point lay

d = distance in inches from the focal point of the camera to the plane, normal to the optical axis, for which the basic conversion factor (f_c) is calculated

f_c = conversion factor in inches per count applied to reference plane readings

X = project image displacement from optical axis in counts.

The equation used to calculate the cumulative error was:

$$S_Q = \sqrt{\left(\frac{d_1}{d} f_c\right)^2 \sigma_X^2 + \left(\frac{d_1}{d} X\right)^2 \sigma_{f_c}^2 + \left(\frac{f_c}{d} X\right)^2 \sigma_{d_1}^2 + \left(\frac{d_1}{d^2} f_c X\right)^2 \sigma_d^2}$$

The ranges of estimated error incurred in solutions to data acquired during the Restraint System Dynamics (Nylon/Operational/Rigid) comparison and the Upper Torso Retraction study were quite similar, however the errors in solutions to the data from the $-50G_x$ Injury Protection Comparison tests were considerably larger, due primarily to the increased digitizing error.

The ranges of estimated error for the above tests were:

Restraint System Dynamics (N/O/R)

Y_{SCS}	d_1	X	S_Q
0	67.01	100	.083
		2500	.101
12	55.01	100	.068
		2500	.084

The estimate of error accumulating from lateral motion of the elbow at maximum extension was .233 inch at X=900 counts. This was based on the d_1=56.17 inches (mean of pretest lateral displacements) and σ_{d_1}=2 inches.

Upper Torso Retraction

Y_{SCS}	d_1	X	S_Q
0	63.36	100	.087
		2500	.106
12	51.36	100	.071
		2500	.087

$-50G_x$ Injury Protection Comparison

Y_{SCS}	d_1	X	S_Q
0	60.63	100	.147
		2000	.149
		4000	.154
12	48.63	100	.118
		2000	.120
		4000	.125

The error accumulating from the lateral motion of the elbow at maximum extention was estimated to be .2236 inches based upon d_1=55.23 inches and σ_{d_1}=1.23 inches.

PROCESSING THE DIGITIZED DATA

For the past five years the UDRI has been using the Hyge Impact Facility Photo Data Analysis Program (HIFPD) to compute resultant displacement, velocity and acceleration data from digitized photographic data. This program applies an 11-point quadratic least square smoothing technique to each step in the computation of smoothed X and Z-axis displacements and resultant velocity and acceleration data. In the remainder of this report we will use data from tests 172 and 173 to define the accuracy of the digital photo data as well as the effect of the 11-point smoothing on the resultant displacement, velocity, and acceleration data. These tests (172 and 173) were conducted on the Body Positioning Restraint Device (BPRD) in Building 824 at Wright-Patterson Air Force Base.

Frequently throughout the remainder of this report we will compare Piston Z-axis data derived from digitized photo data with Piston Z-axis acceleration data recorded with a Piezo resistive damped linear accelerometer and with piston Z-axis displacement data recorded with a displacement transducer. The symbols used to identify these different types of data in the text as well as in the tables and plots are PH for photo data, PZ for Piezo accelerometer data and PD for displacement transducer data. The PZ and PD data are all digitized at 1024 samples per second (or DT = .0009766 seconds per sample) while the PH data are digitized from film at 500 frames per second (DT = .002 seconds per frame). The sample rate and DT notation are used interchangeably throughout this report. Also the notation "11-point" is used in the text and on the tables and plots to refer to data derived using the 11-point quadratic least square fit routine.

Later in this report we also refer to HX and HZ head acceleration data. These are X-axis and Z-axis data, respectively, recorded with an undamped Piezo resistive accelerometer attached to the roof of the mouth of the test subject. The sample rates are the same as for the PZ data - 1024 samples per second.

ACCURACY OF DIGITIZED PHOTOMETRIC DATA

We have already discussed the accuracy of the digitized photo data in a previous section; however, the HIFPD program also provides at least three additional checks on the quality of the digital data. First, one of the optional printouts from the HIFPD program is a tabulation of the frame to frame differences (in counts) in the digitized X- and Z-axis data for each reference and target point. By scanning these difference data one can quickly spot frame to frame differences which appear abnormally large. Second, subroutine MEAN1 in the HIFPD program computes and prints the standard deviation about the mean sled[2] reference data. Third, subroutine MEAN2 in the HIFPD program computes and prints the mean and standard deviation of the difference between smoothed and unsmoothed data for each parameter (target). If any of these means and/or standard deviations are larger than expected or are larger than are normal for that type of data, the digitized data should be checked and, if necessary, should be redigitized.

In the next two subsections we will present examples of the accuracy of our digital photo data by presenting the standard deviations about the mean sled reference data and the mean and standard deviations of the difference between unsmoothed and smoothed displacement data for each parameter for tests 172 and 173.

Accuracy of Sled Reference Data

Each frame of digital photo data includes two stationary reference points - a range and a sled reference point - plus two to ten target points on the subject or equipment. The HIFPD program rotates and/or translates all points to adjust for fluctuations in each range reference reading. If data are both translated and rotated, the initial angle between the sled and range reference is maintained throughout the run. All other digitized points are also

[2]The term "sled" reference is used here and throughout the text to be consistent with the terminology used in the HIFPD program. For tests 172 and 173 the "sled" reference is really the "seat" reference.

rotated and/or translated using the same adjustment factors applied to the sled reference data.

Ideally the frame to frame readings for the range and sled stationary reference points should be the same; however, in the real world the digitized data for these reference points fluctuate from frame to frame. These fluctuations are caused by a number of factors such as slight variations in the locations of the image in the film frame and the sensitivity of the film reading equipment. To adjust for these frame to frame variations we translate all data to the coordinate system whose origin is the range reference point. Next we determine the angle between the sled and the range reference points for the first frame. The sled reference point as well as all other data points in all subsequent frames are then translated to the range reference point and rotated to maintain a constant angle between the range and the sled reference points (same angle as for the initial sled-range reference point).

The translation and rotation of these data can best be described by presenting the equations together with a few very general illustrations. In Figure 3a, let points R_1, S_1, R_2, and S_2 represent the range and sled reference readings for the first and second frames plotted in the film coordinate system. Figure 3b contains these same reference points translated to a coordinate system through the range reference point. The equations for this translation are:

$$XS_1' = XS_1 - XR_1 \qquad XR_1' = XR_1 - XR_1$$

$$ZS_1' = ZS_1 - ZR_1 \qquad ZR_1' = ZR_1 - ZR_1$$

$$XS_2' = XS_2 - XR_2 \qquad XR_2' = XR_2 - XR_2$$

$$ZS_2' = ZS_2 - ZR_2 \qquad ZR_2' = ZR_2 - ZR_2$$

Figure 3c contains these same points with the angles between the sled and range reference points defined as Θ_1 and Θ_2. The equations for these angles are:

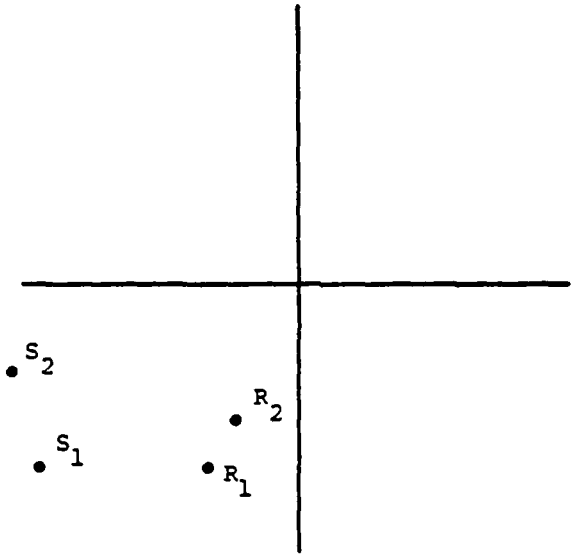

Figure 3a. First Two Sled and Range Reference Points.

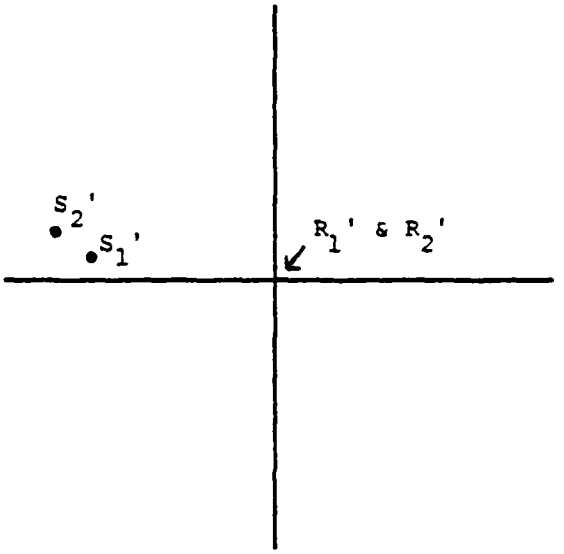

Figure 3b. Same Points After Translation.

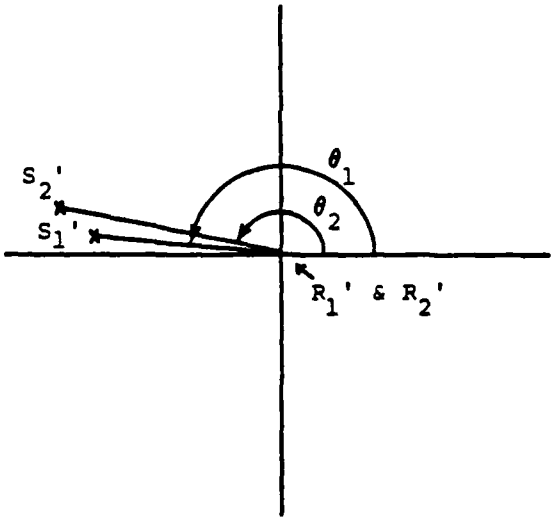

Figure 3c. Angles Between Sled and Range Reference Points.

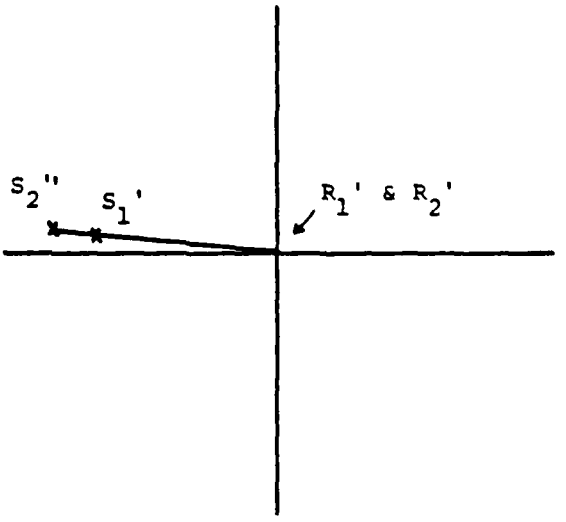

Figure 3d. Sled Reference Points After Rotation.

$$\theta_1 = \tan^{-1} \left[\frac{ZS_1' - ZR_1'}{XS_1' - XR_1'} \right]$$

$$\theta_2 = \tan^{-1} \left[\frac{ZS_2' - ZR_2'}{XS_2' - XR'} \right]$$

The data for all sled reference points after the initial point are rotated such that the angle between the sled and the range reference is the same as angle θ_1 above. In the HIFPD program we assume that the coordinate system of the second sled reference point has been rotated through angel θ where

$$\theta = \theta_2 - \theta_1 .$$

Thus the equations for the inverse rotation are:

$$XS_2'' = XS_2' \cos \theta + ZS_2' \sin \theta$$

$$ZS_2'' = -XS_2' \sin \theta + ZS_2' \cos \theta$$

Figure 3d contains points S_1' and S_2'' after rotating S_2' through angle θ. The HIFPD program then translates all points back to the film coordinate system of the initial range reference point. The equations for this translation are:

$$XS_2''' = XS_2'' + XR_1$$

$$ZX_2''' = ZS_2'' + ZR_1$$

$$XR_2''' = XR_1$$

$$ZR_2''' = ZR_1$$

After these sled reference data are translated and rotated, fluctuations in the data should represent the sensitivity of our film readings. Subroutine MEAN1 in the HIFPD program computes the standard deviation about the mean of these sled reference readings. Table 4 contains these standard deviation data for tests 172 and 173.

Inspection of these data shows that the Z-axis data are very small and are constant for these two tests. This very small constant value is a function of angle Θ_1 defined above. When Θ_1 is between approximately 175 and 185 degrees as is the case in this test configuration, the resulting Z-axis adjustment forces the Z-axis coordinate value to be approximately the same for all frames. Thus this Z-axis data cannot be used to estimate our film reading accuracy. The X-axis standard deviations are much larger and are not as sensitive to the rotation angle as are the Z-axis data; thus the X-axis data should provide a good estimate of our film reading accuracy.

TABLE 4

STANDARD DEVIATION ABOUT THE MEAN SLED REFERENCE

Run	X-Axis (feet)	Z-Axis (feet)
172	.0025	.00017
173	.0030	.00017

Compare Smoothed and Unsmoothed Data

Subroutine MEAN2 was added to the HIFPD program to compute the mean and standard deviation of the difference between the unsmoothed and smoothed X and Z-axis displacement data. The mean difference data should always be in the order of 10^{-4} to 10^{-5} feet; larger means may indicate a bias in the smoothing technique. The standard deviations give us a feel for the fluctuations in the data as well as the effect of the smoothing technique. If these standard deviations are considerably larger than the sled reference standard deviations,

we may be doing too much smoothing or the reading accuracy for this parameter may not be as good as for the sled reference data. Inspection of the velocity and acceleration versus time data as well as a rerun using a fewer point fit should be used to judge whether or not we are doing too much smoothing.

Some representative standard deviation data are presented in Table 5. All mean data are in the 10^{-4} to 10^{-6} range and are thus not tabulated. Inspection of this table shows that only the Hip, Knee and Elbow have standard deviations approximately the same as for the sled reference X-axis data. These three parameters are also similar to the sled reference data in that they exhibit very little motion in these tests. Many of the remaining parameters have standard deviations more than two or three times as large as for the sled reference. Most of these parameters also show considerably more movement than the sled reference. These large standard deviations do not decrease significantly for the 7 and 9-point fits. This is probably an indication that the error in the sled reference X-axis data is not representative of the other parameters, particularly those which exhibit greater movement and may not be as clearly defined on the film. The standard deviations in Table 5 are probably more representative of the film reading accuracy for these parameters.

Appendix A contains the standard velocity and acceleration (resultant) plots generated by the HIFPD program for all ten parameters for test 172 using 7, 9, 11 and 13-point fits. These plots are included primarily to illustrate the effect of different point fits on the final velocity and acceleration data. These plots show that the oscillations in the acceleration increase considerably for the 7 and 9-point fits; thus, we are probably not over smoothing. In fact, a 13 or higher point fit would do a better job of smoothing out some of the point to point fluctuations in the digitized data; however, it would also further degrade the true peak accelerations and additional points would be lost at the beginning and end of each plot. Thus the 11-point fit appears to be a reasonable compromise.

TABLE 5

STANDARD DEVIATION BETWEEN UNSMOOTHED AND SMOOTHED DISPLACEMENT DATA IN FEET

	TEST 172		TEST 173	
	x-axis	z-axis	x-axis	z-axis
		(11-Point Smoothing)		
Hip	.0027	.0024	.0027	.0030
Knee	.0024	.0038	.0034	.0041
Shoulder	.0062	.0036	.0080	.0046
Elbow	.0034	.0027	.0048	.0039
Head Point 1	.0074	.0059	.0090	.0060
Head Point 2	.0090	.0074	.0128	.0085
Piston	.0044	.0055	.0062	.0072
T1	.0071	.0039	.0093	.0045
Helmet 1	.0063	.0037	.0099	.0038
Helmet 2	.0061	.0035	.0086	.0038
		(9-Point Smoothing)		
Hip	.0026	.0024		
Knee	.0023	.0037		
Shoulder	.0063	.0034		
Elbow	.0034	.0027		
Head Point 1	.0071	.0056		
Head Point 2	.0094	.0070		
Piston	.0043	.0057		
T1	.0072	.0037		
Helmet 1	.0064	.0037		
Helmet 2	.0062	.0033		
		(7-Point Smoothing)		
Hip	.0025	.0022		
Knee	.0021	.0035		
Shoulder	.0058	.0034		
Elbow	.0032	.0027		
Head Point 1	.0069	.0052		
Head Point 2	.0086	.0067		
Piston	.0040	.0050		
T1	.0064	.0032		
Helmet 1	.0058	.0035		
Helmet 2	.0055	.0031		
		(13-Point Smoothing)		
Hip	.0023	.0025		
Knee	.0024	.0039		
Shoulder	.0063	.0037		
Elbow	.0034	.0029		
Head Point 1	.0075	.0061		
Head Point 2	.0095	.0073		
Piston	.0045	.0055		
T1	.0071	.0041		
Helmet 1	.0062	.0040		
Helmet 2	.0060	.0037		

USE SAMPLE DATA TO EVALUATE THE SMOOTHING TECHNIQUE USED IN THE HIFPD PROGRAM

In this section we will evaluate the smoothing technique used in the HIFPD computer program. This evaluation will include:

1) the comparison of the PZ Piston acceleration for runs 172 and 173 with the corresponding photo data smoothed using 9, 11 and 13-point fits;

2) the comparison of the PZ, PD, and PH given or derived acceleration and displacement data to determine the quality of the PH and PZ data;

3) the comparison of electronically recorded Piston (PZ) or Head (HX and HZ) acceleration with the corresponding acceleration computed by applying the 11-point smoothing technique to displacement derived by double integration[3] of the given PZ, HX or HZ acceleration;

4) the derivation from sample theory of a frequency response function which will give us "worst case" estimates of the frequency response and accuracy of our 11-point smoothing;

5) the derivation of the frequency response of our smoothing technique by applying our 11-point smoothing to a series of Sine functions;

6) the application of this frequency response function to data smoothed with the 11-point fit routine.

The HIFPD program uses a moving 11-point quadratic least square fit to smooth the X and Z-axis displacement data. For each set of 11 points only the displacement at the midpoint is computed; then one point is added and one dropped to compute the displacement for the next time increment. This 11-point fit is applied a second and third time using the X and Z-axis displacement to compute the X and Z-axis

[3]The integrated data referred to throughout this text were computed with subroutine QSF from the IBM Scientific Subroutine Package available in the ASD Computer Center Subprogram Library. QSF uses a combination of Simpson's Rule and Newton's 3/8 Rule to integrate equidistant data points.

velocity and the X and Z-axis velocity to compute acceleration data. These velocity and acceleration data are computed by applying the least square coefficients to the derivative of the quadratic least square equation. When we originally developed the HIFPD program, we tried numerous types of smoothing techniques and finally settled for this 11-point method.

The 11-point smoothing used in this evaluation is the same as used in the HIFPD program; however, in these analyses it is applied to either X- or Z-axis data and the resultant is not computed as in the HIFPD program. Here data for each axis are evaluated independently.

Compare PZ and Quadratic Fit Data

Appendix B contains plots of the Piston PZ acceleration data with the 9, 11, and 13-point fits of the corresponding Piston Z-axis photo data from tests 172 and 173. These PZ data which were recorded at 1024 samples per second were interpolated[4] at 500 samples per second to obtain a one to one correspondence with the photo sampling rate. These plots illustrate how high frequency oscillations resulting from point to point digitizing errors are reduced or removed with the 11 and 13-point fits. However, the amplitude of the large high frequency acceleration pulse is also reduced with the higher point fits; thus, the 11-point fit appears to be a reasonable compromise.

These plots also indicate a very poor correspondence between the PZ and photo acceleration data during what should be the constant velocity segment as well as at the acceleration spike. The poor correspondence at the acceleration spike can be explained by the frequency response of our quadratic fit technique which is derived later in this report. The poor correspondence during what should be the constant velocity segment is at least partially due to the questionable PZ

[4]The interpolated data referred to here and throughout this text were computed with subroutine INTRPL which is part of Algorithm 433 - Interpolating and Smooth Curve Fitting Based on Local Procedures -- from Communications of the ACM, October 1972, Volume 15, Number 12. This interpolation method is devised in such a way that the computed curve from which the data are interpolated passes through all given data points and appear smooth and natural.

acceleration data which is discussed in greater detail in the following paragraphs.

The first two displacement graphs (figures) in Appendix C contain plots of the Piston Z-axis displacement versus time for tests 172 and 173. Each graph contains two displacement versus time traces; one recorded at 1024 samples per second using a displacement transducer (PD) and the other derived from 500 sample per second photo data smoothed using our 11-point smoothing technique (PH-11PT). These graphs show reasonably good agreement between the transducer data and the photo data. They also illustrate that the piston moved with a constant or nearly constant velocity during the time interval from .06 to .21 seconds; thus the acceleration should also be approximately zero during this time interval.

The two acceleration graphs in Appendix C contain plots of the Piston Z-axis acceleration versus time for tests 172 and 173. Each graph contains plots of the Piston PZ acceleration, the Piston acceleration derived from the transducer displacement using the 11-point smoothing technique (PD-11PT), and the Piston acceleration derived from the photo displacement data also using the 11-point smoothing technique (PH-11PT). These graphs show reasonably good agreement between the transducer and photo derived acceleration data during the .06 to .21 second time interval (constant velocity segment); also, both acceleration traces oscillate about the zero acceleration level as expected with nearly constant velocity. In contrast, the PZ acceleration decreases from approximately 4 g's to approximately 1 g during this same time interval. The poor agreement between the three traces at the two acceleration pulses can be explained by the 11-point fit frequency response derived later in this report.

The last set of displacement graphs in Appendix C contains plots of the Piston Z-axis displacement derived from the PZ acceleration data by double integration of these PZ data. These two plots do not agree with the transducer displacement data (PD); they show the piston moving in the wrong direction and do not indicate a constant

velocity segment. There is obviously considerable disagreement between the acceleration data recorded by the Piezo resistive damped linear accelerometer (PZ) and the displacement recorded by the displacement transducer (PD).

In conclusion, since there is such poor agreement between the PZ acceleration and the PD displacement, we do not think one can make a valid comparison between the PZ acceleration and the acceleration derived from the photo data. Nevertheless, it is important to note that the displacement and acceleration data derived from the photo data do agree reasonably well with the corresponding data derived from the PD displacement.

Evaluation of 11-Point Fit Technique Using Accelerometer Data

In this section we evaluate our 11-point smoothing technique by first deriving velocity and displacement versus time data from accelerometer data (by single and double integration of the accelerometer data). Next we apply our 11-point smoothing technique to this derived displacement data to compute velocity and acceleration data. A comparison is then made between these computed data and the data derived directly from the accelerometer for the purpose of evaluating our 11-point smoothing technique. Plots of these comparisons are presented in Appendix D.

We computed the derived velocity and displacement versus time data from the given PZ, HX, and HZ accelerometer data by integrating these accelerometer data to obtain velocity and then integrating the velocity to obtain the derived displacement. These derived velocity and displacement data were computed at the same 1024 samples per second as the given PZ, HX, and HZ accelerometer data. Next we applied the 11-point smoothing technique to these derived displacement data and computed the smoothed displacement, velocity, and acceleration versus time data. Plots comparing the derived and smoothed displacement, the derived and smoothed velocity, and the original and smoothed acceleration for the PZ, HX, and HZ data are presented in Appendix D.

Next in order to evaluate the 11-point smoothing techniques at the standard photo data sample rate, we computed a second set of smoothed displacement, velocity and acceleration data sampled at 500 samples per second. To accomplish this we interpolated the derived displacement at 500 samples per second and then applied the standard 11-point smoothing technique to compute the smoothed displacement, velocity and acceleration data. For plotting purposes the derived velocity and the original accelerometer data were also interpolated at 500 samples per second. Plots comparing these derived and smoothed data for PZ, HX, and HZ are also presented in Appendix D.

Examination of the plots described above (presented in Appendix D) shows that all 11-point fit velocity and displacement data agree very well with the corresponding integrated data. The 11-point fit of HX and HZ acceleration at the .0009766 second sampling rate (1024 samples per second) also does a very good job of smoothing out the original high frequency noise. These same data at the .002 second sampling rate (500 samples per second) are not as good, particularly at the peak and minimum points. The 11-point fit of the PZ acceleration at both sampling rates is good except at the large amplitude pulses at the beginning and end. The high sampling rate response is also much better at these large amplitude pulses. Thus, if the photo data could be recorded at 1000 to 2000 frames per second, the computed acceleration would show considerable improvement. Also by doubling or tripling the sampling rate, we could add two or four points to the quadratic smoothing technique (that is, use a 13 or 15 point fit) and thus smooth out more of the high frequency noise and still approximate the peak acceleration more accurately.

In the above 11-point fit test cases where we compare the smoothed and original acceleration data we assumed that the effect of the integration routine used to compute the integrated displacement was negligible. We can verify this assumption by applying a 3-point fit technique (analogous to the 11-point fit technique) to the derived displacement and once again compare the resulting smoothed acceleration with the original acceleration data. This 3-point quadratic fit technique does not smooth the data; it was used for convenience here

to avoid writing another routine to compute unsmoothed velocity and acceleration data. Plots of these 3-point fit displacement, velocity and acceleration data are presented at the end of Appendix D. Inspection of the plots shows that the differences between the given and computed accelerations are very small (less than 1 g) which demonstrates that the integration routine introduces only a very small error in the derived displacement data. Thus the differences between the original and 11-point fit data are due to the 11-point fit and not the integration routine.

DERIVE A FREQUENCY RESPONSE FUNCTION TO EVALUATE THE SMOOTHING TECHNIQUE USED IN THE HIFPD PROGRAM

In the previous sections we evaluated the 11-point quadratic fit technique by applying it to derived displacement data which was computed from given accelerometer data. This demonstrated that the 11-point fit technique did a good job of approximating the given acceleration everywhere except for large transient spikes in the acceleration; that is, it qualitatively demonstrated the frequency response limitations of the 11-point fit technique. In the following sections we will apply theoretical principles used in Sampled - Data Control Systems[5] in a partial attempt to explain the frequency response limitations of our 11-point fit technique. We will also apply our 11-point smoothing technique to analyze a series of pure Sine functions, in the frequency range of 2 to 35 Hz, in order to actually compute the frequency response of this smoothing technique. The frequency response data are presented in two ways; first in a table of frequency versus distortion factor and, secondly, in a plot of frequency response (in dB) versus frequency (in Hz). (In the following sections the frequency response will often be presented and referred to as a distortion factor.)

[5] "Digital and Sampled-Data Control Systems" by Julius T. Tou, McGraw-Hill, 1959.

Derivation of a Frequency Distortion Factor for Electronic Systems

Our purpose here is to study theoretical concepts of an electronic sampled data system in order to obtain an insight into how our 11-point fit technique could possibly impact upon photo sampled data systems. Most of the theoretical work on electronic sampled data systems to be presented here is taken from Tou[5]. This study will also help explain the actual frequency response characteristics to be presented later.

When we apply the 11-point fit technique we have, in essence, arrived at an estimation of the function by using a "weighted" average of 11 consecutive points which span a period of time equivalent to 10 basic sampling intervals. Thus, if the basic sampling period is 0.002 sec (500 samples or frames per sec) then the effective sampling period for the 11-point weighted average is ten times this basic sampling period or 0.02 seconds (50 samples or frames per sec). By Shannon's Theorem a sampling period of 0.02 seconds limits the information bandwidth to 25 Hz which is 1/2 the effective sampling rate of 50 samples/second (a sampling period of 0.02 seconds implies a rate of 50 samples/second).

However, the basic nature of photographic data is very similar to that for a fully-clamped electronic system in that data levels remain fixed and constant for the full duration of each data frame. Consequently, study of an electronic system may shed some light on our photo system. Tou[5] shows in equation 3.4-13 on page 78 that, for a fully clamped electronic sampling system, there is a frequency related distortion factor that operates on the information in addition to the Shannon limitation. This distortion factor is a function of the frequency of the data signal. Let f_s be the sampling frequency, T_s be the sampling interval (thus $f_s = \frac{1}{T_s}$) and let f_o be the frequency of the data signal which is being sampled. Then for the fully clamped case Tou[5] shows that the distortion factor (F) is given by:

$$F = \frac{a \sin (\pi f_o T_s)}{\pi f_o T_s}$$

It is also understood, and necessary, that $f_o \leq \frac{1}{2} f_s = \frac{1}{2T_s}$. Now let $f_o = r\, f_s = \frac{r}{T_s}$, then we can express F as:

$$F = \frac{a \sin (\pi\, r)}{\pi\, r}$$

where $0 \leq r \leq 0.5$. For convenience, since it is a constant, let a = 1, then the frequency effect of letting f_o vary from 0 to $\frac{1}{2} f_s$ (or $0 \leq r \leq 0.5$) is given in Table 6.

TABLE 6

FREQUENCY RATIO (r) VERSUS DISTORTION FACTOR (F)
FOR A FULLY-CLAMPED ELECTRONIC SAMPLED DATA SYSTEM

$r = \frac{f_o}{f_s}$	F
0.10	0.9836
0.15	0.9634
0.20	0.9355
0.25	0.9003
0.30	0.8584
0.40	0.7568
0.50	0.6366

There is an old "rule-of-thumb" used by data acquisition engineers which states that for a sampled-data system at least five samples per cycle of a periodic signal are required to be able to make a fairly good reproduction of that signal. Shannon's Theorem states that the absolute limit is two samples per cycle. These two measures are described above for the cases where r=0.2 (5 samples per cycle) and r=0.5 (2 samples per cycle). Recall that the data in Table 6 above are for a fully-clamped electronic sampling system which represents a perturbation to Shannon's Theorem. Our purpose here is to apply this characteristic of an electronic sampled data system to our photo sampled data system to obtain some measure of what could possibly be expected for the photo system.

Thus by analyzing the data in the above table one could expect, for a photographic system running at 500 frames per second and fitting a smoothing curve over 11 points, that for data at frequencies of 10 Hz or less ($r \leq 0.2$) the distortion factor will be on the order of 0.9355 or better and that data at frequencies approaching the Shannon limit of 25 Hz ($r=0.5$) could be expected to have a distortion factor on the order of 0.6366.

This distortion function for fully clamped electronic sampling systems may well apply to our smoothed photographic displacement data. To compute velocity and acceleration, the HIFPD program applies the 11-point smoothing a second and third time; therefore the distortion function would also have to be applied a second and third time or in effect it would have to be squared for the velocity and cubed for the acceleration data. Thus, the resulting acceleration at 25 Hz would be distorted by almost 75 percent. However, since our 11-point smoothing technique employs both a "running average" and a quadratic least square fit rather than a simple 11-point average, one could possibly expect less distortion (higher F) for our system for a given r than for the electronic system. Therefore, the distortion factors in Table 6 could be considered to be a measure of the "worst-case" conditions for our 11-point smoothing technique and may well represent an upper bound on the frequency distortion.

Actual Frequency Response For the 11-Point Fit Smoothing Technique

In this section we will precisely derive a distortion or frequency response function which is directly applicable to our 11-point quadratic fit smoothing technique. This frequency response function will demonstrate how our 11-point fit technique responds to high frequency sinusoidal data. It will also show why it would be desirable to sample photo data at a rate higher than 500 samples per second.

We computed a precise distortion factor for our smoothing technique by applying the 11-point fit three times (just as in the HIFPD program) in order to derive displacement, velocity, and acceleration data using as input data a pure Sine function sampled at 500 points per second (.002 second sample period). This process was repeated for

a number of frequencies over the range of 2 to 35 Hz. The exact equations relating sinusoidal displacement (D), velcoity (V), and acceleration (A) functions are:

$$D = a \sin(\omega t)$$
$$V = a\,\omega \cos(\omega t)$$
$$A = -a\,\omega^2 \sin(\omega t)$$

where

a = amplitude
$\omega = 2\pi$ times frequency in Hz
t = time in seconds

Each input Sine function, representing displacement, was sampled at 0.002 sec intervals and these data were used as input to the 11-point fit routine. The ratios of the resultant smoothed output data to the actual true data (including displacement, velocity, and acceleration) provided distortion factors (FK) for our 11-point smoothing technique. The tabulation of this precisely computed frequency dependent distortion function is presented in Table 7. Also presented in Table 7 is the F factor derived for the electronic systems for comparison purposes. The frequency dependent distortion function is more commonly presented as a frequency response plot where

$$\text{frequency response in dB} = 20 \log_{10} (FK).$$

A plot of the frequency response data for displacement, velocity, and acceleration is given in Figure 4.

We also computed similar tabulations using 7-point and 9-point fits of the Sine functions. They are not presented here since they showed that for a given $r(r = \frac{f_o}{f_s})$ the distortion factors are approximately the same (differ by .02 to .03). Thus the r given in Table 7 can be used, independent of the f_o frequency, to determine the distortion factor FK for sampling rates greater than or less than 500 samples per second. This computation of FK is also valid for 7-point, 9-point, and 11-point smoothing techniques.

TABLE 7

DISTORTION FACTOR (FK) COMPUTED FROM
MULTIPLE FREQUENCY SINE FUNCTIONS

f_o (Hz)*	$r = \frac{f_o}{f_s}$	F	Distortion Factor (FK)		
			DISPL	VEL	ACCEL
2	.04	.9974	1.0000	.9981	.9963
4	.08	.9895	1.0000	.9925	.9851
6	.12	.9765	.9999	.9831	.9667
8	.16	.9584	.9997	.9700	.9413
10	.20	.9355	.9993	.9532	.9093
12	.24	.9079	.9985	.9327	.8713
14	.28	.8759	.9972	.9086	.8278
16	.32	.8399	.9953	.8809	.7796
18	.36	.8000	.9926	.8498	.7275
20	.40	.7568	.9888	.8154	.6724
22	.44	.7106	.9838	.7779	.6151
24	.48	.6618	.9975	.7376	.5567
26	.52	.6109	.9695	.6949	.4981
28	.56	.5583	.9597	.6500	.4403
30	.60	.5046	.9479	.6034	.3841
32	.64	.4500	.9340	.5556	.3305
34	.68	.3952	.9177	.5070	.2801
35	.70	.3679	.9086	.4826	.2563

*f_o applies only to an 11-point fit of data sampled at 500 samples per second; use r to determine FK for other fits and/or sample rates.

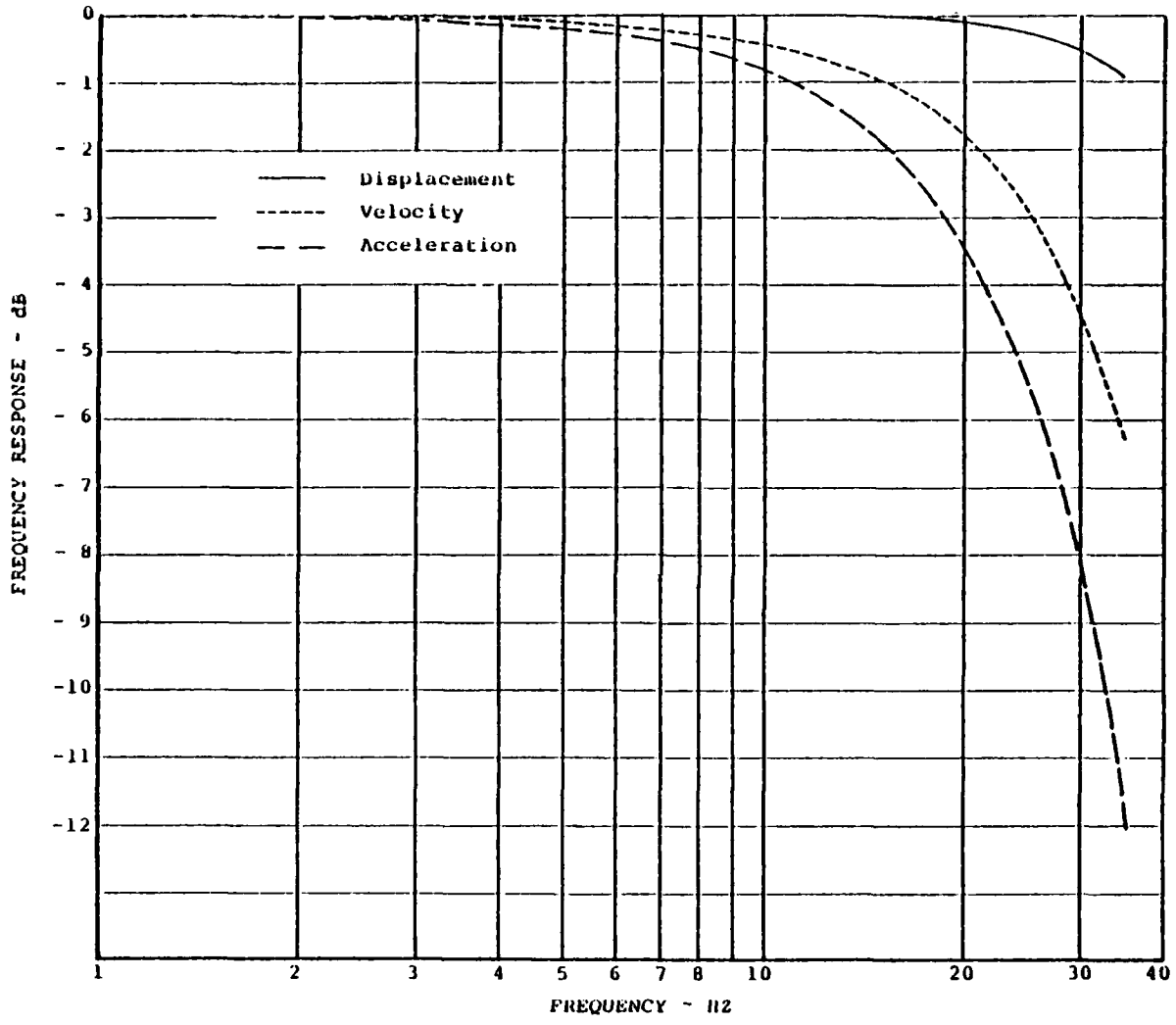

Figure 4. Frequency Response of the 11-Point Smoothing Technique as Applied in the HIFPD Program.

An analysis of the data in Table 7 also shows that the actual frequency related distortion is less than predicted by sample theory i.e., the frequency response for our 11-point smoothing technique is better than would be predicted for the fully-clamped electronic sampling system. For example, FK is .9086 at f_o=35 Hz (r=.70) compared to a predicted value of F=.3679. As stated previously, this can probably be attributed to our quadratic least square fit which produces a weighted average over the effective data sampling period. We should also note that an r>.5 still gives good results for the 11-point fit system which means that the effective sampling rate is actually greater than 50 Hz (1/10 sampling rate) as one might expect for a running weighted average technique such as we use in the HIFPD program.

We can also use the data in Table 7 to compute the sampling rate which will give a satisfactory distortion factor (FK) at a specific f_o frequency. For example, if we want computed acceleration data with less than 5 percent distortion (FK=.95) for frequencies up to 30 Hz, we can use the equation

$$f_s = f_o/r = 30/.15 = 200 \text{ Hz}.$$

The 200 Hz effective sampling rate must be adjusted for the number of points used in the smoothing technique. For our 11-point fit, the adjustment factor is ten, giving us a required sampling rate of 2000 samples per second. Consequently, to insure good data having frequency components in the range of 0 to 30 Hz, one must obtain photo data at a rate of 2000 frames per second when employing the 11-point smoothing technique of program HIFPD.

Apply Derived Distortion Function to Smoothed Acceleration Data

The 172 PZ and 173 PZ acceleration plots presented in Appendix D can be used to see how well our acceleration distortion factor predicts the 11-point fit data. Since these data are sampled at 1024 samples per second, the r ratio is computed using an f_s=102 rather than f_s=50 as in Table 7; thus, the f_o for a specific r is approximately twice the table value. A comparison of the 11-point computed acceleration

data with the data predicted by the FK distortion factor (Table 7) are presented in Table 8.

The following example from Table 8 will help illustrate how the data were computed. Run 172 has a 22.45 g positive acceleration spike with a time duration and shape which suggests a major frequency component of approximately 42.3 Hz. The r for this frequency is .415 (r = 42.3/102) which corresponds to a FK of .645; thus the predicted acceleration is .645 x 22.45 or 14.48 g's. This compares very well with the computed 13.97 g's.

The data in the bottom half of Table 8 is from 500 sample per second PZ Piston data in Appendix D. These data were generated to evaluate the 11-point fit at the normal sampling rate of the photo data. Table 8 also shows a reasonably good correspondence between the predicted and computed data for this reduced sampling rate. Thus, the FK distortion factor appears to predict with reasonable accuracy the acceleration response of the 11-point fit routine used in the HIFPD program; nevertheless, since we do not know the major frequency components of the exact acceleration pulse, FK should not be used to adjust or otherwise correct the HIFPD resultant acceleration (or velocity) data.

TABLE 8

APPLICATION OF ACCELERATION DISTORTION FACTOR TO 11-POINT FIT OF PZ ACCELERATION DATA IN APPENDIX D

Run ID	Frequency of Peak	r	FK	Given Accel	Predicted Accel	Computed Accel
(f_s = 102, DT = .0009766)						
172PZ	18.3	.18	.93	- 5.34	- 4.97	- 4.70
172PZ	42.3	.415	.645	22.45	14.48	13.97
173PZ	18.3	.18	.93	- 5.75	- 5.34	- 4.52
173PZ	42.3	.415	.645	20.6	13.28	13.0
(f_s = 50, DT = .002)						
172PZ	18.3	.366	.72	- 5.34	- 3.84	- 3.60
172PZ	34.4	.69	.32	22.3	7.10	8.0
173PZ	18.3	.366	.72	- 5.75	- 4.10	- 3.65
173PZ	31.4	.63	.345	21.34	7.36	7.34

CONCLUSIONS FROM ANALYSIS OF DIGITAL PROCESSING TECHNIQUES

The frequency response data presented in Table 7 and Figure 4 provides the best overall summary of the effect of our 11-point fit routine on the displacement, velocity, and acceleration data. Table 2 shows that acceleration data computed from our 500 sample per second photo data will be within 5 percent of the true acceleration only for acceleration pulses having major frequency components of less than 7 Hz. The frequency response could be increased to approximately 30 Hz by increasing the sample rate to 2000 samples per second. This increase in accuracy with increased sampling rate is demonstrated by the data in Appendix D where we apply the 11-point fit to data digitized at both 500 and 1024 samples per second.

Displacement plots in Appendix C show a very good correspondence between the Piston Z-axis displacement recorded with a displacement transducer (PD) and displacement derived from photo data using the 11-point smoothing technique (PH-11PT). The acceleration data in this same appendix show reasonably good correspondence between the 11-point smoothed PD and photo acceleration data except at the acceleration spikes. The agreement between the recorded PZ acceleration (with a Piezo resistive damped linear accelerometer) and these same smoothed PD and photo acceleration is not nearly as good. The differences during the constant velocity segment (0.6 to 0.21 seconds) are at least partially due to a suspected problem with the PZ acceleration while the disagreement at the spikes can be explained by the frequency response function discussed in the above paragraphs.

In summary, we believe that the analyses of 500 frame per second data with the 11-point fit routine in this report show that acceleration pulse data having major frequency components of less than 7 to 8 Hz are accurate within 5 percent while serious degradation exists for higher frequency data.

RECOMMENDATIONS

The conclusions drawn previously lead to the following recommendations.

Data Acquisition

Have anthropometric points located by either an anthropologist or the medical monitor and identified with a semi-permanent mark.

Investigate the feasibility of obtaining a portable three dimensional measuring system with digital readout to expedite recording of initial seat coordinates of fiducials on reference and anthropometric points with improved accuracy.

Investigate the feasibility of interposing a grid between the cameras and the subject. Such a grid could be fabricated from fine wire (.002 inch - .006 inch music wire) and would provide calibration and orientation data on each film frame.

An accurate grid board should be photographed on each camera at two or more distances from the camera prior to the initiation of each test program for calibration purposes.

Data Digitization

The sponsoring agency recently procured a sophisticated automatic digitizing system. The specifications to which the system was designed should greatly improve the accuracy of the digitized data. If the foregoing suggestions to photograph a calibration grid prior to each test program is implemented, improved accuracy in calibration should also be realized.

Electronic Data Processing

A method of applying a Fast Fourier Transform to the displacement data and its derivatives has been developed by Mr. Ints Kaleps and Mr. Dave Brungart of the Mathematical Analysis Branch (AMRL/BBM). This method promises to yield derived data which predicts much more

accurately the motion demonstrated during the experiment. Utilization of this method as an alternative to the quadratic smoothing method should be studied further since it may be a beneficial method.

If, as suggested above, a feasible method of measuring coordinate positions of anthropometric points prior to each test run is developed and implemented, it is recommended that the program be modified to provide a comparison between the initial coordinate solutions and the measured values, thus providing a prompt indication of the accuracy of the seat coordinate displacement solutions.

APPENDIX A

This appendix contains velocity and acceleration plots generated by the HIFPD program for Run 172 using 7, 9, 11 and 13-point smoothing. These plots are presented here to illustrate the effect of the four types of smoothing. Also, since the HIFPD program can process only six parameters in each pass, Run 172 required two passes to process the ten parameters. Thus to make the two HIFPD input datasets unique, test numbers 172 and 10172 were assigned for the first and second passes, respectively.

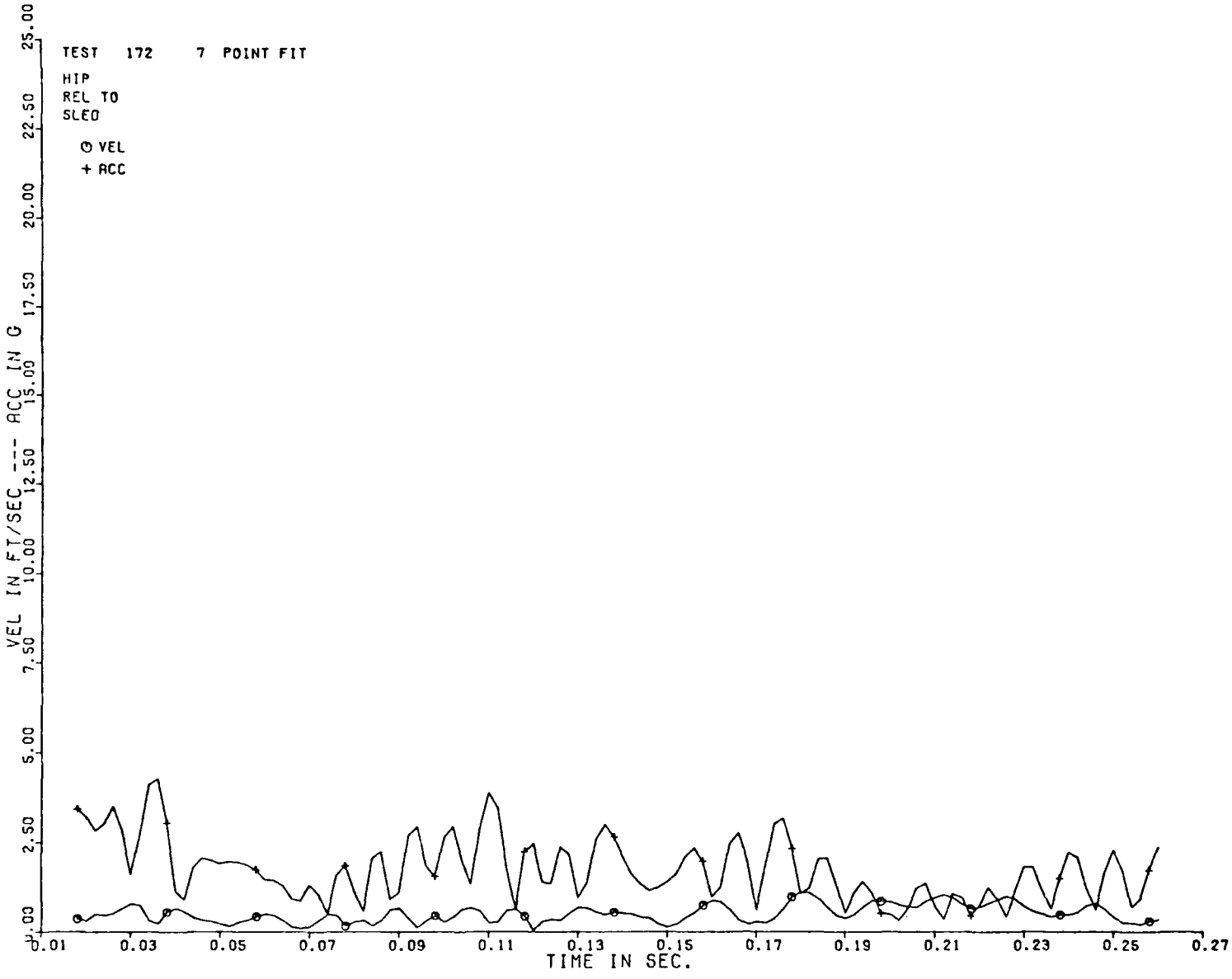
TEST 172 7 POINT FIT
HIP
REL TO
SLED
⊙ VEL
+ ACC
VEL IN FT/SEC --- ACC IN G
0.00
2.50
5.00
7.50
10.00
12.50
15.00
17.50
20.00
22.50
25.00
0.01
0.03
0.05
0.07
0.09
0.11
0.13
0.15
0.17
0.19
0.21
0.23
0.25
0.27
TIME IN SEC.

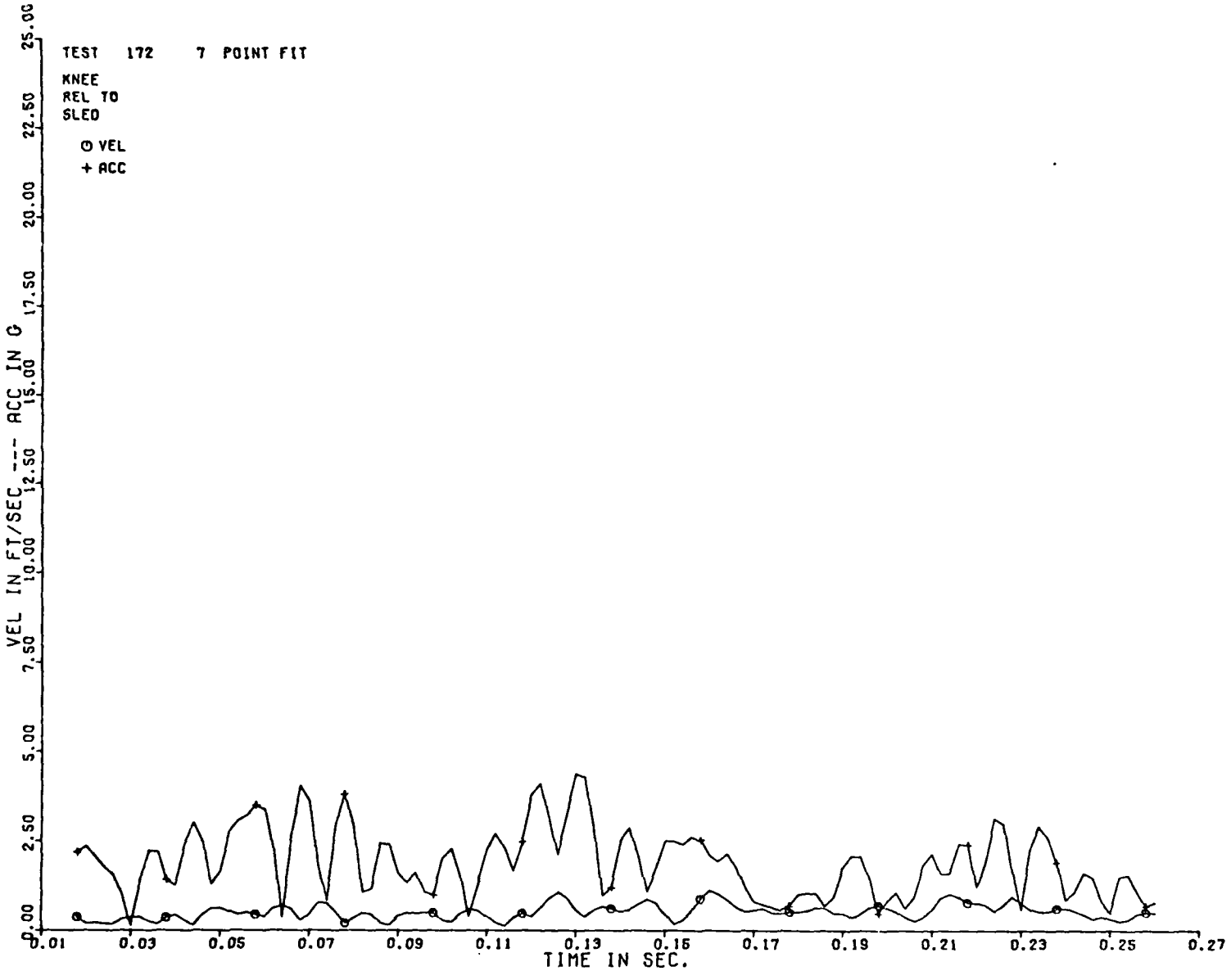
TEST 172 7 POINT FIT
KNEE
REL TO
SLED
⊙ VEL
+ ACC
VEL IN FT/SEC --- ACC IN G
0.00
2.50
5.00
7.50
10.00
12.50
15.00
17.50
20.00
22.50
25.00
0.01
0.03
0.05
0.07
0.09
0.11
0.13
0.15
0.17
0.19
0.21
0.23
0.25
0.27
TIME IN SEC.

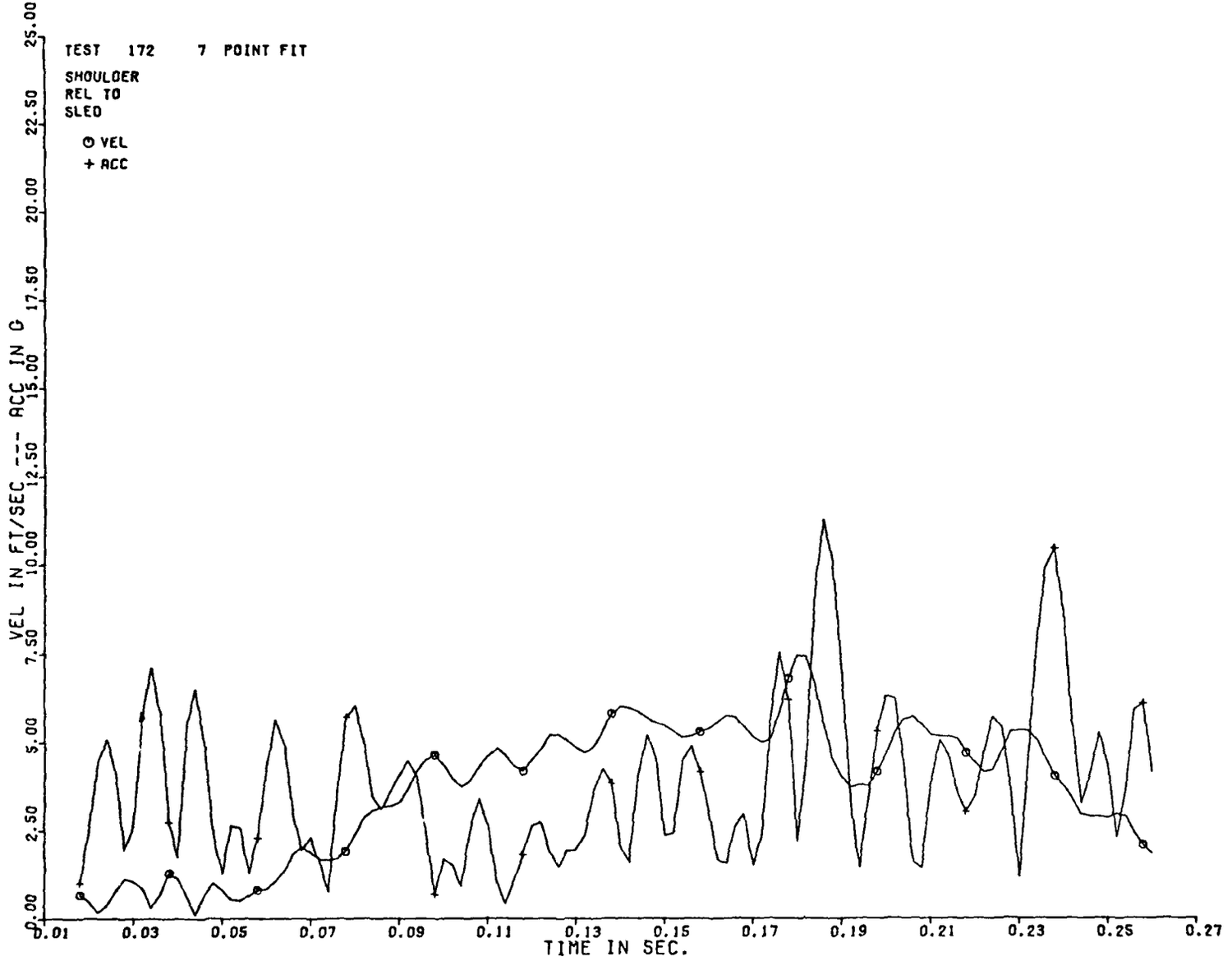
TEST 172 7 POINT FIT
SHOULDER
REL TO
SLED
VEL
ACC
VEL IN FT/SEC --- ACC IN G
0.00
2.50
5.00
7.50
10.00
12.50
15.00
17.50
20.00
22.50
25.00
0.01
0.03
0.05
0.07
0.09
0.11
0.13
0.15
0.17
0.19
0.21
0.23
0.25
0.27
TIME IN SEC.

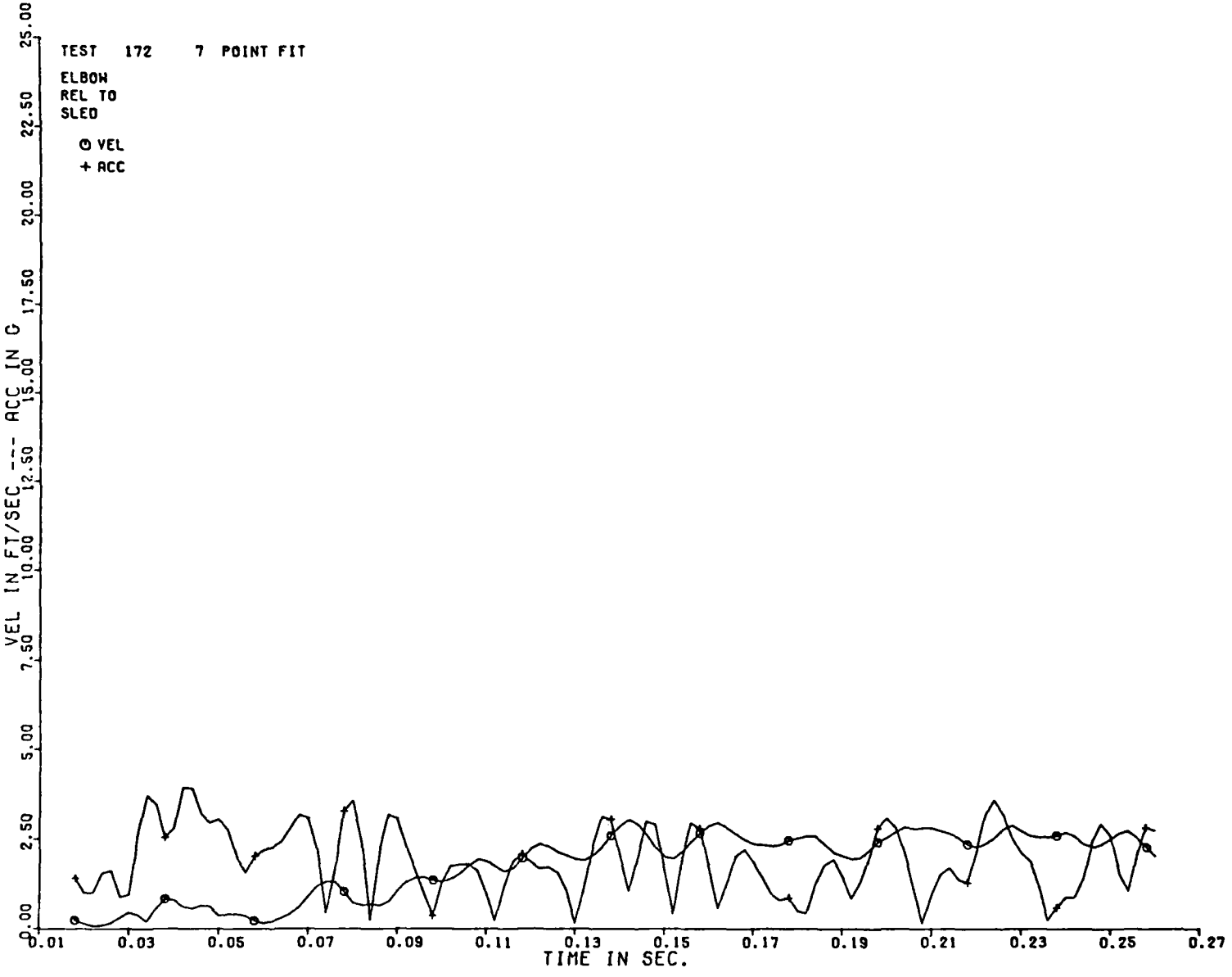
TEST 172 7 POINT FIT
ELBOW
REL TO
SLED
VEL
ACC
VEL IN FT/SEC --- ACC IN G
0.00
2.50
5.00
7.50
10.00
12.50
15.00
17.50
20.00
22.50
25.00
0.01
0.03
0.05
0.07
0.09
0.11
0.13
0.15
0.17
0.19
0.21
0.23
0.25
0.27
TIME IN SEC.

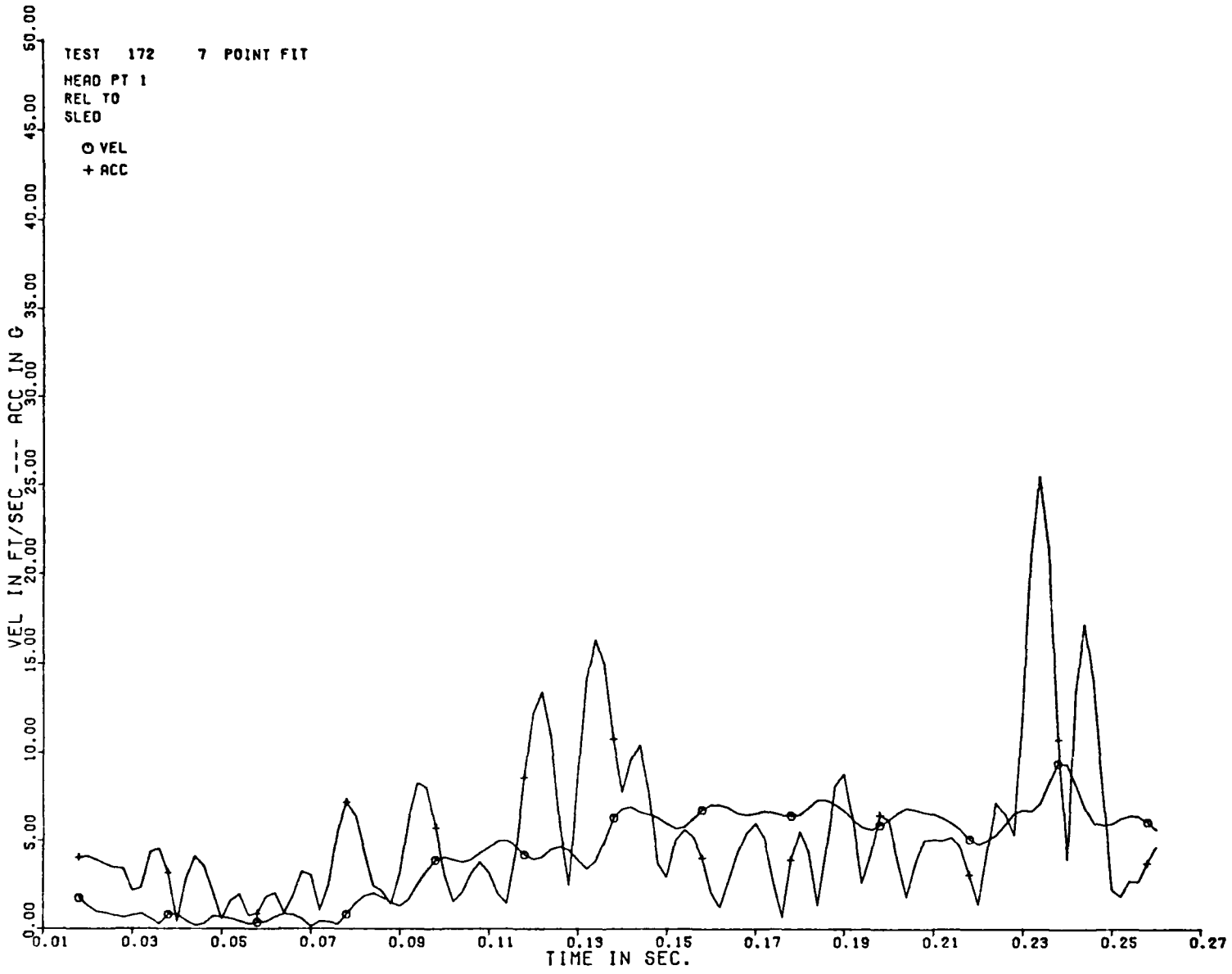
TEST 172 7 POINT FIT
HEAD PT 1
REL TO
SLED
⊙ VEL
+ ACC
VEL IN FT/SEC --- ACC IN G
0.00
5.00
10.00
15.00
20.00
25.00
30.00
35.00
40.00
45.00
50.00
0.01
0.03
0.05
0.07
0.09
0.11
0.13
0.15
0.17
0.19
0.21
0.23
0.25
0.27
TIME IN SEC.

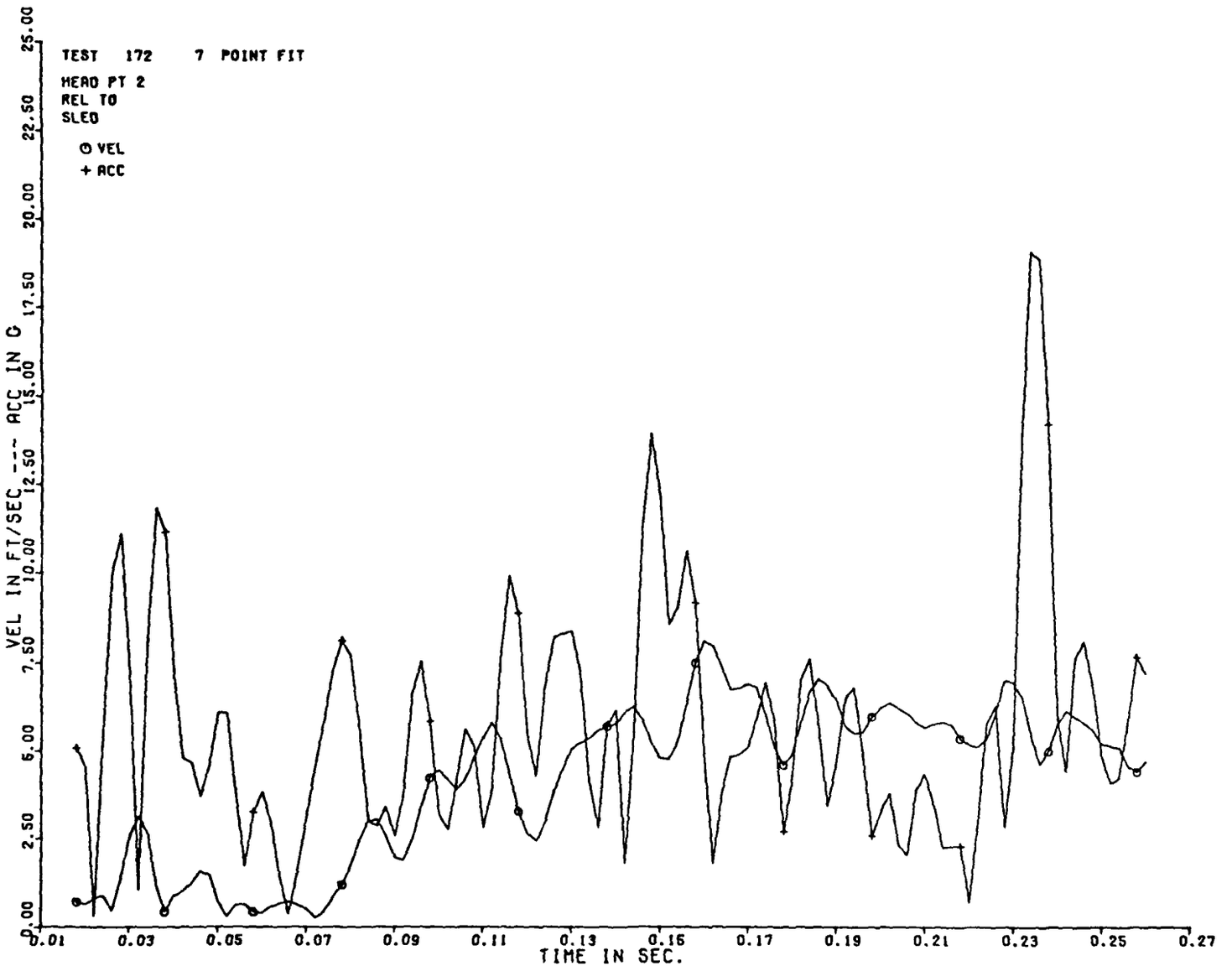
TEST 172 7 POINT FIT
HEAD PT 2
REL TO
SLED
VEL
ACC
VEL IN FT/SEC --- ACC IN G
0.00
2.50
5.00
7.50
10.00
12.50
15.00
17.50
20.00
22.50
25.00
0.01
0.03
0.05
0.07
0.09
0.11
0.13
0.15
0.17
0.19
0.21
0.23
0.25
0.27
TIME IN SEC.

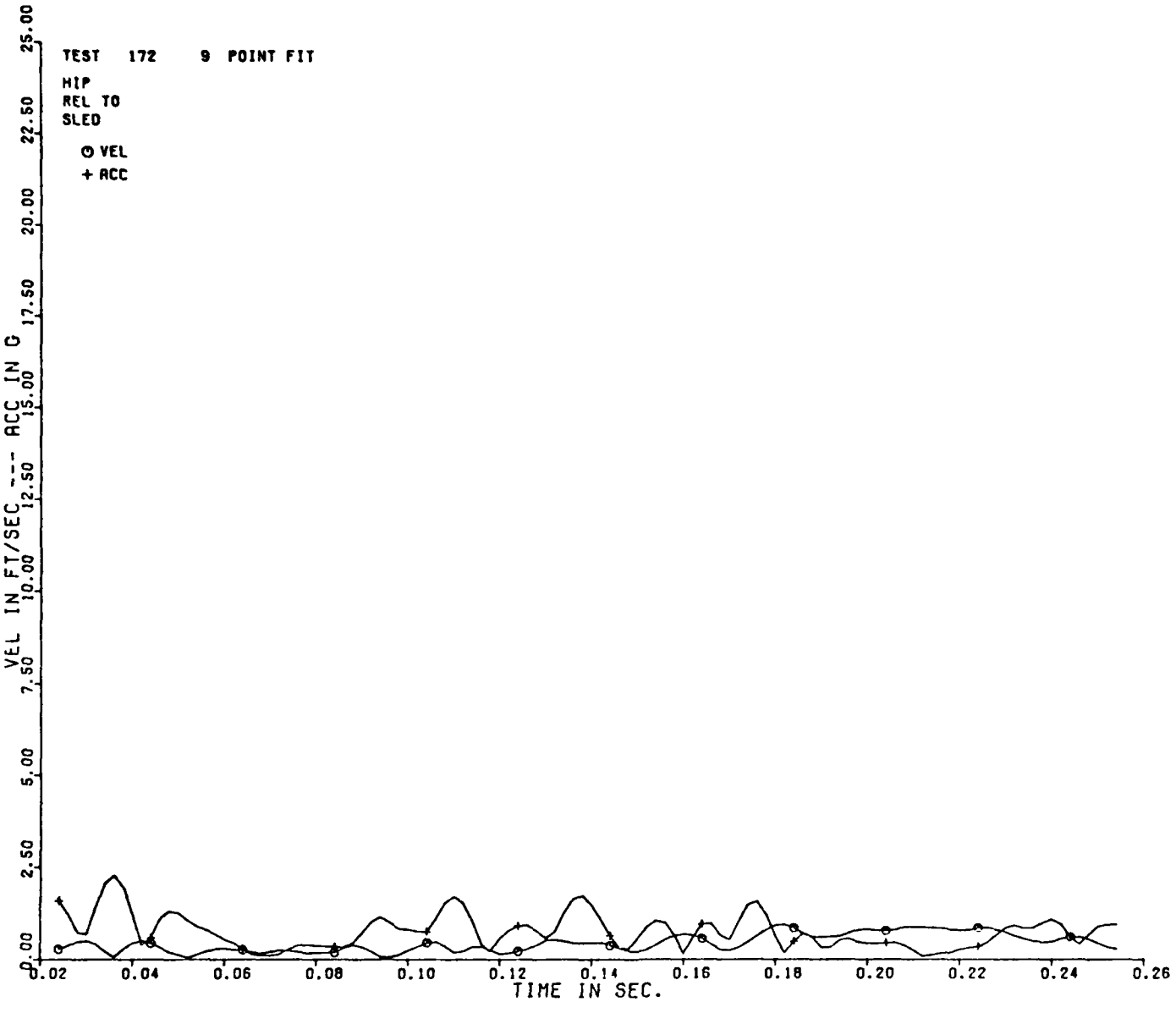
TEST 172 9 POINT FIT
HIP
REL TO
SLED
⊙ VEL
+ ACC
VEL IN FT/SEC --- ACC IN G
0.00
2.50
5.00
7.50
10.00
12.50
15.00
17.50
20.00
22.50
25.00
0.02
0.04
0.06
0.08
0.10
0.12
0.14
0.16
0.18
0.20
0.22
0.24
0.26
TIME IN SEC.

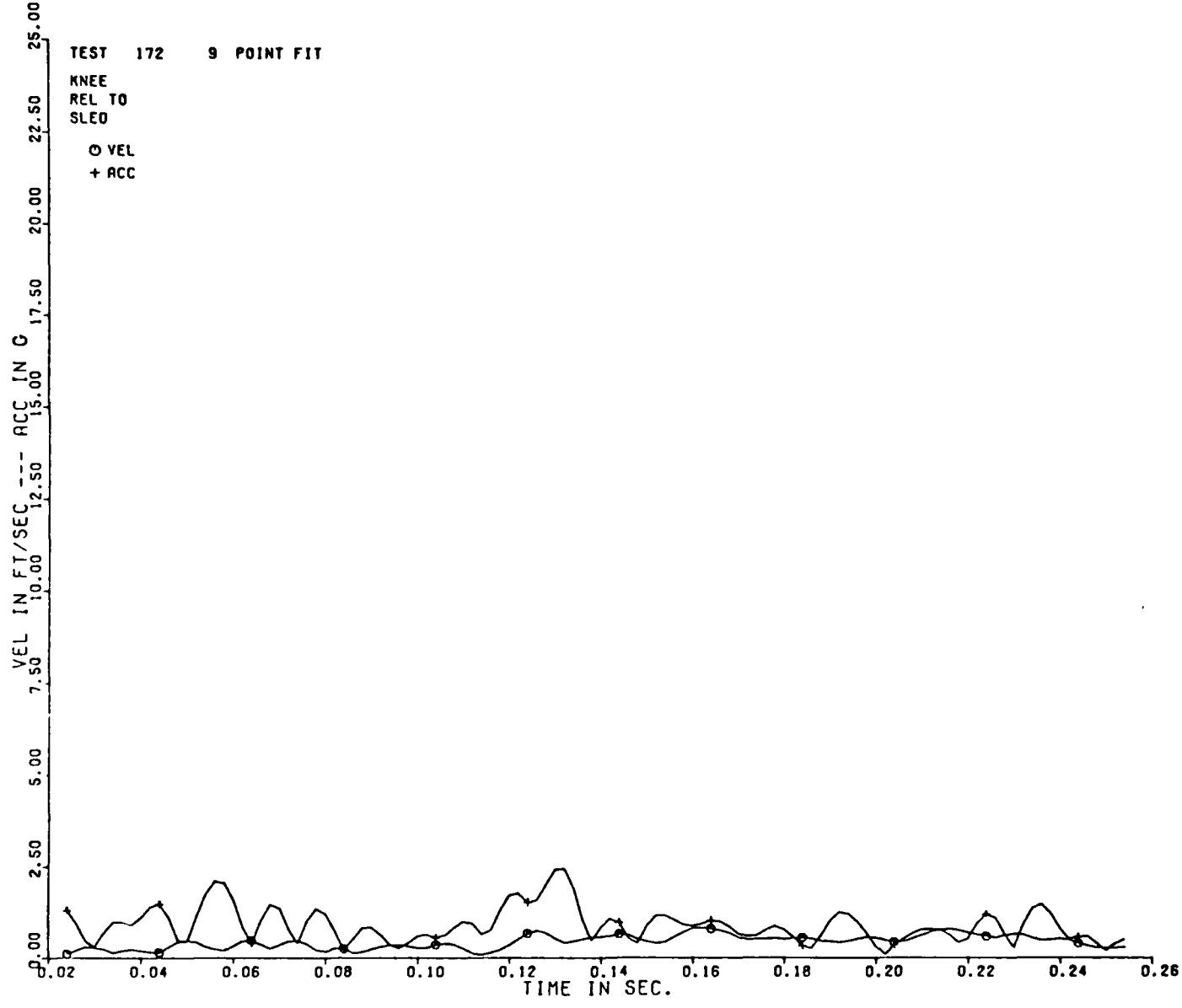
TEST 172 9 POINT FIT
KNEE
REL TO
SLED
VEL
ACC
VEL IN FT/SEC --- ACC IN G
0.00
2.50
5.00
7.50
10.00
12.50
15.00
17.50
20.00
22.50
25.00
0.02
0.04
0.06
0.08
0.10
0.12
0.14
0.16
0.18
0.20
0.22
0.24
0.26
TIME IN SEC.

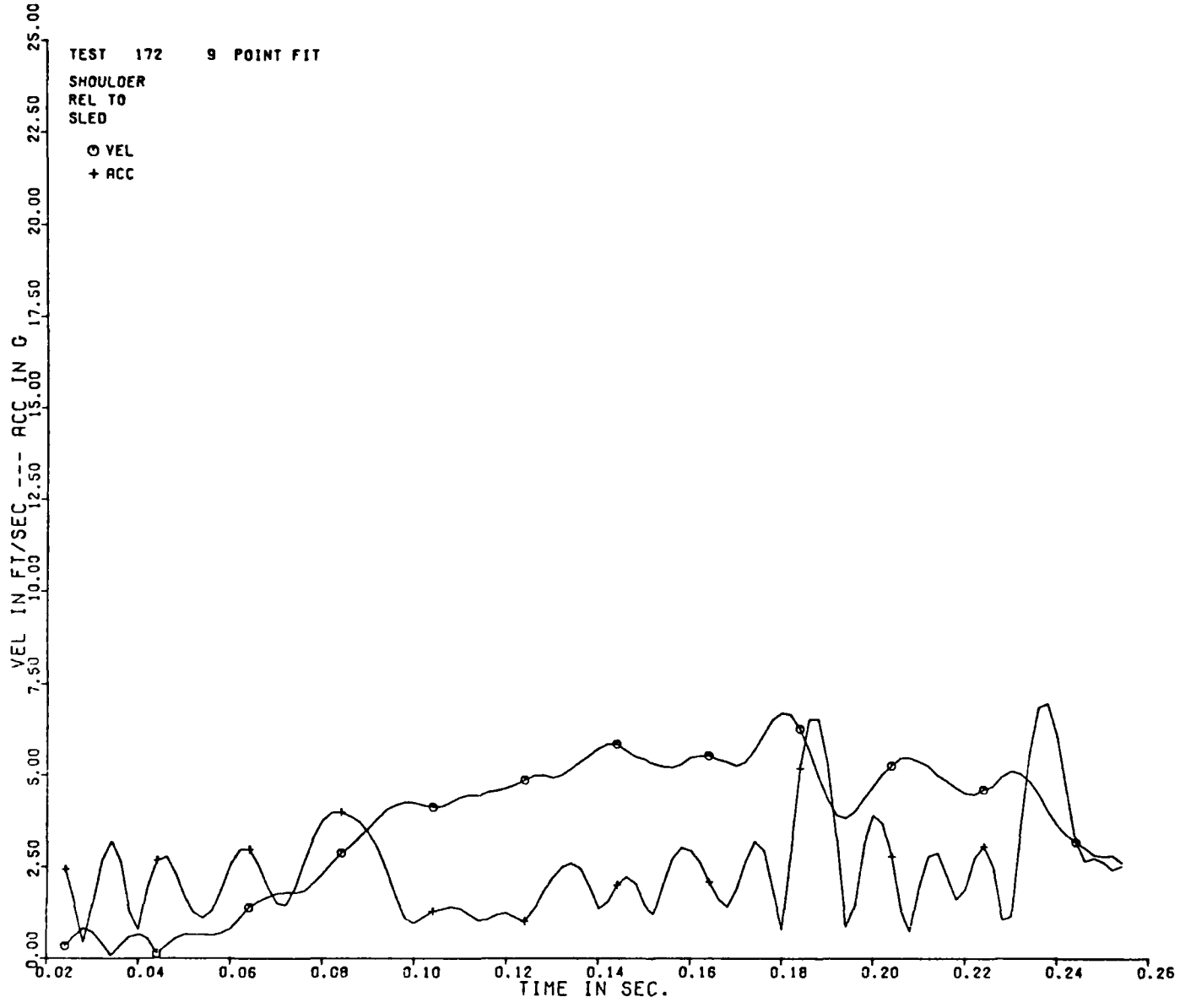
TEST 172 9 POINT FIT
SHOULDER
REL TO
SLED
⊙ VEL
+ ACC
VEL IN FT/SEC --- ACC IN G
0.00
2.50
5.00
7.50
10.00
12.50
15.00
17.50
20.00
22.50
25.00
0.02
0.04
0.06
0.08
0.10
0.12
0.14
0.16
0.18
0.20
0.22
0.24
0.26
TIME IN SEC.

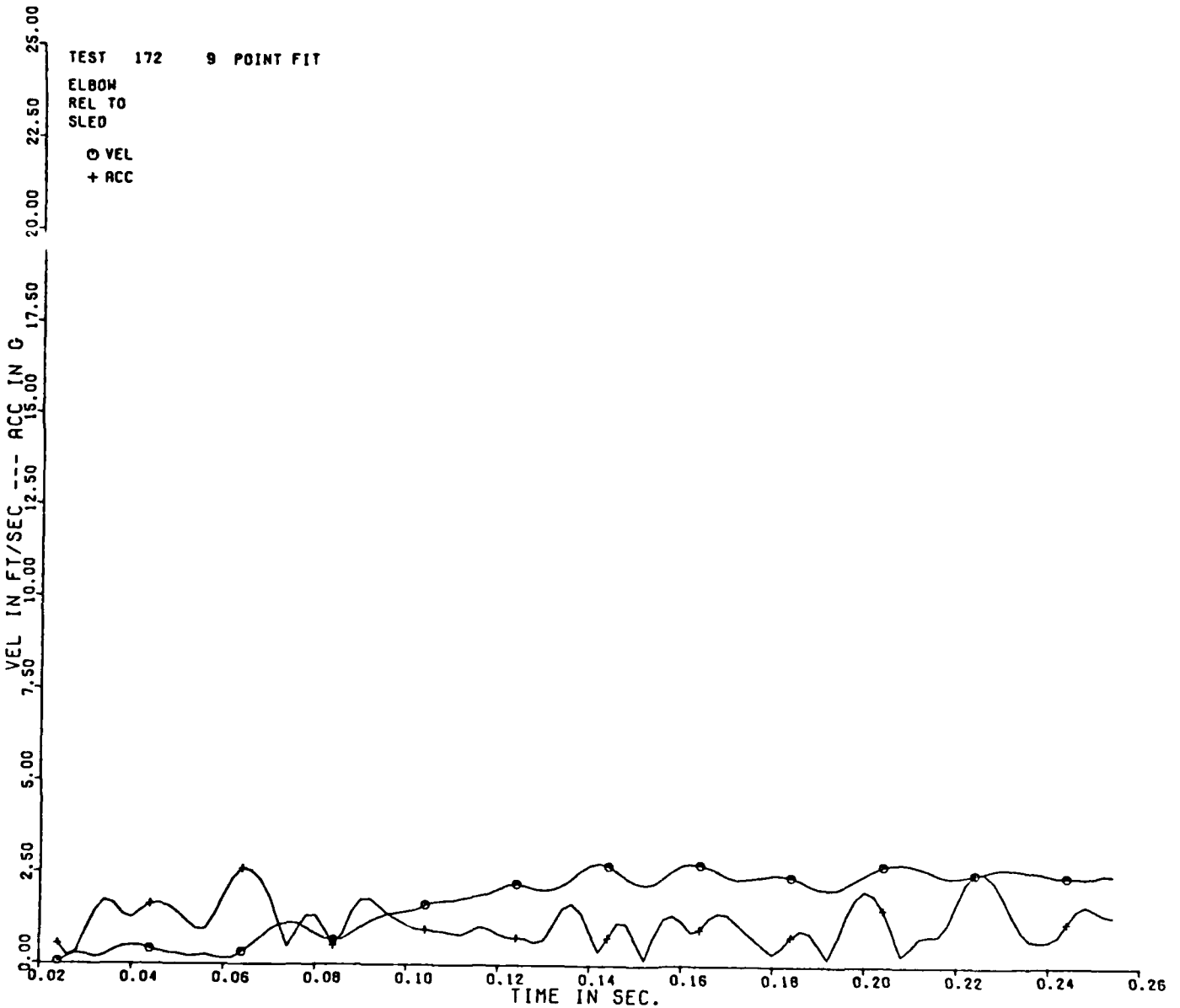
TEST 172 9 POINT FIT
ELBOW
REL TO
SLED
⊙ VEL
+ ACC
VEL IN FT/SEC --- ACC IN G
0.00
2.50
5.00
7.50
10.00
12.50
15.00
17.50
20.00
22.50
25.00
0.02
0.04
0.06
0.08
0.10
0.12
0.14
0.16
0.18
0.20
0.22
0.24
0.26
TIME IN SEC.

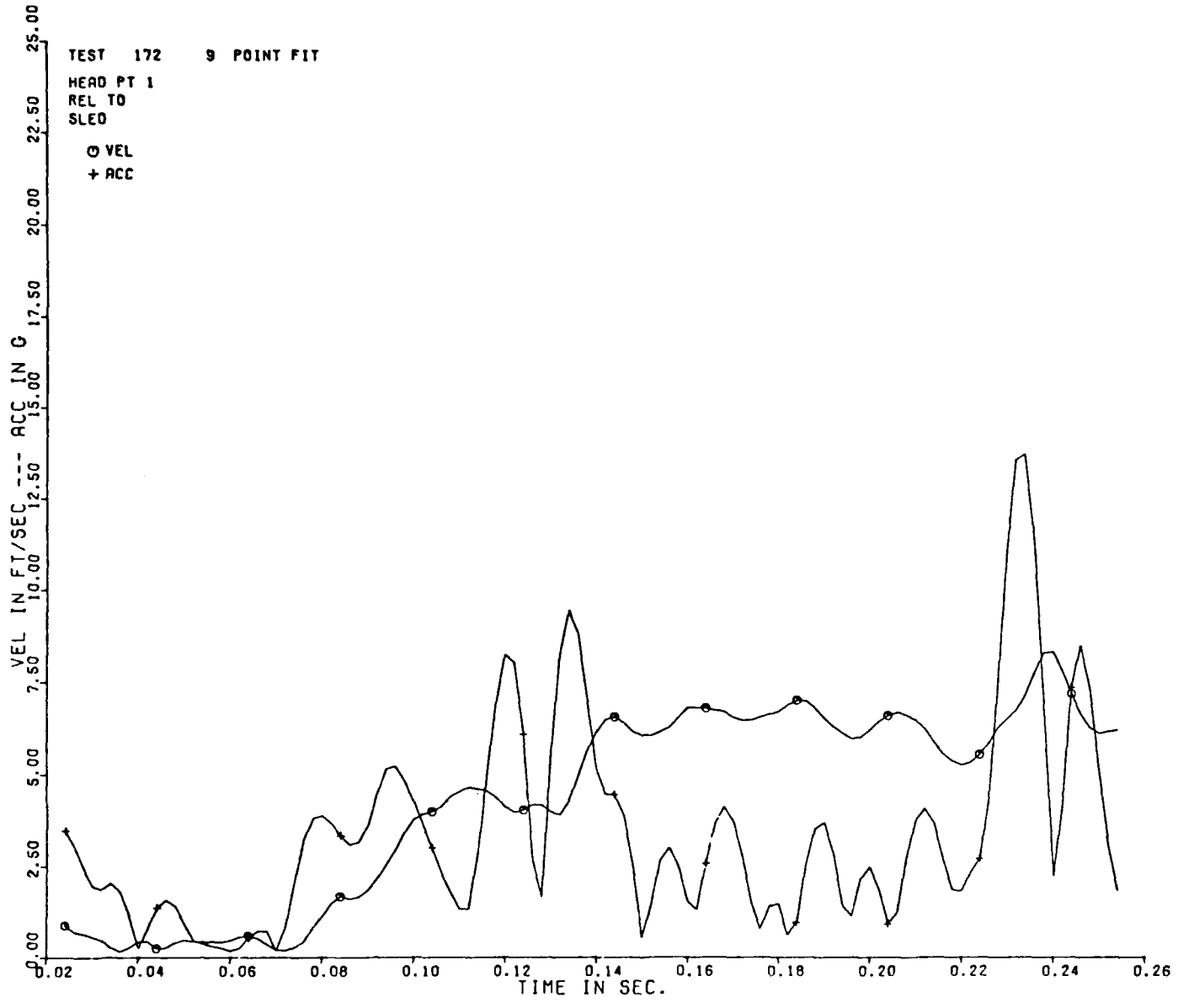
TEST 172 9 POINT FIT
HEAD PT 1
REL TO
SLED
⊙ VEL
+ ACC
VEL IN FT/SEC --- ACC IN G
0.00
2.50
5.00
7.50
10.00
12.50
15.00
17.50
20.00
22.50
25.00
0.02
0.04
0.06
0.08
0.10
0.12
0.14
0.16
0.18
0.20
0.22
0.24
0.26
TIME IN SEC.

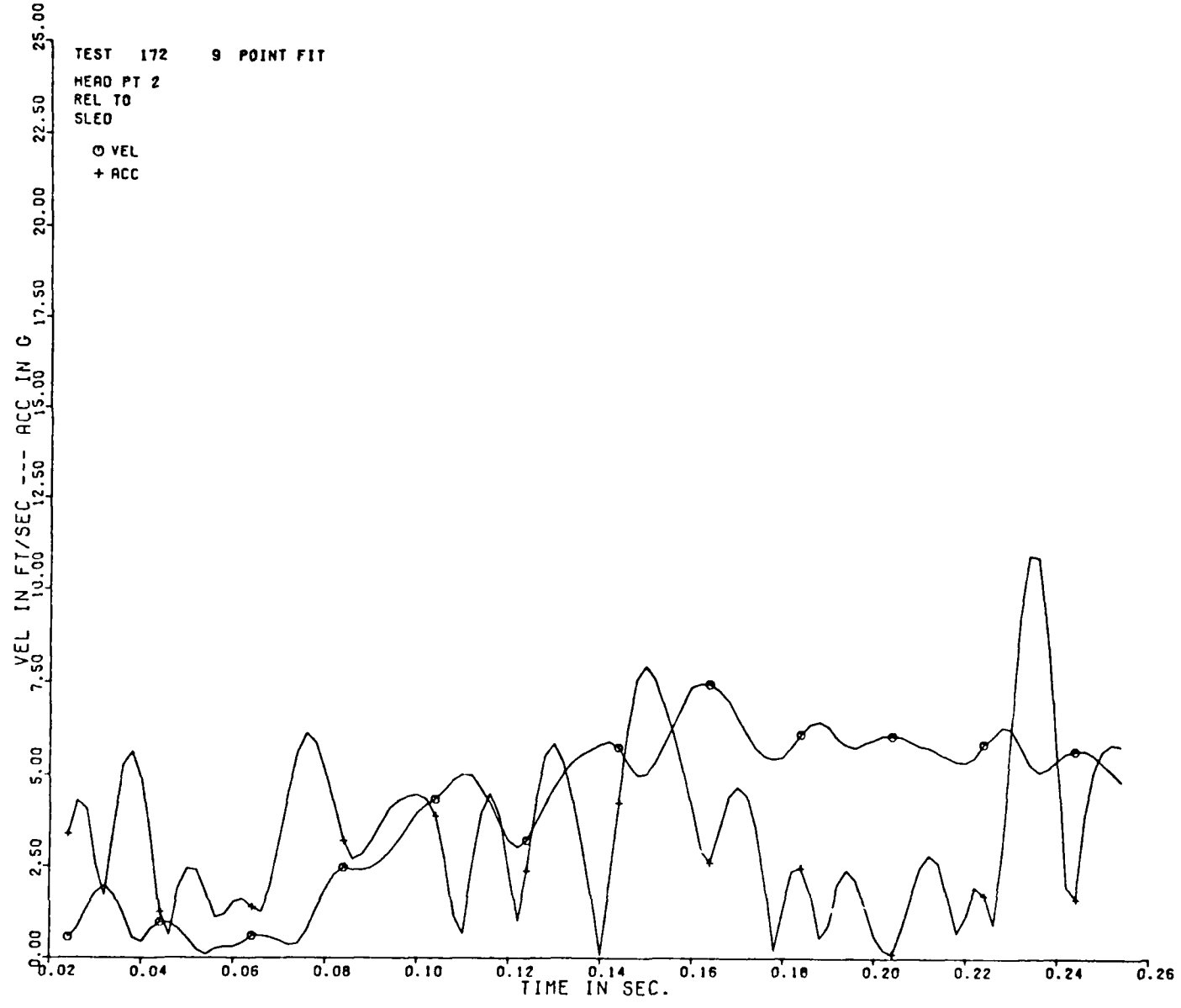
TEST 172 9 POINT FIT
HEAD PT 2
REL TO
SLED
⊙ VEL
+ ACC
VEL IN FT/SEC --- ACC IN G
0.00
2.50
5.00
7.50
10.00
12.50
15.00
17.50
20.00
22.50
25.00
0.02
0.04
0.06
0.08
0.10
0.12
0.14
0.16
0.18
0.20
0.22
0.24
0.26
TIME IN SEC.

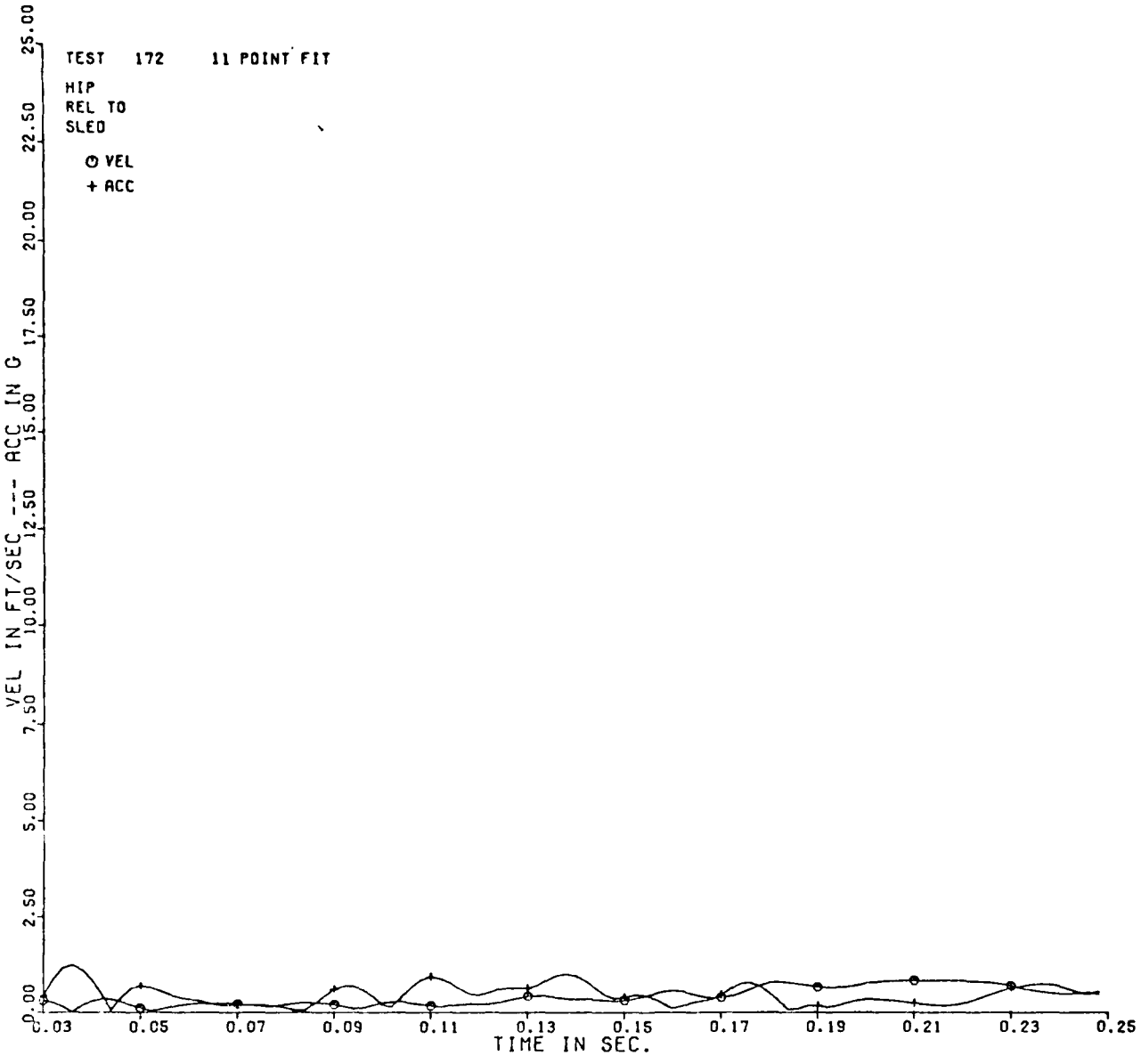
TEST 172 11 POINT FIT
HIP
REL TO
SLED
⊙ VEL
+ ACC
VEL IN FT/SEC --- ACC IN G
0.00
2.50
5.00
7.50
10.00
12.50
15.00
17.50
20.00
22.50
25.00
0.03
0.05
0.07
0.09
0.11
0.13
0.15
0.17
0.19
0.21
0.23
0.25
TIME IN SEC.

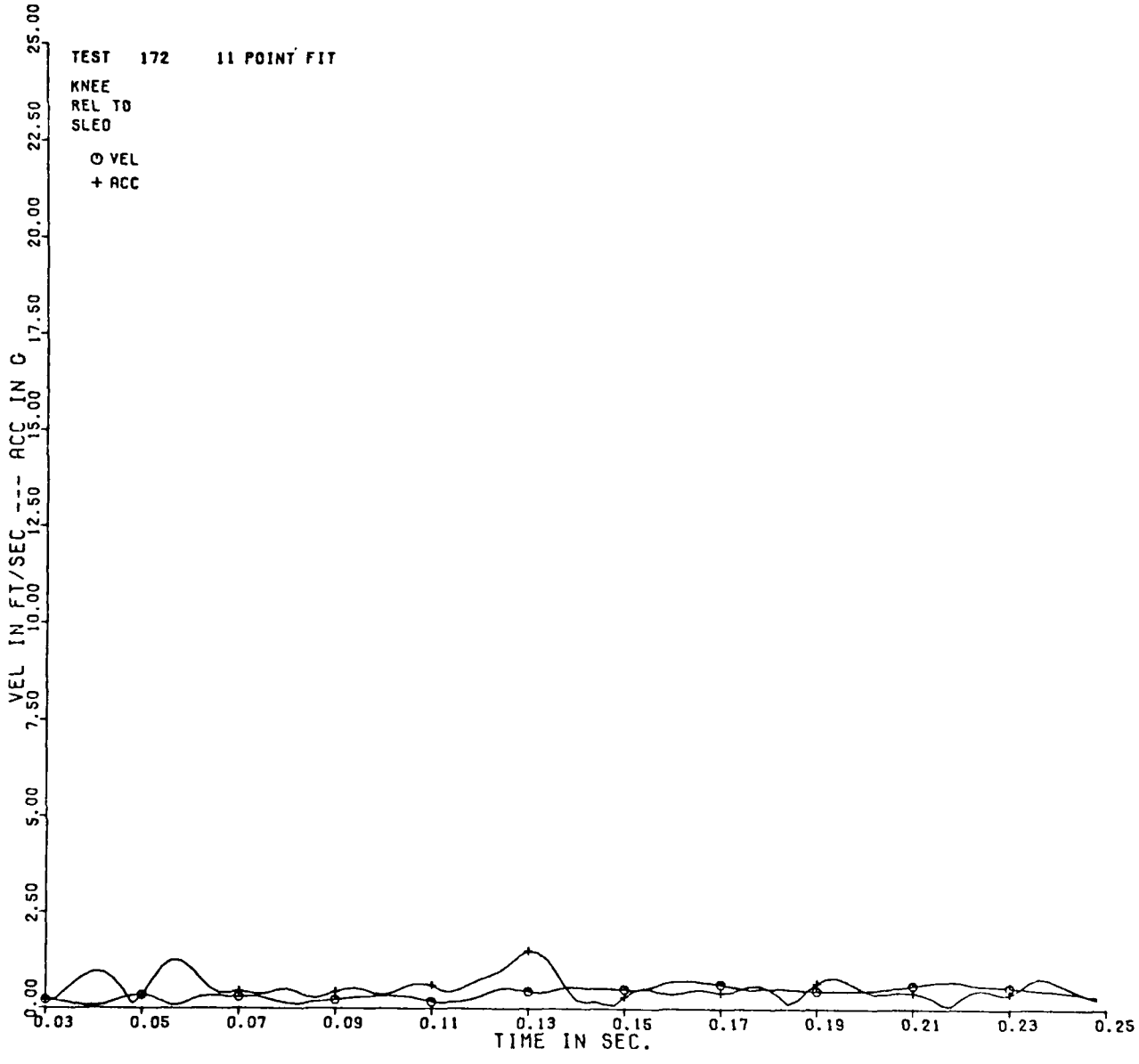
TEST 172 11 POINT FIT
KNEE
REL TO
SLED
⊙ VEL
+ ACC
VEL IN FT/SEC --- ACC IN G
0.00
2.50
5.00
7.50
10.00
12.50
15.00
17.50
20.00
22.50
25.00
0.03
0.05
0.07
0.09
0.11
0.13
0.15
0.17
0.19
0.21
0.23
0.25
TIME IN SEC.

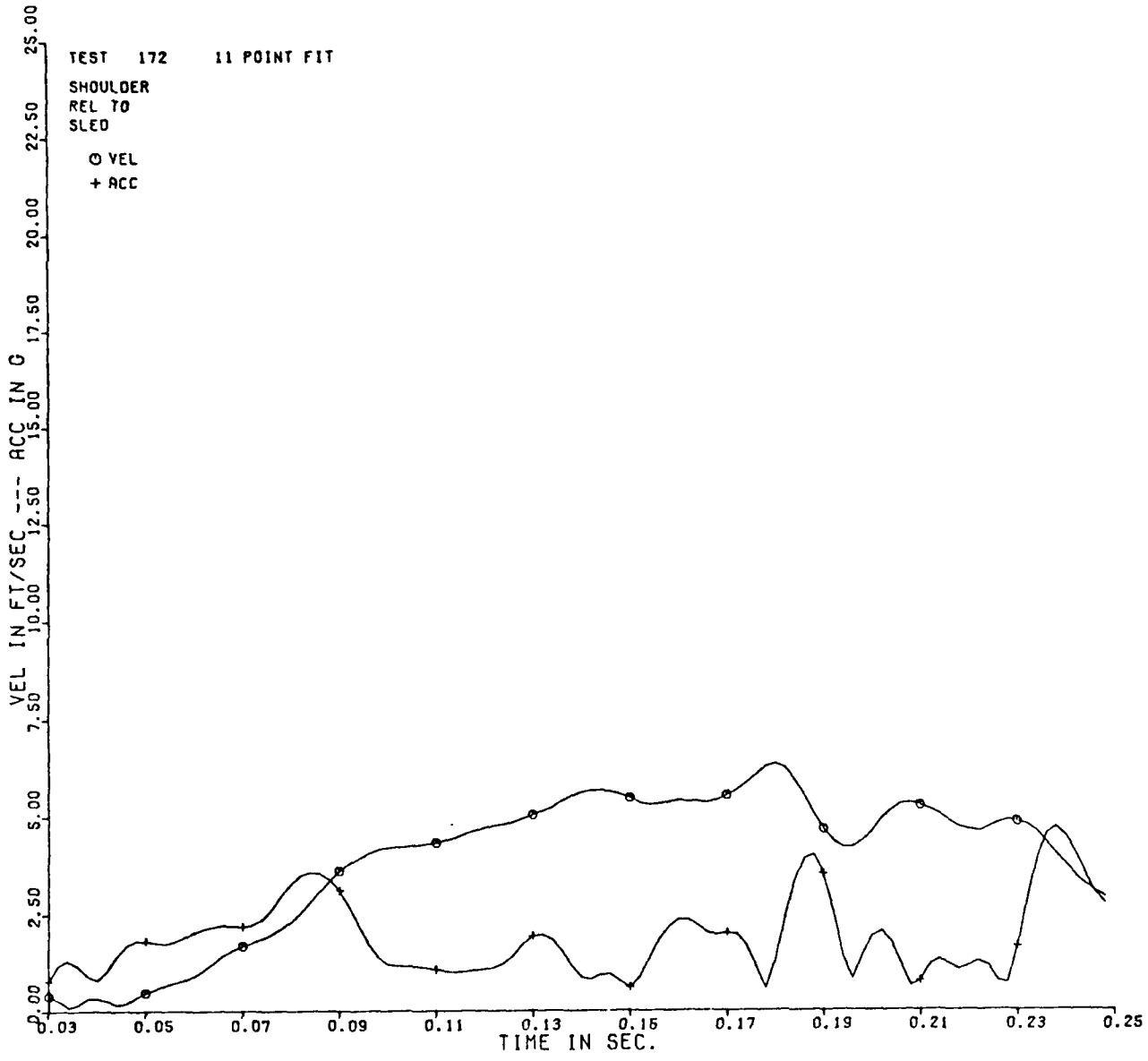
TEST 172 11 POINT FIT
SHOULDER
REL TO
SLED
⊙ VEL
+ ACC
VEL IN FT/SEC --- ACC IN G
0.00
2.50
5.00
7.50
10.00
12.50
15.00
17.50
20.00
22.50
25.00
0.03
0.05
0.07
0.09
0.11
0.13
0.15
0.17
0.19
0.21
0.23
0.25
TIME IN SEC.

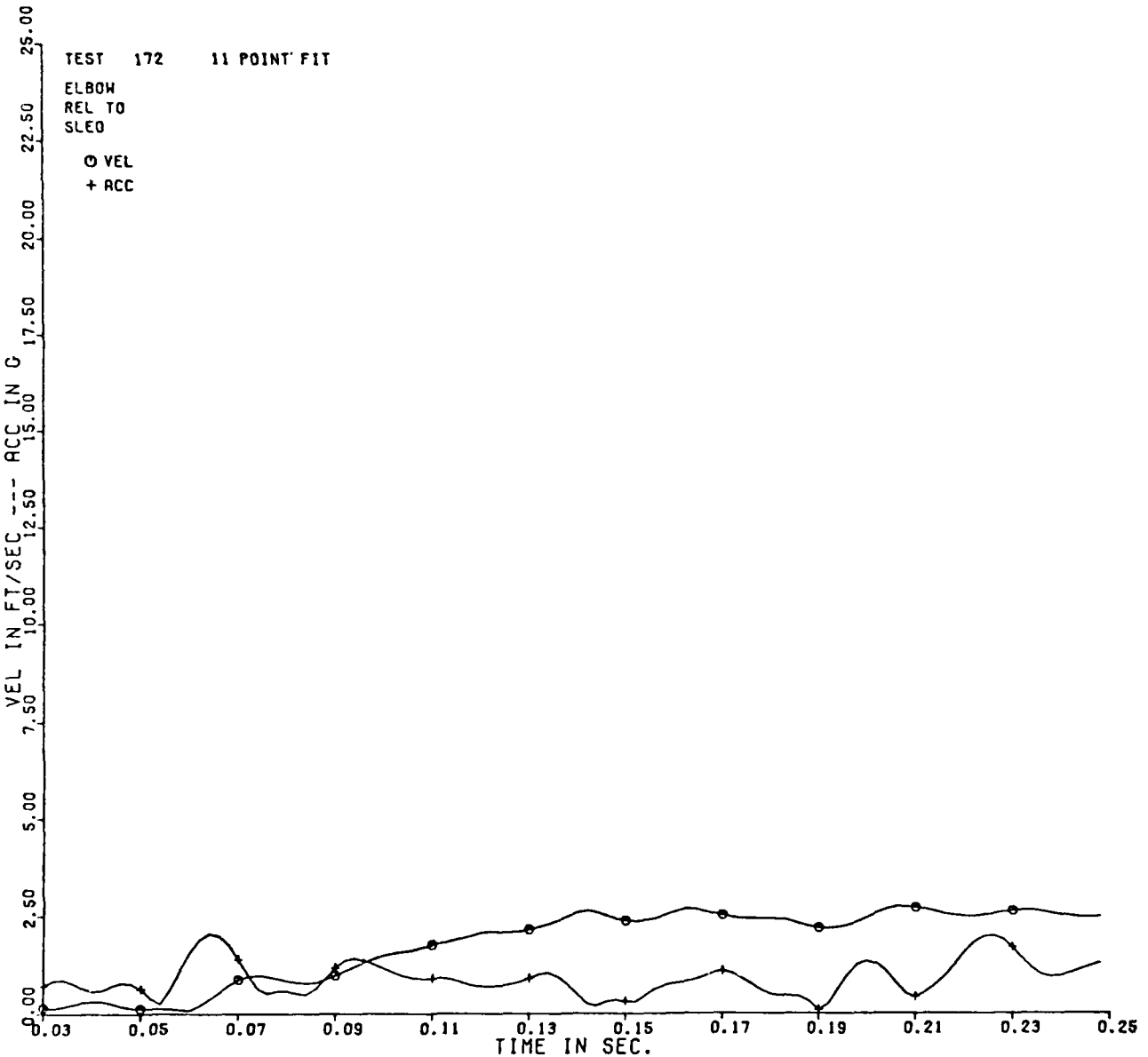
TEST 172 11 POINT FIT
ELBOW
REL TO
SLEO
⊙ VEL
+ ACC
VEL IN FT/SEC --- ACC IN G
0.00
2.50
5.00
7.50
10.00
12.50
15.00
17.50
20.00
22.50
25.00
0.03
0.05
0.07
0.09
0.11
0.13
0.15
0.17
0.19
0.21
0.23
0.25
TIME IN SEC.

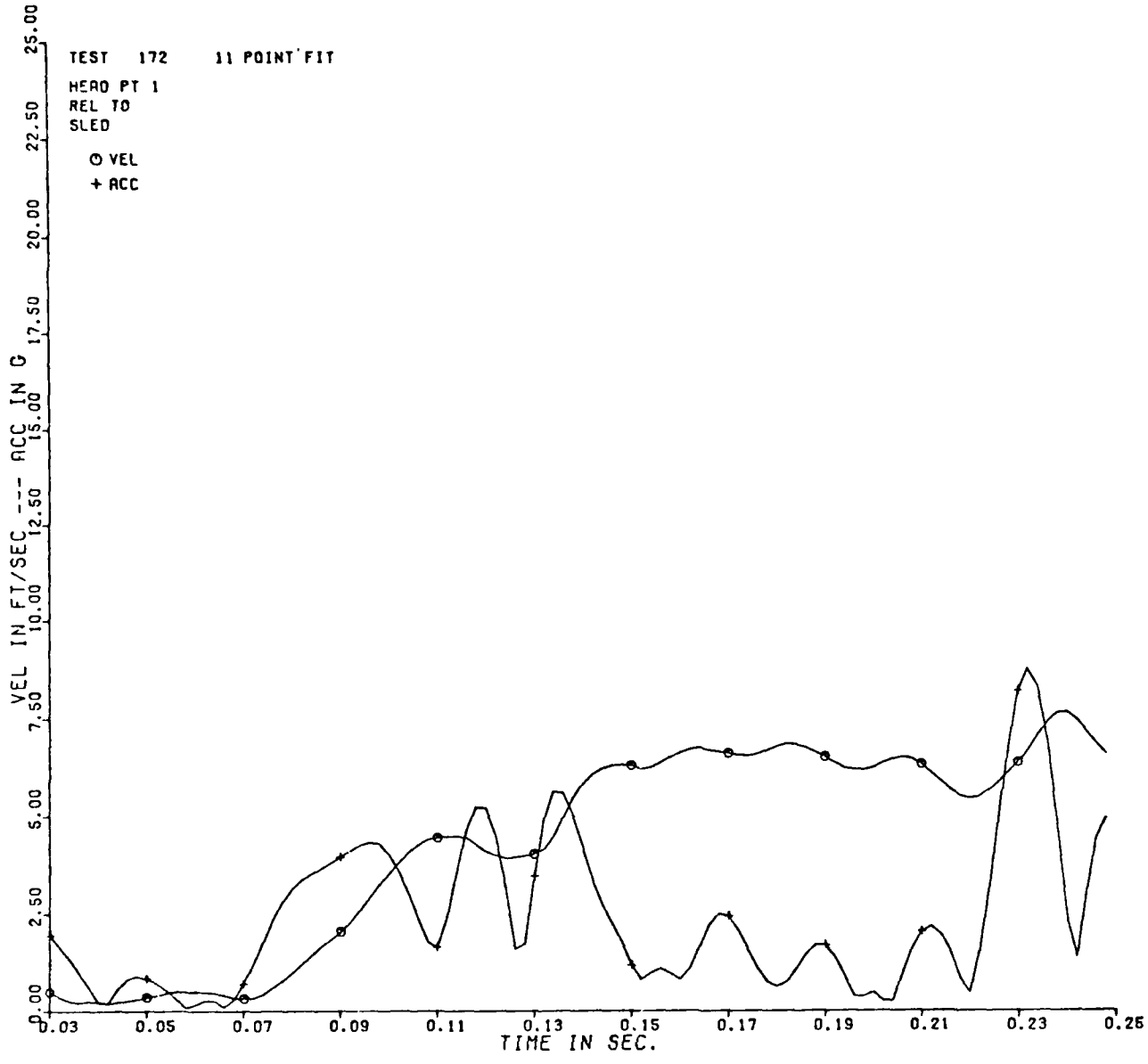
TEST 172 11 POINT FIT
HEAD PT 1
REL TO
SLED
⊙ VEL
+ ACC
VEL IN FT/SEC --- ACC IN G
0.00
2.50
5.00
7.50
10.00
12.50
15.00
17.50
20.00
22.50
25.00
0.03
0.05
0.07
0.09
0.11
0.13
0.15
0.17
0.19
0.21
0.23
0.25
TIME IN SEC.

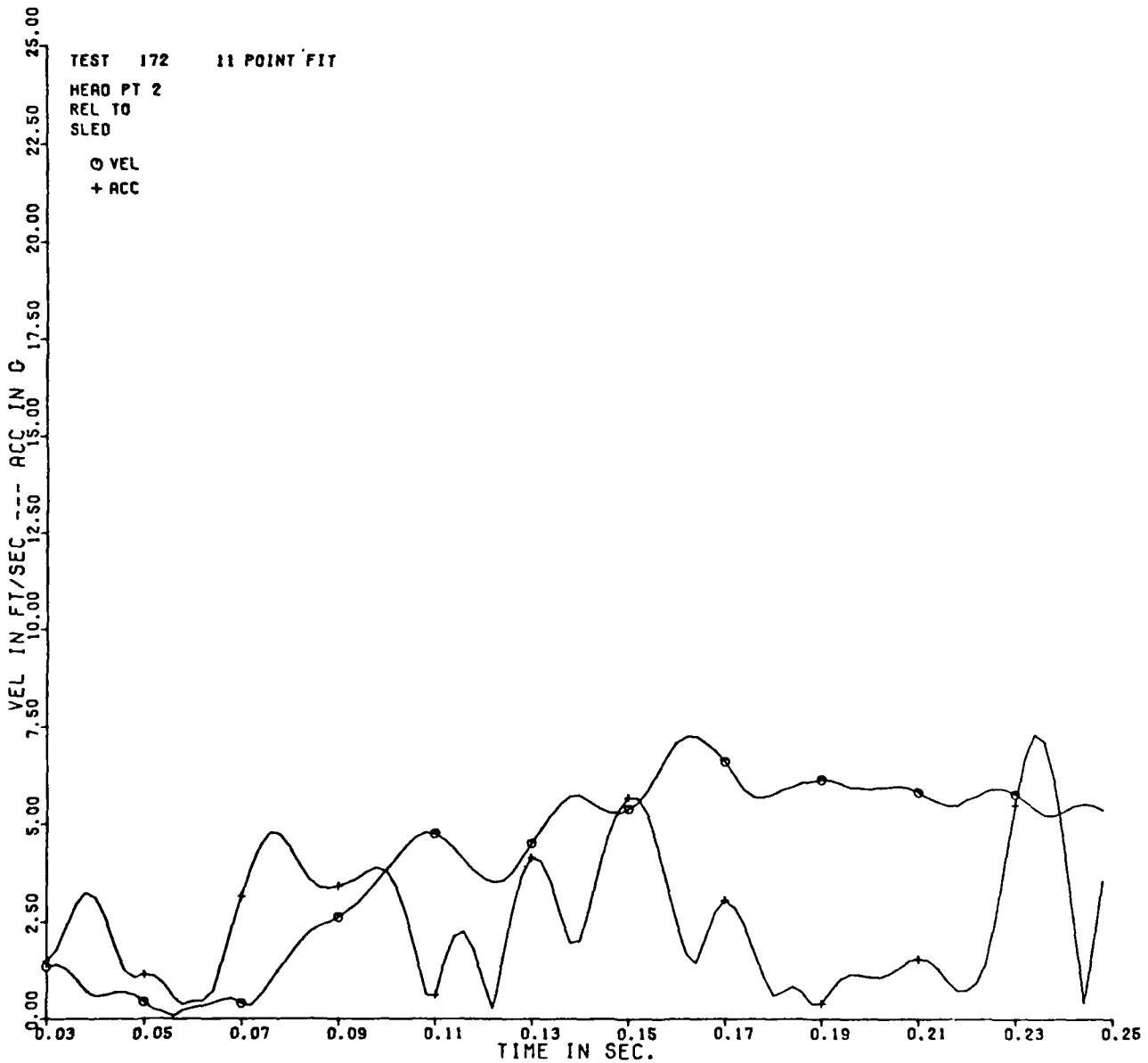
TEST 172 11 POINT FIT
HEAD PT 2
REL TO
SLED
⊙ VEL
+ ACC
VEL IN FT/SEC --- ACC IN G
0.00
2.50
5.00
7.50
10.00
12.50
15.00
17.50
20.00
22.50
25.00
0.03
0.05
0.07
0.09
0.11
0.13
0.15
0.17
0.19
0.21
0.23
0.25
TIME IN SEC.

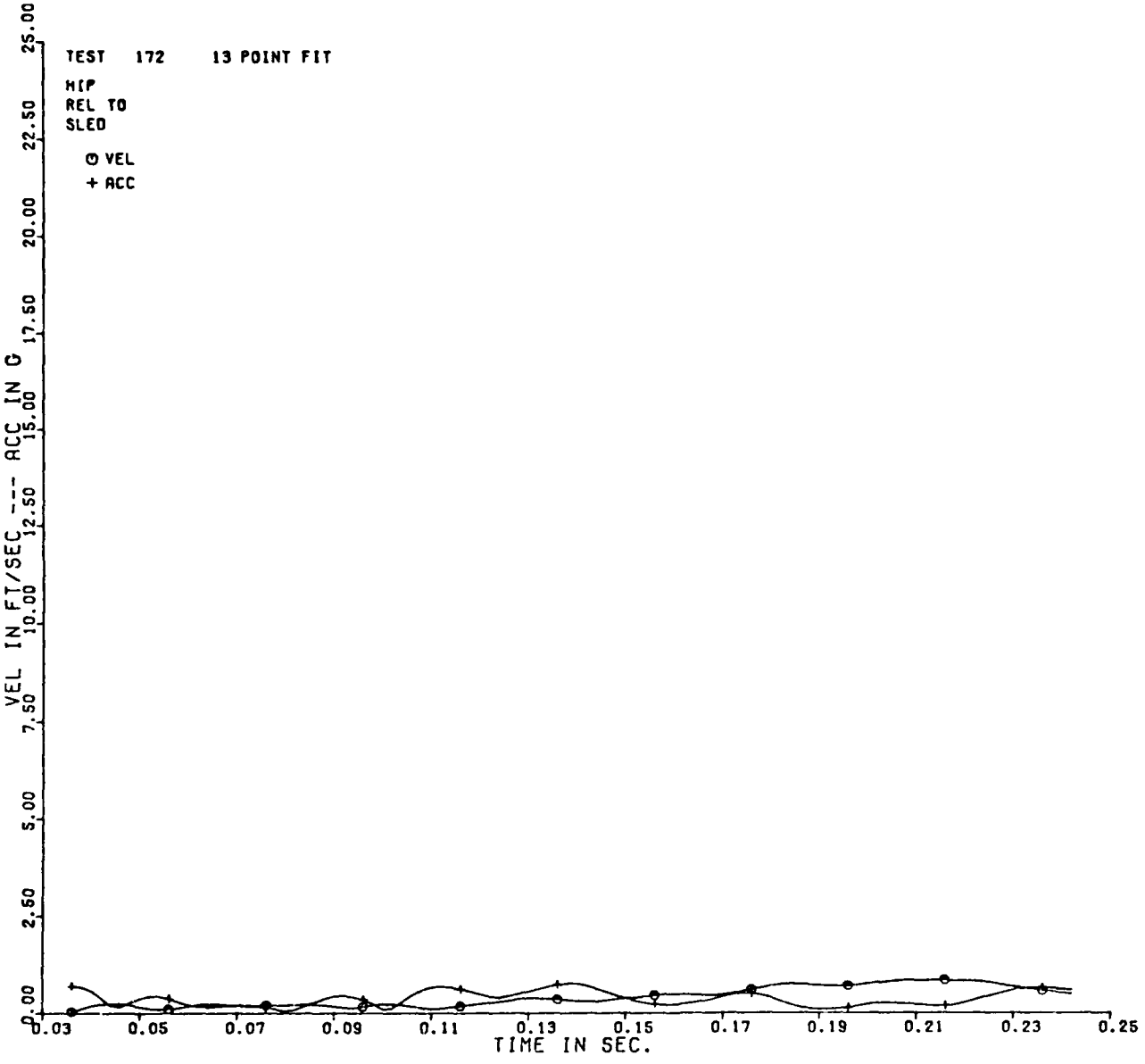
TEST 172 13 POINT FIT
HIP
REL TO
SLED
O VEL
+ ACC
VEL IN FT/SEC --- ACC IN G
0.00
2.50
5.00
7.50
10.00
12.50
15.00
17.50
20.00
22.50
25.00
0.03
0.05
0.07
0.09
0.11
0.13
0.15
0.17
0.19
0.21
0.23
0.25
TIME IN SEC.

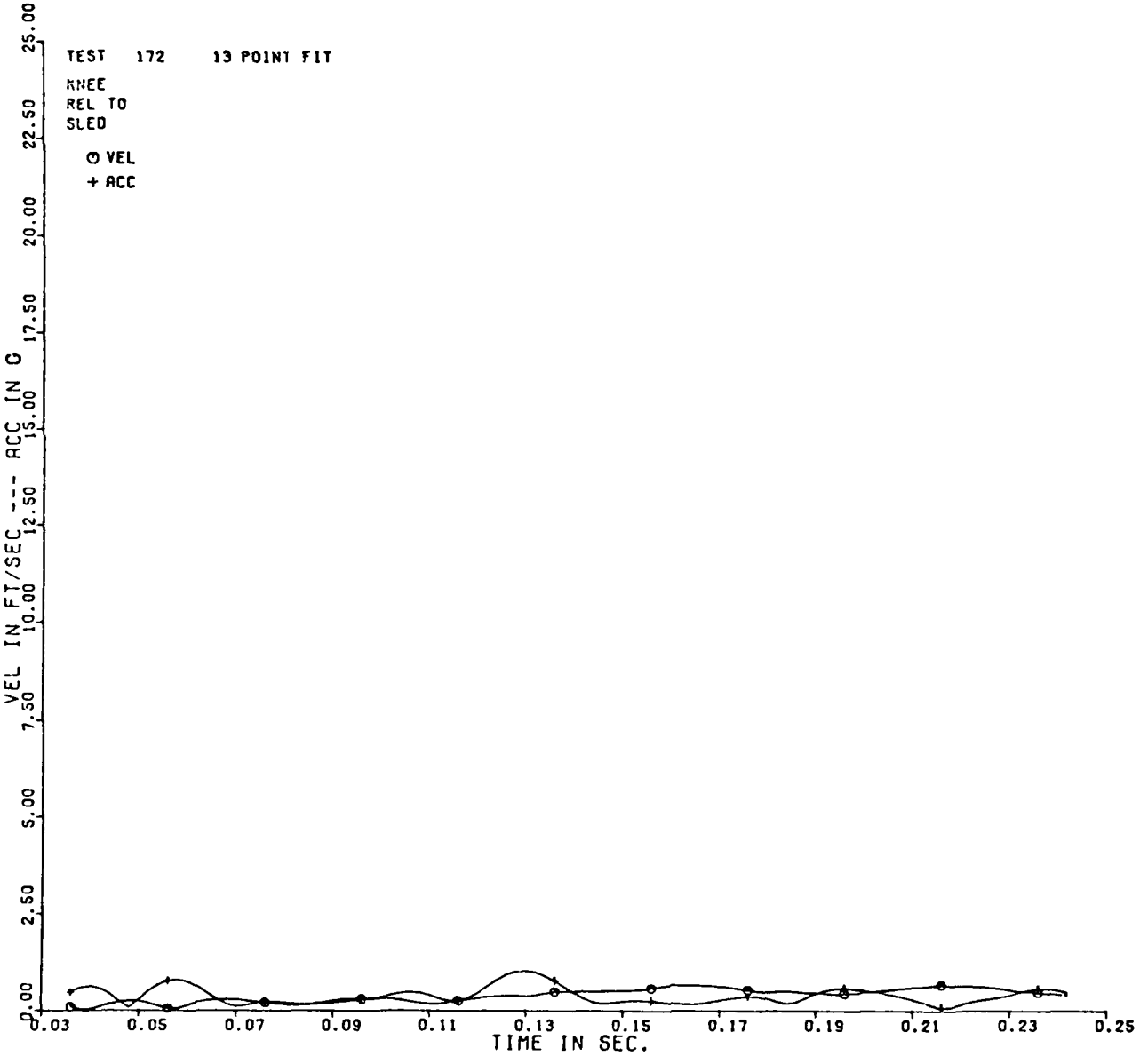
TEST 172 13 POINT FIT
KNEE
REL TO
SLED
⊙ VEL
+ ACC
VEL IN FT/SEC --- ACC IN G
0.00
2.50
5.00
7.50
10.00
12.50
15.00
17.50
20.00
22.50
25.00
0.03
0.05
0.07
0.09
0.11
0.13
0.15
0.17
0.19
0.21
0.23
0.25
TIME IN SEC.

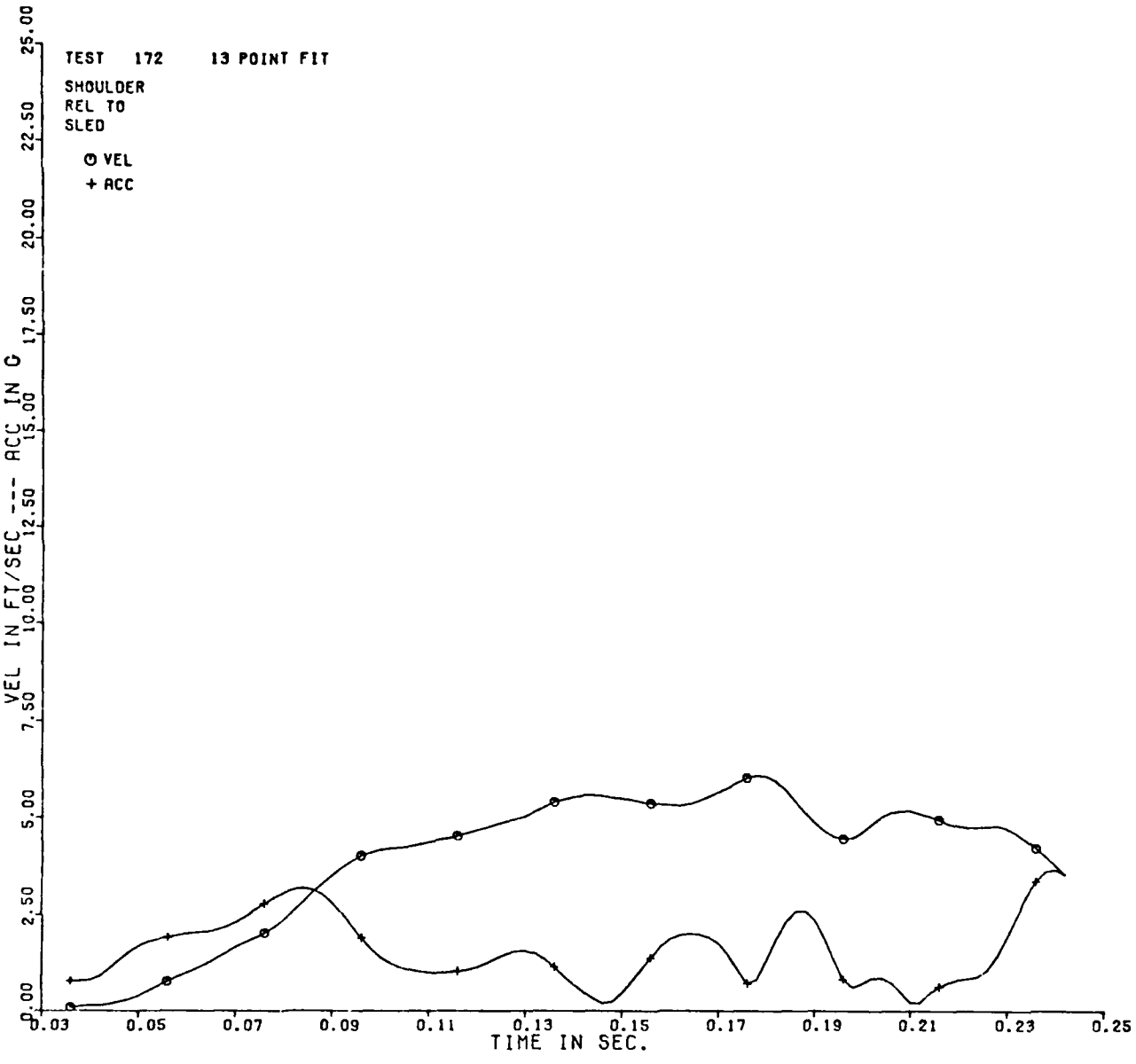
TEST 172 13 POINT FIT
SHOULDER
REL TO
SLED
⊙ VEL
+ ACC
VEL IN FT/SEC --- ACC IN G
0.00
2.50
5.00
7.50
10.00
12.50
15.00
17.50
20.00
22.50
25.00
0.03
0.05
0.07
0.09
0.11
0.13
0.15
0.17
0.19
0.21
0.23
0.25
TIME IN SEC.

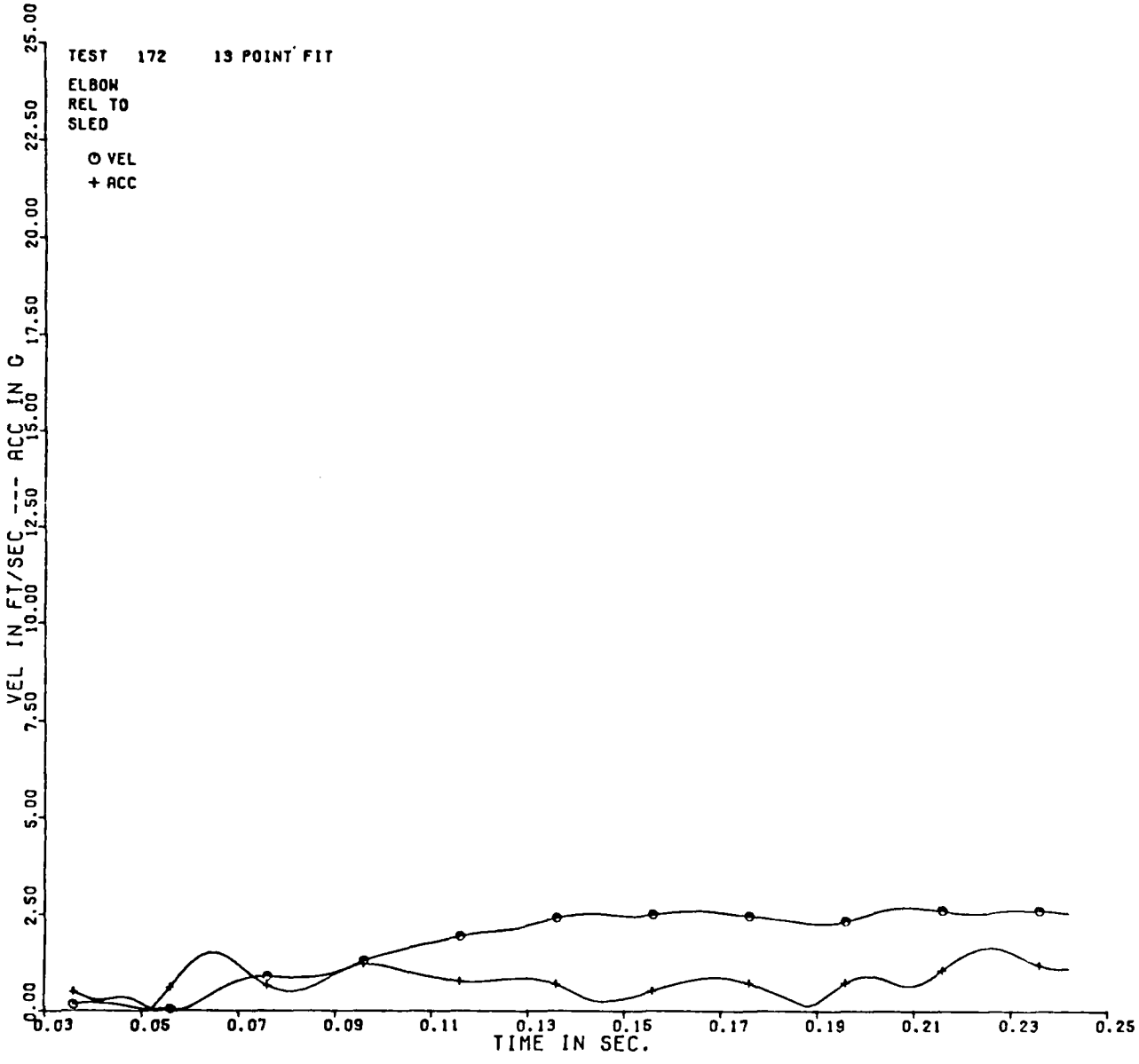
TEST 172 13 POINT FIT
ELBOW
REL TO
SLED
⊙ VEL
+ ACC
VEL IN FT/SEC --- ACC IN G
0.00
2.50
5.00
7.50
10.00
12.50
15.00
17.50
20.00
22.50
25.00
0.03
0.05
0.07
0.09
0.11
0.13
0.15
0.17
0.19
0.21
0.23
0.25
TIME IN SEC.

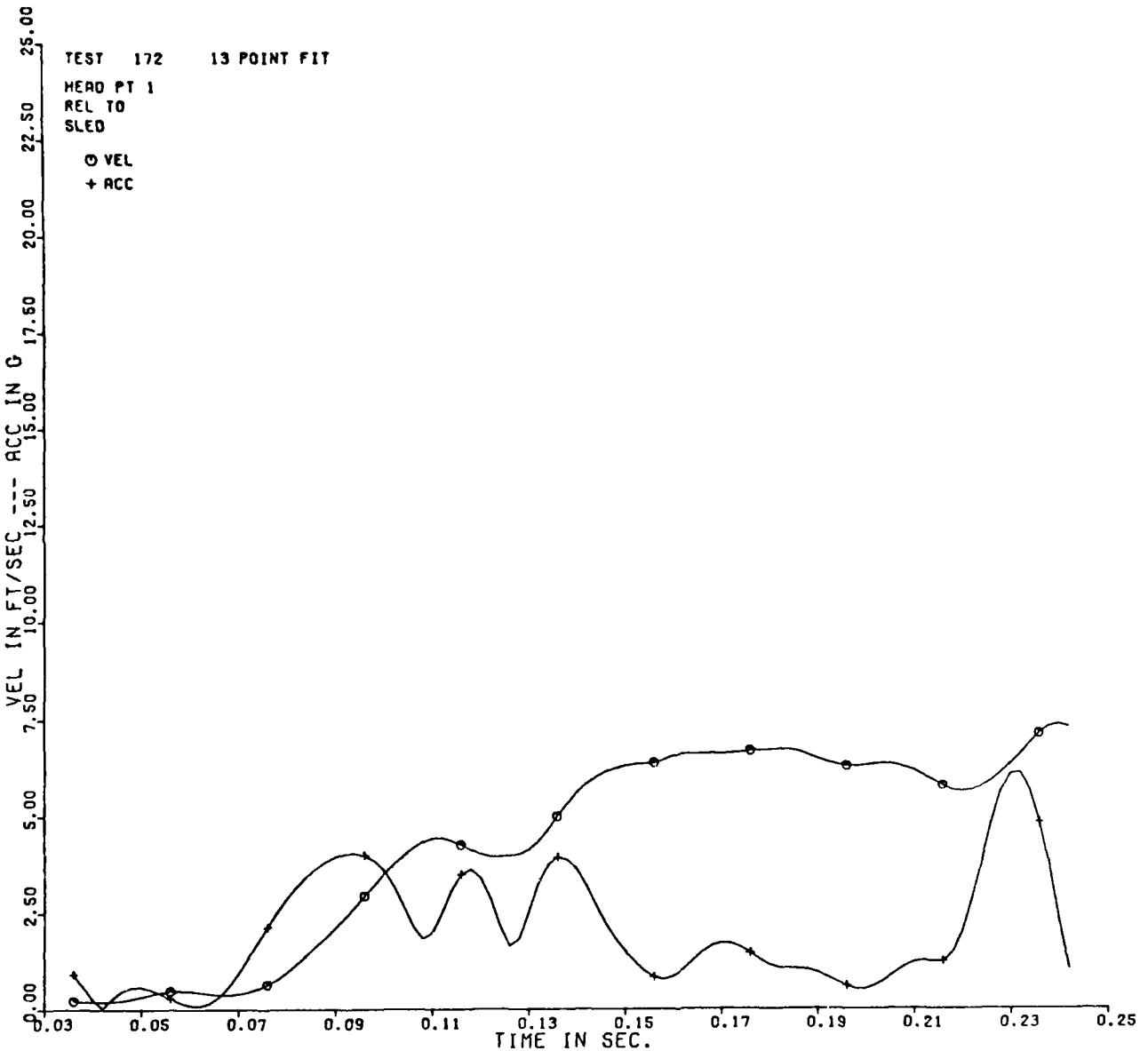
TEST 172 13 POINT FIT
HEAD PT 1
REL TO
SLED
⊙ VEL
+ ACC
VEL IN FT/SEC --- ACC IN G
0.00
2.50
5.00
7.50
10.00
12.50
15.00
17.50
20.00
22.50
25.00
0.03
0.05
0.07
0.09
0.11
0.13
0.15
0.17
0.19
0.21
0.23
0.25
TIME IN SEC.

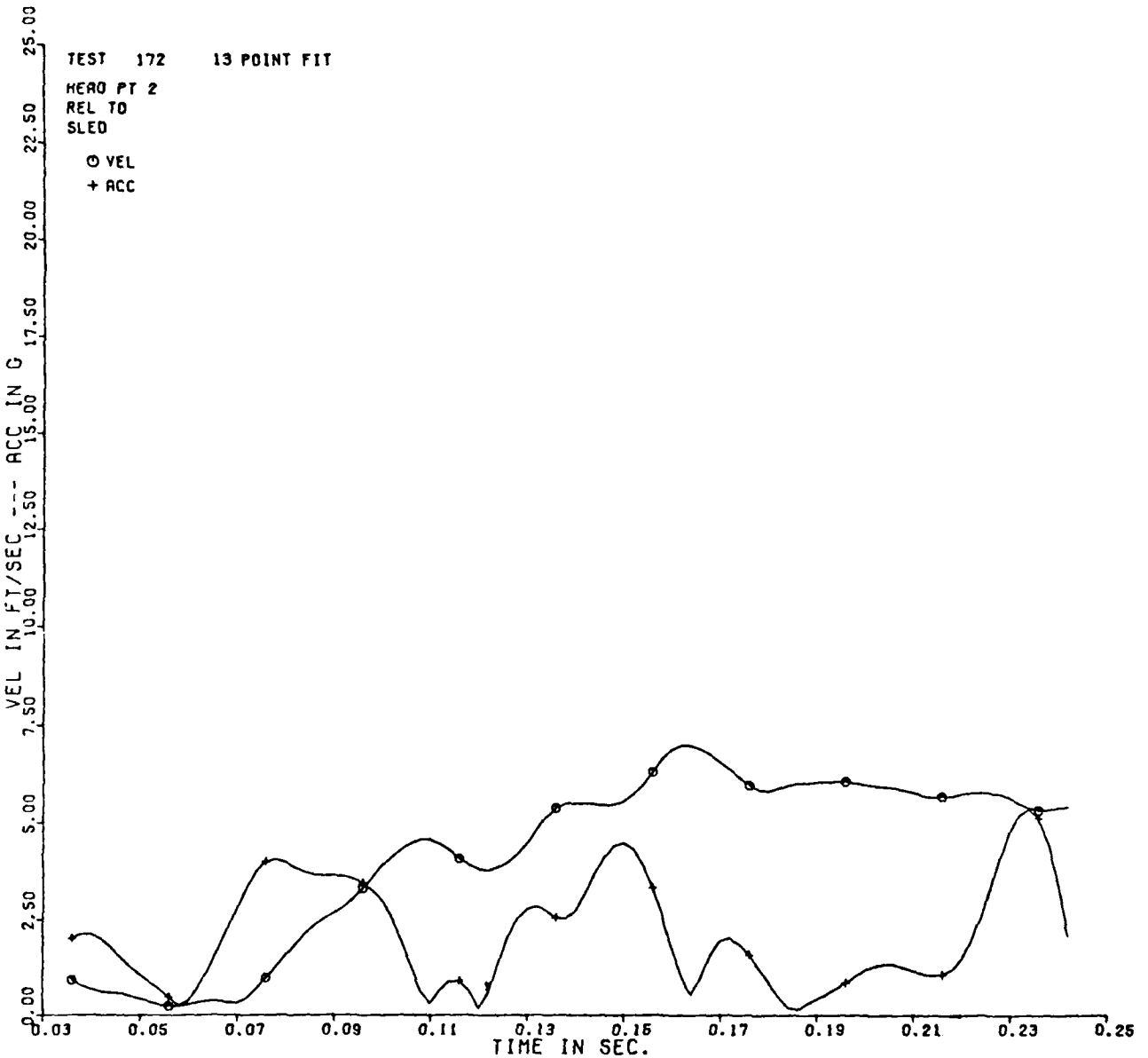
TEST 172 13 POINT FIT
HEAD PT 2
REL TO
SLED
⊙ VEL
+ ACC
VEL IN FT/SEC --- ACC IN G
0.00
2.50
5.00
7.50
10.00
12.50
15.00
17.50
20.00
22.50
25.00
0.03
0.05
0.07
0.09
0.11
0.13
0.15
0.17
0.19
0.21
0.23
0.25
TIME IN SEC.

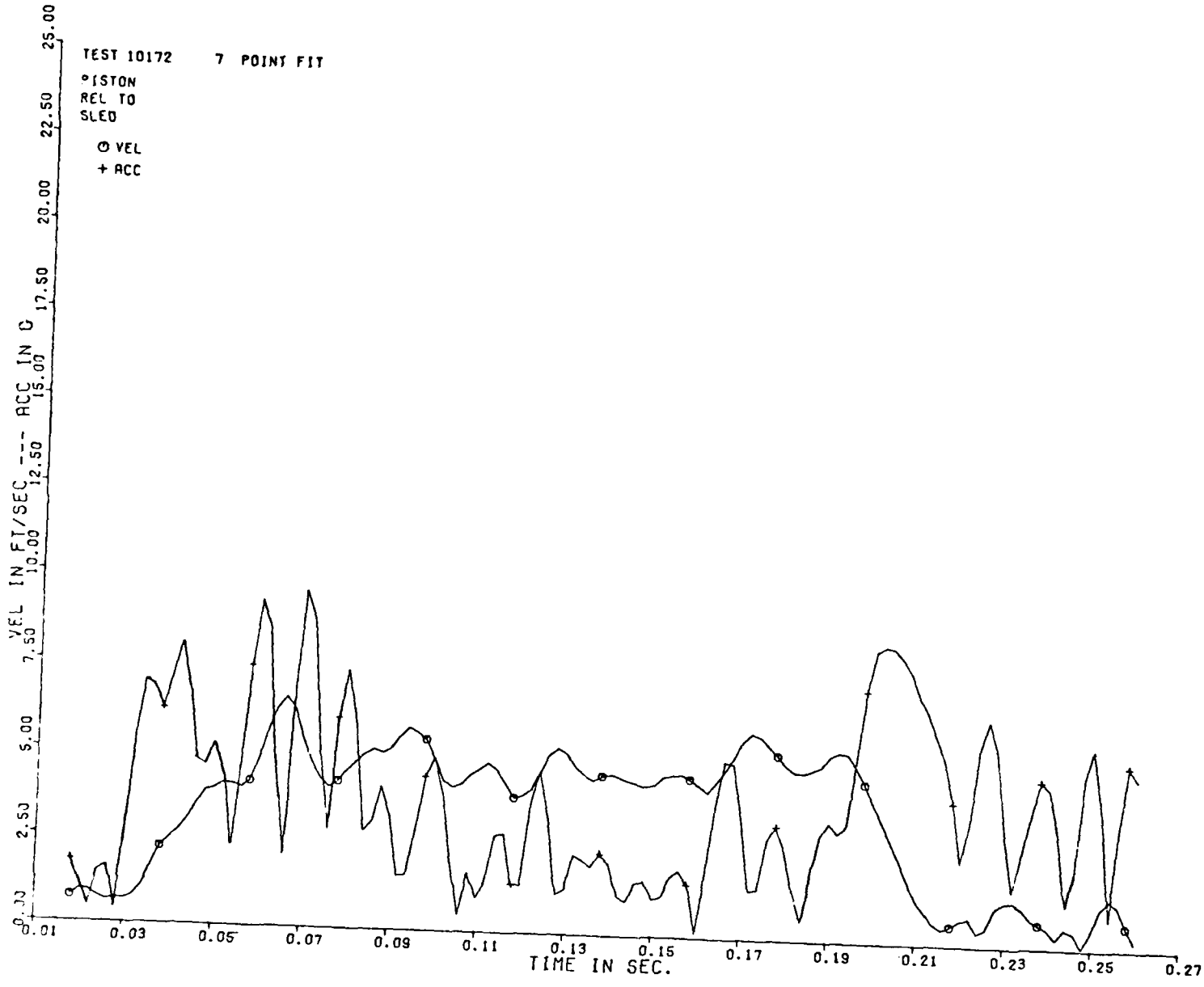
TEST 10172 7 POINT FIT
PISTON
REL TO
SLED
⊙ VEL
+ ACC
VEL IN FT/SEC --- ACC IN G
0.00
2.50
5.00
7.50
10.00
12.50
15.00
17.50
20.00
22.50
25.00
0.01
0.03
0.05
0.07
0.09
0.11
0.13
0.15
0.17
0.19
0.21
0.23
0.25
0.27
TIME IN SEC.

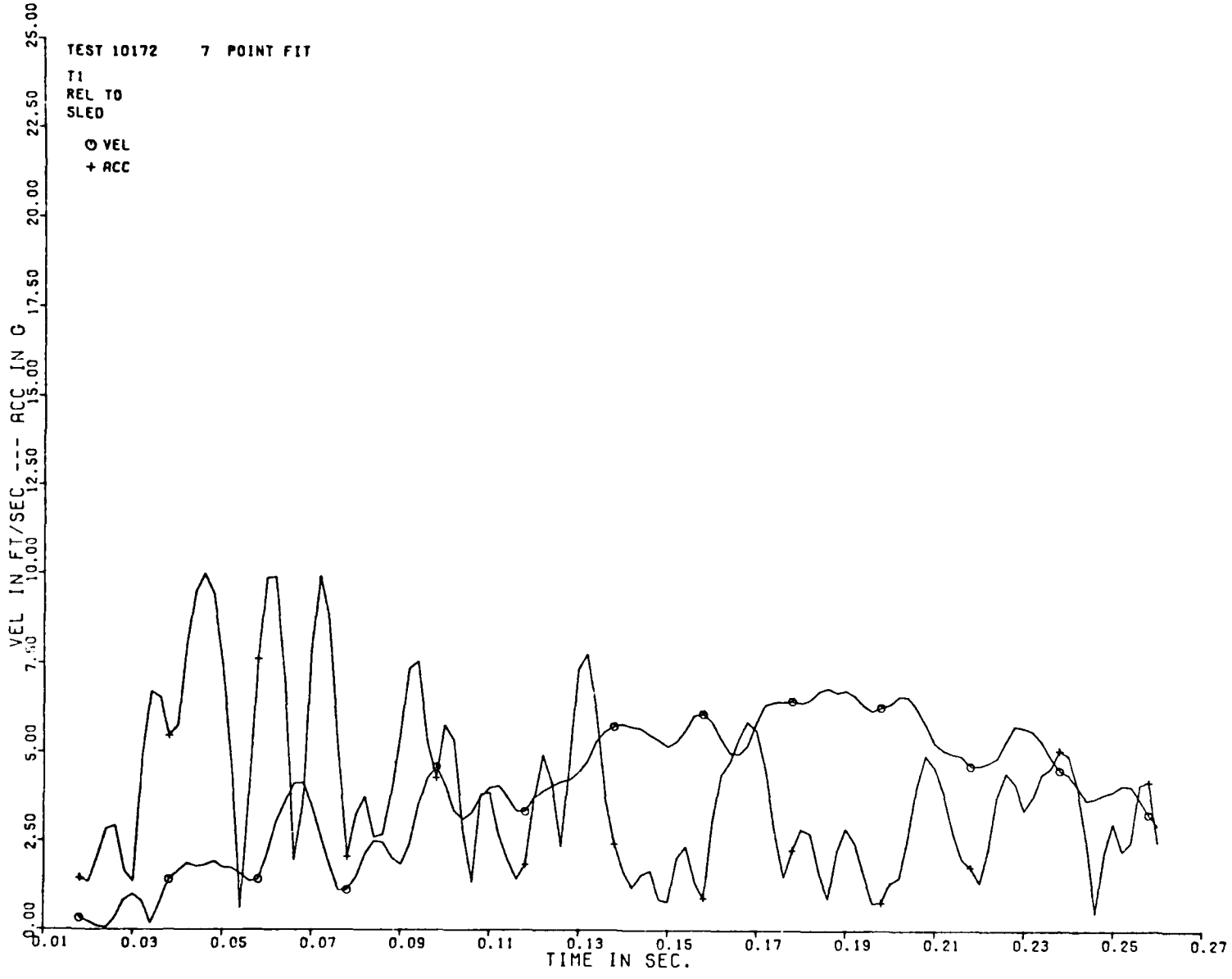
TEST 10172 7 POINT FIT
T1
REL TO
SLED
⊙ VEL
+ ACC
VEL IN FT/SEC --- ACC IN G
0.00
2.50
5.00
7.50
10.00
12.50
15.00
17.50
20.00
22.50
25.00
0.01
0.03
0.05
0.07
0.09
0.11
0.13
0.15
0.17
0.19
0.21
0.23
0.25
0.27
TIME IN SEC.

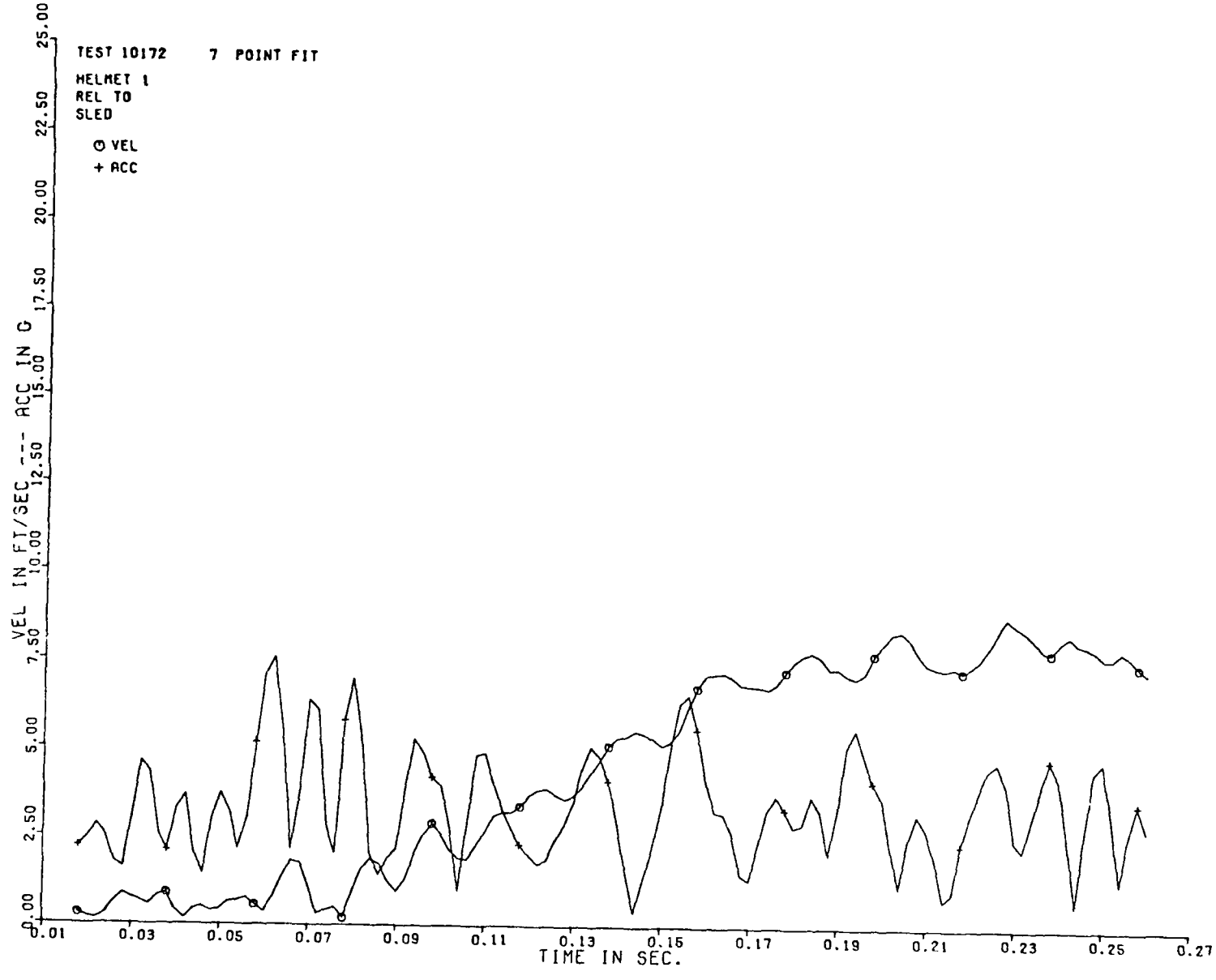
TEST 10172 7 POINT FIT
HELMET 1
REL TO
SLED
⊙ VEL
+ ACC
VEL IN FT/SEC --- ACC IN G
0.00
2.50
5.00
7.50
10.00
12.50
15.00
17.50
20.00
22.50
25.00
0.01
0.03
0.05
0.07
0.09
0.11
0.13
0.15
0.17
0.19
0.21
0.23
0.25
0.27
TIME IN SEC.

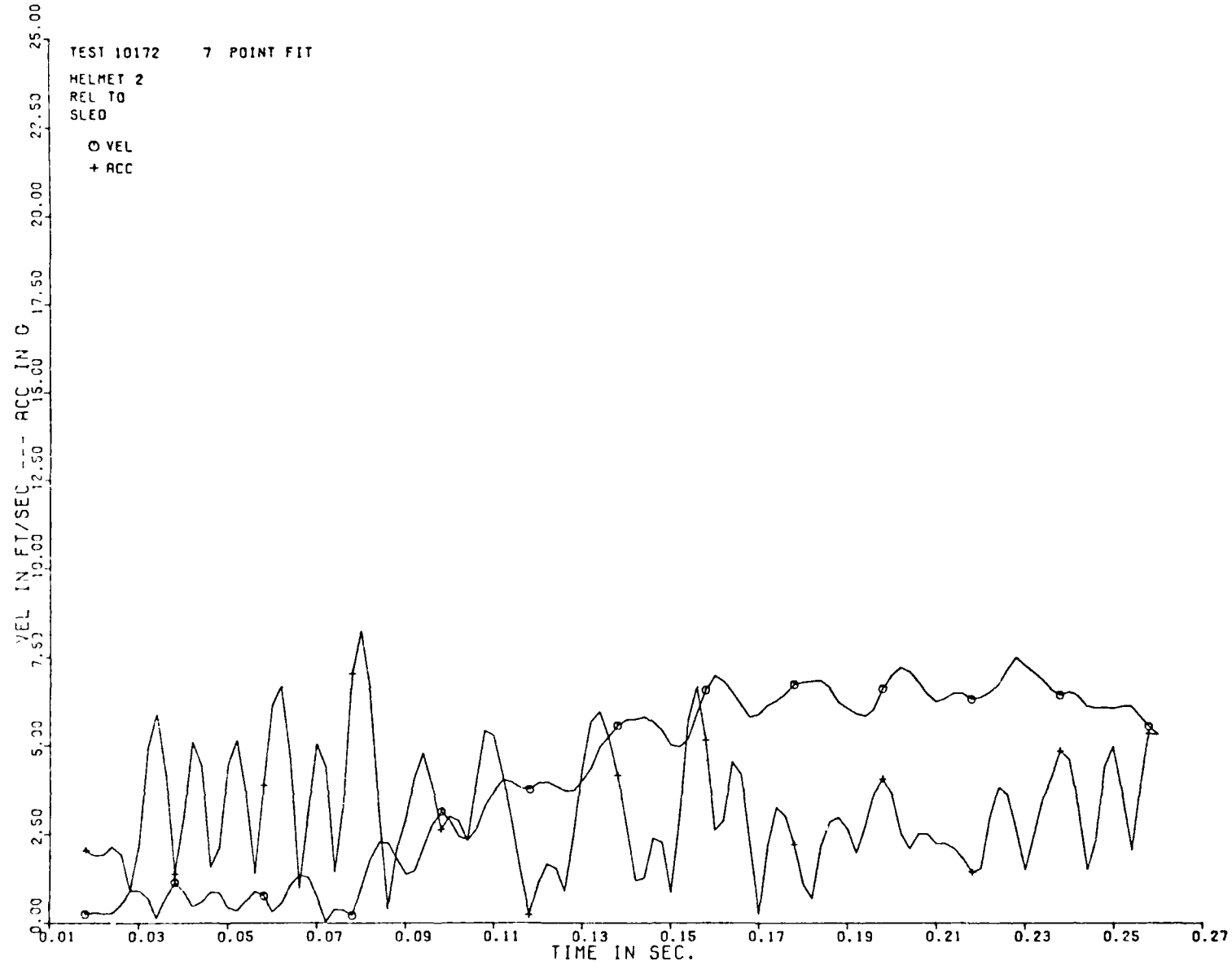
TEST 10172 7 POINT FIT
HELMET 2
REL TO
SLED
VEL
ACC
VEL IN FT/SEC --- ACC IN G
0.00
2.50
5.00
7.50
10.00
12.50
15.00
17.50
20.00
22.50
25.00
0.01
0.03
0.05
0.07
0.09
0.11
0.13
0.15
0.17
0.19
0.21
0.23
0.25
0.27
TIME IN SEC.

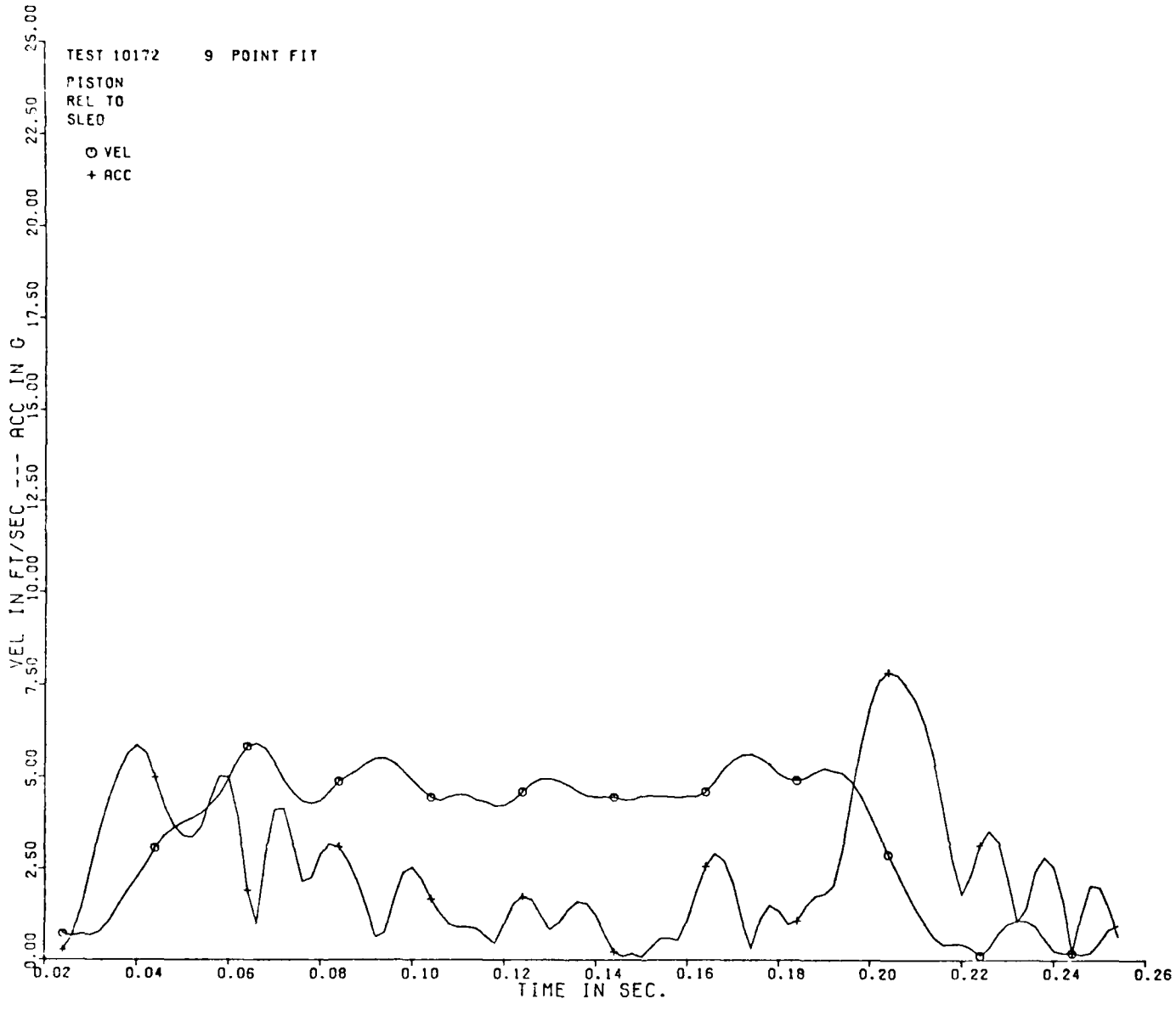
TEST 10172 9 POINT FIT
PISTON
REL TO
SLED
⊙ VEL
+ ACC
VEL IN FT/SEC --- ACC IN G
0.00
2.50
5.00
7.50
10.00
12.50
15.00
17.50
20.00
22.50
25.00
0.02
0.04
0.06
0.08
0.10
0.12
0.14
0.16
0.18
0.20
0.22
0.24
0.26
TIME IN SEC.

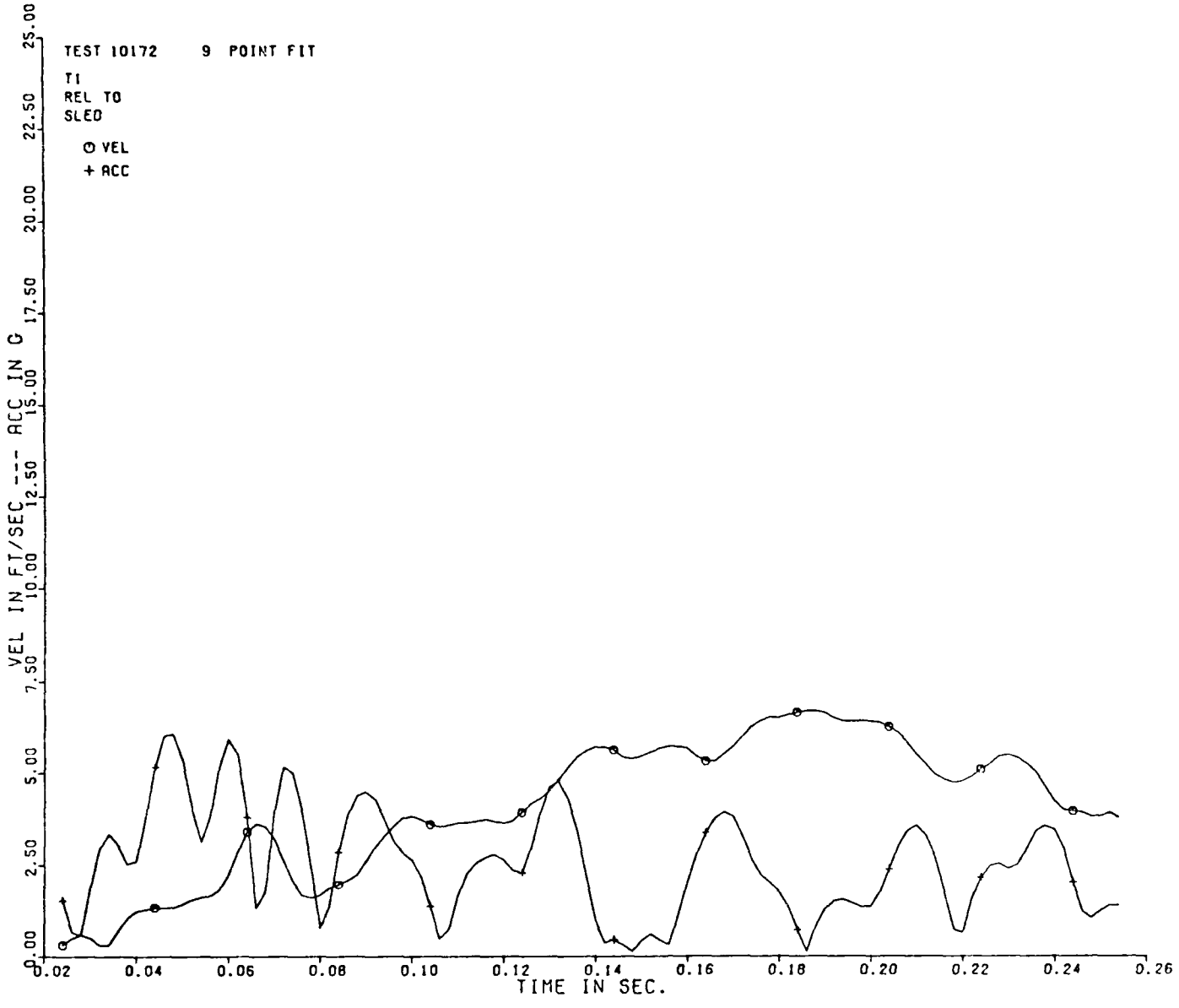
TEST 10172 9 POINT FIT
T1
REL TO
SLED
⊙ VEL
+ ACC
VEL IN FT/SEC --- ACC IN G
0.00
2.50
5.00
7.50
10.00
12.50
15.00
17.50
20.00
22.50
25.00
0.02
0.04
0.06
0.08
0.10
0.12
0.14
0.16
0.18
0.20
0.22
0.24
0.26
TIME IN SEC.

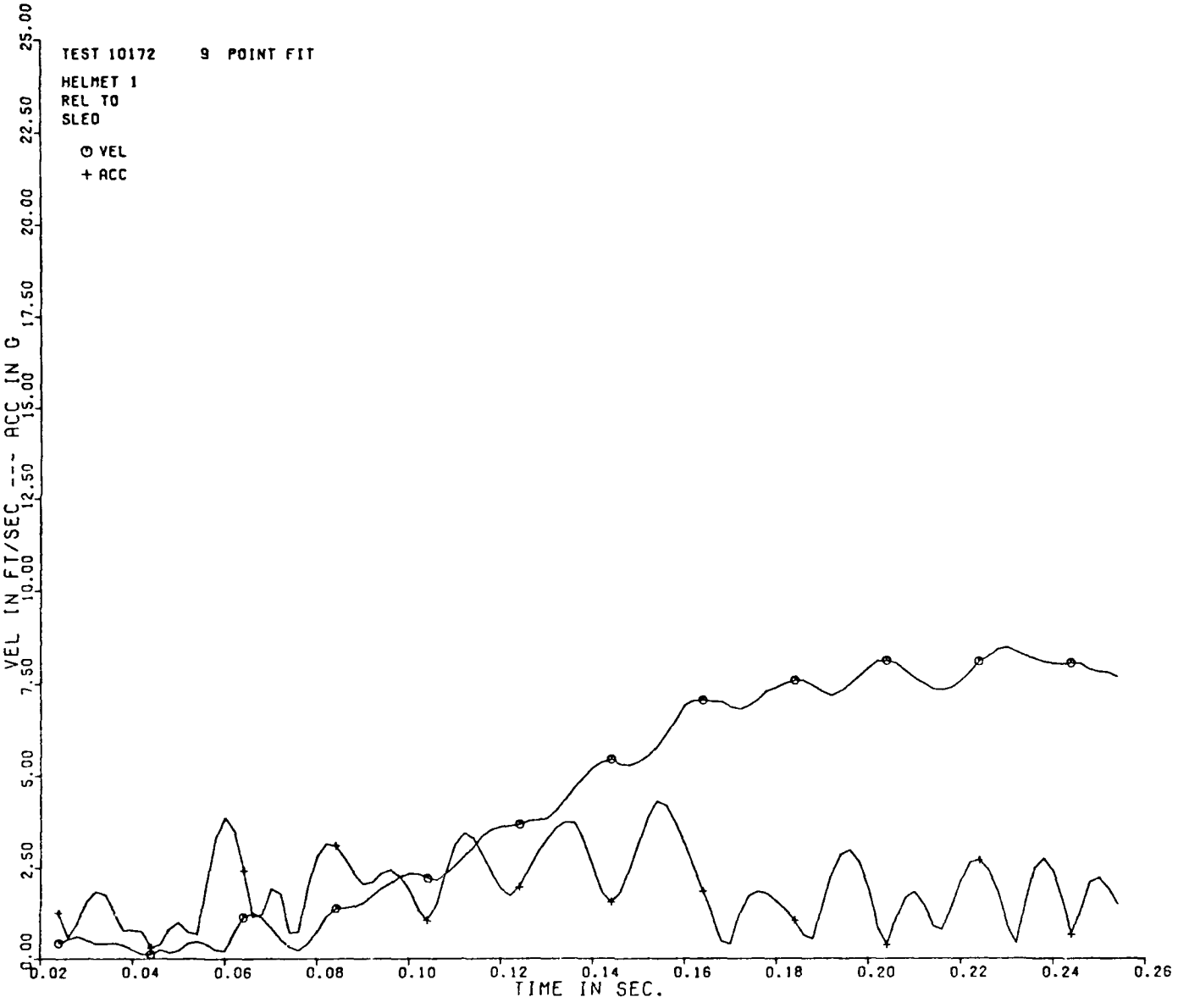
TEST 10172 9 POINT FIT
HELMET 1
REL TO
SLED
⊙ VEL
+ ACC
VEL IN FT/SEC --- ACC IN G
0.00
2.50
5.00
7.50
10.00
12.50
15.00
17.50
20.00
22.50
25.00
0.02
0.04
0.06
0.08
0.10
0.12
0.14
0.16
0.18
0.20
0.22
0.24
0.26
TIME IN SEC.

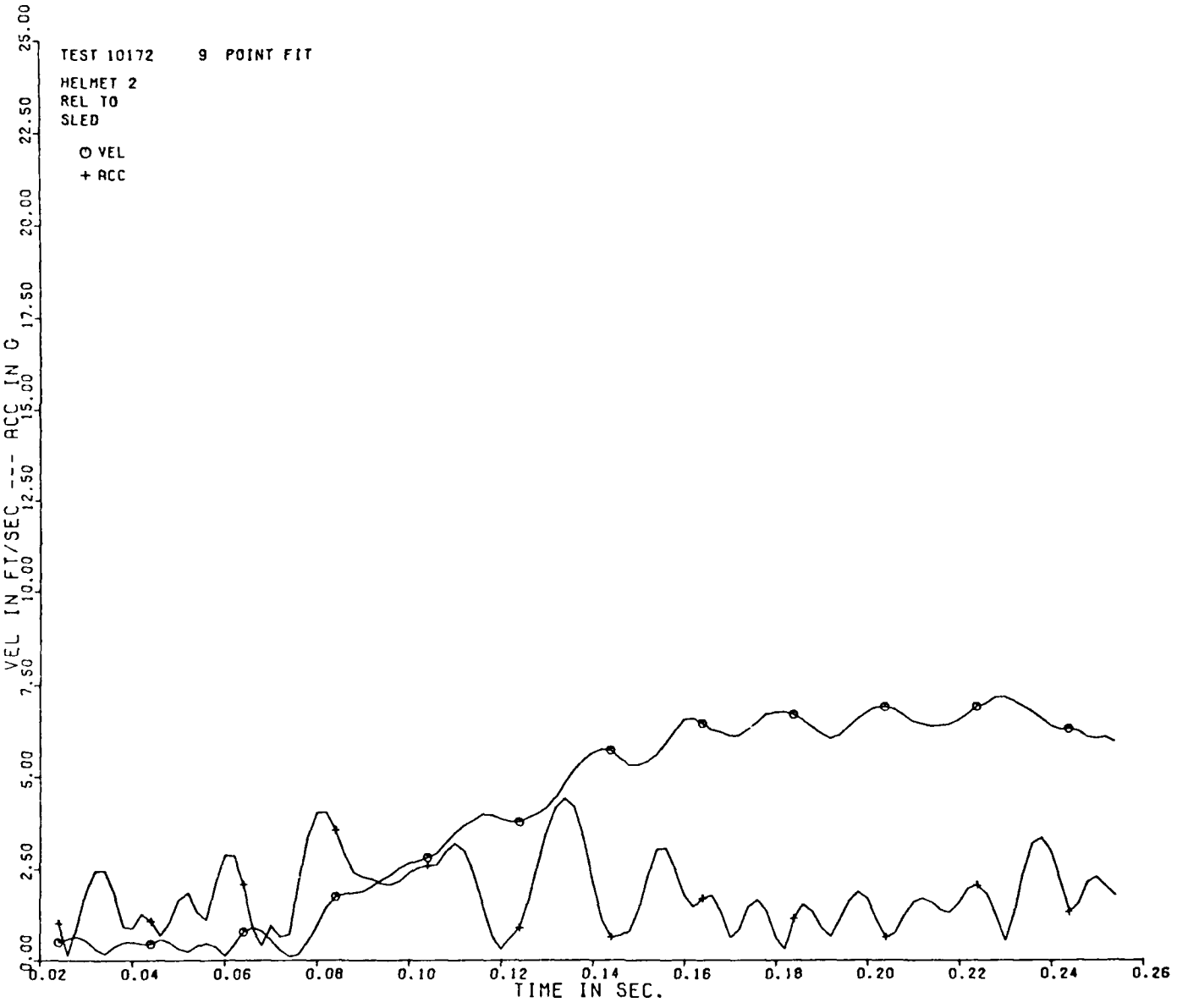
TEST 10172 9 POINT FIT
HELMET 2
REL TO
SLED
O VEL
+ ACC
VEL IN FT/SEC --- ACC IN G
0.00
2.50
5.00
7.50
10.00
12.50
15.00
17.50
20.00
22.50
25.00
0.02
0.04
0.06
0.08
0.10
0.12
0.14
0.16
0.18
0.20
0.22
0.24
0.26
TIME IN SEC.

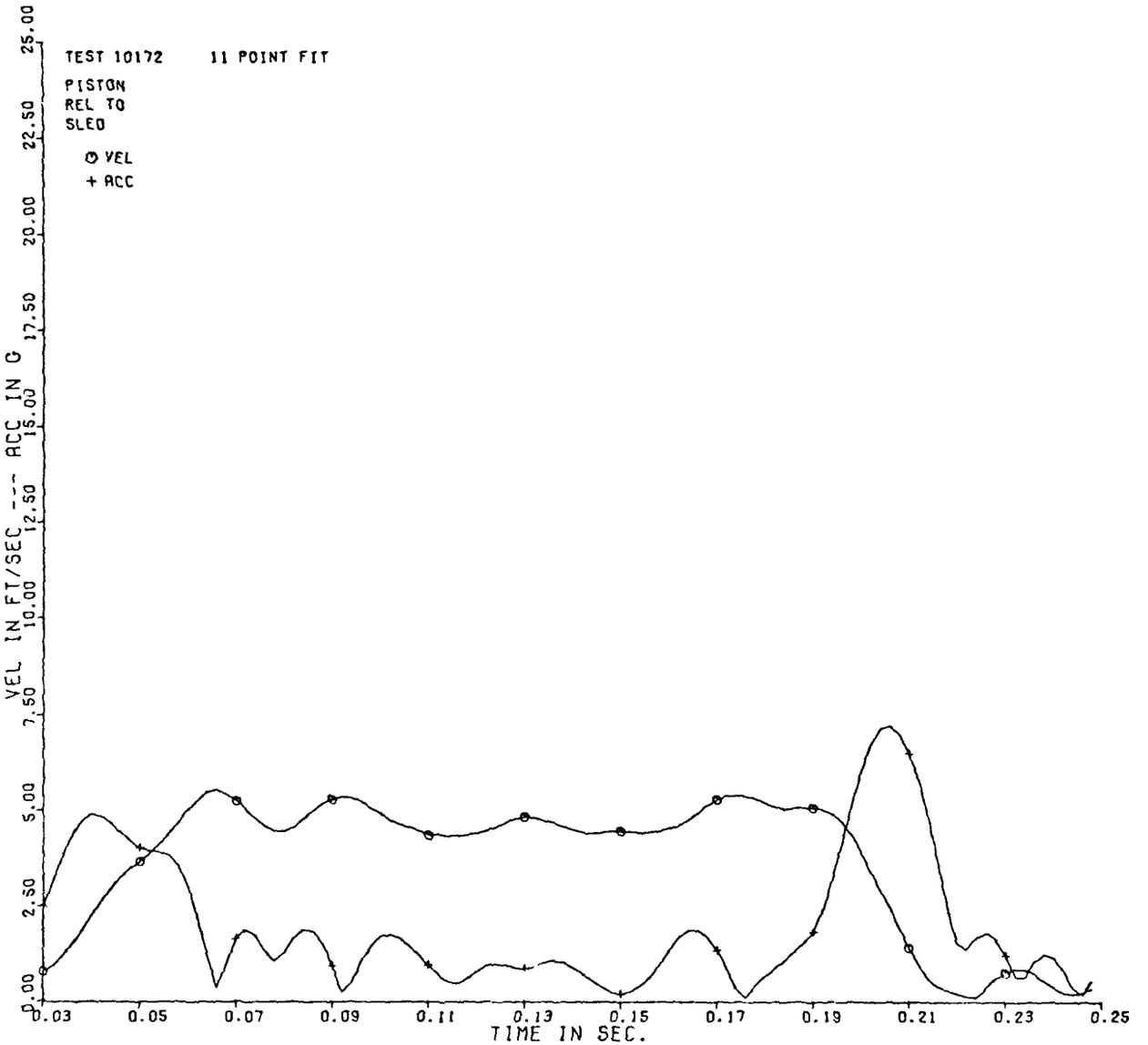
TEST 10172 11 POINT FIT
PISTON
REL TO
SLED
⊙ VEL
+ ACC
VEL IN FT/SEC --- ACC IN G
0.00
2.50
5.00
7.50
10.00
12.50
15.00
17.50
20.00
22.50
25.00
0.03
0.05
0.07
0.09
0.11
0.13
0.15
0.17
0.19
0.21
0.23
0.25
TIME IN SEC.

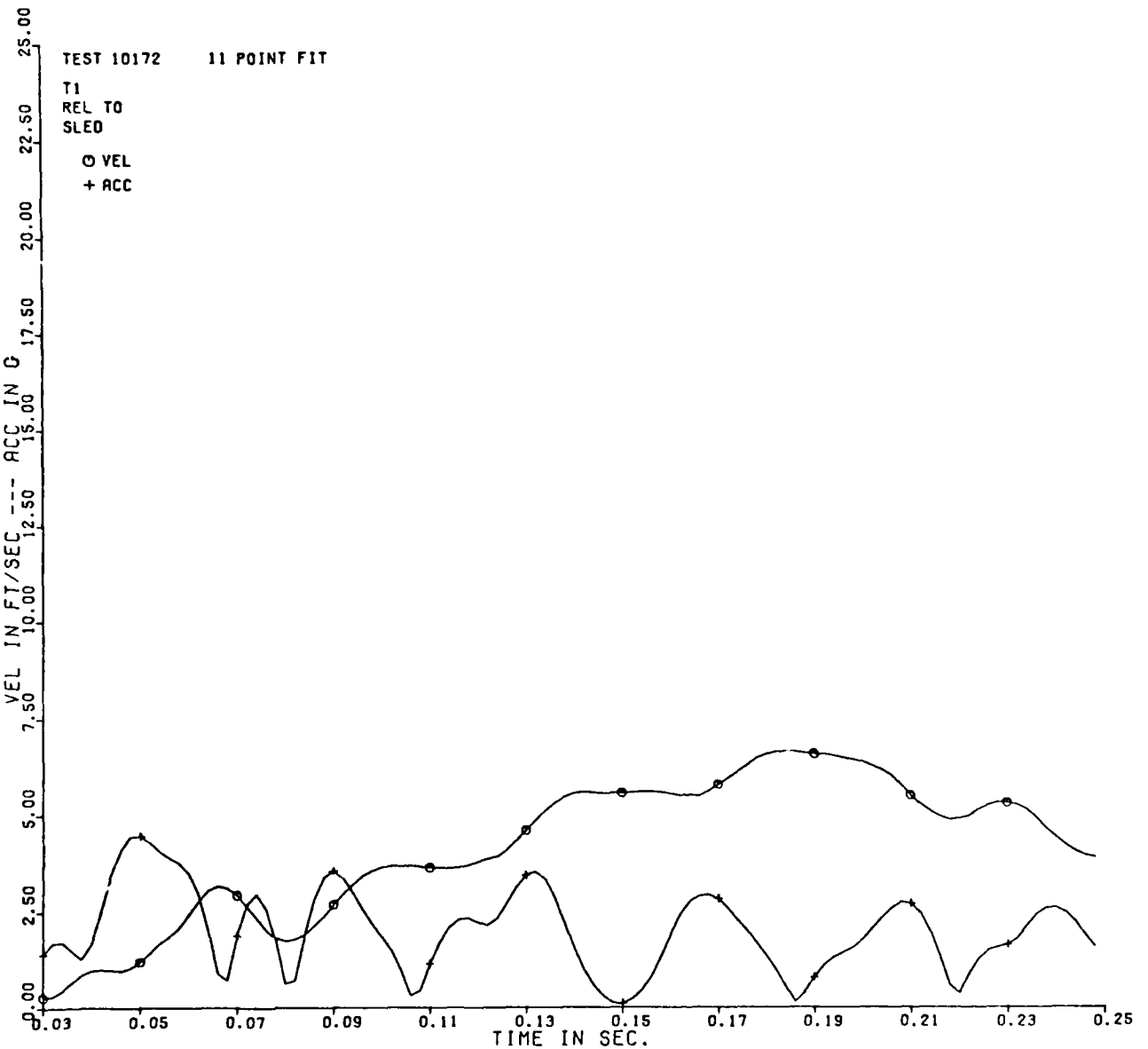
TEST 10172 11 POINT FIT
T1
REL TO
SLED
⊙ VEL
+ ACC
VEL IN FT/SEC --- ACC IN G
0.00
2.50
5.00
7.50
10.00
12.50
15.00
17.50
20.00
22.50
25.00
0.03
0.05
0.07
0.09
0.11
0.13
0.15
0.17
0.19
0.21
0.23
0.25
TIME IN SEC.

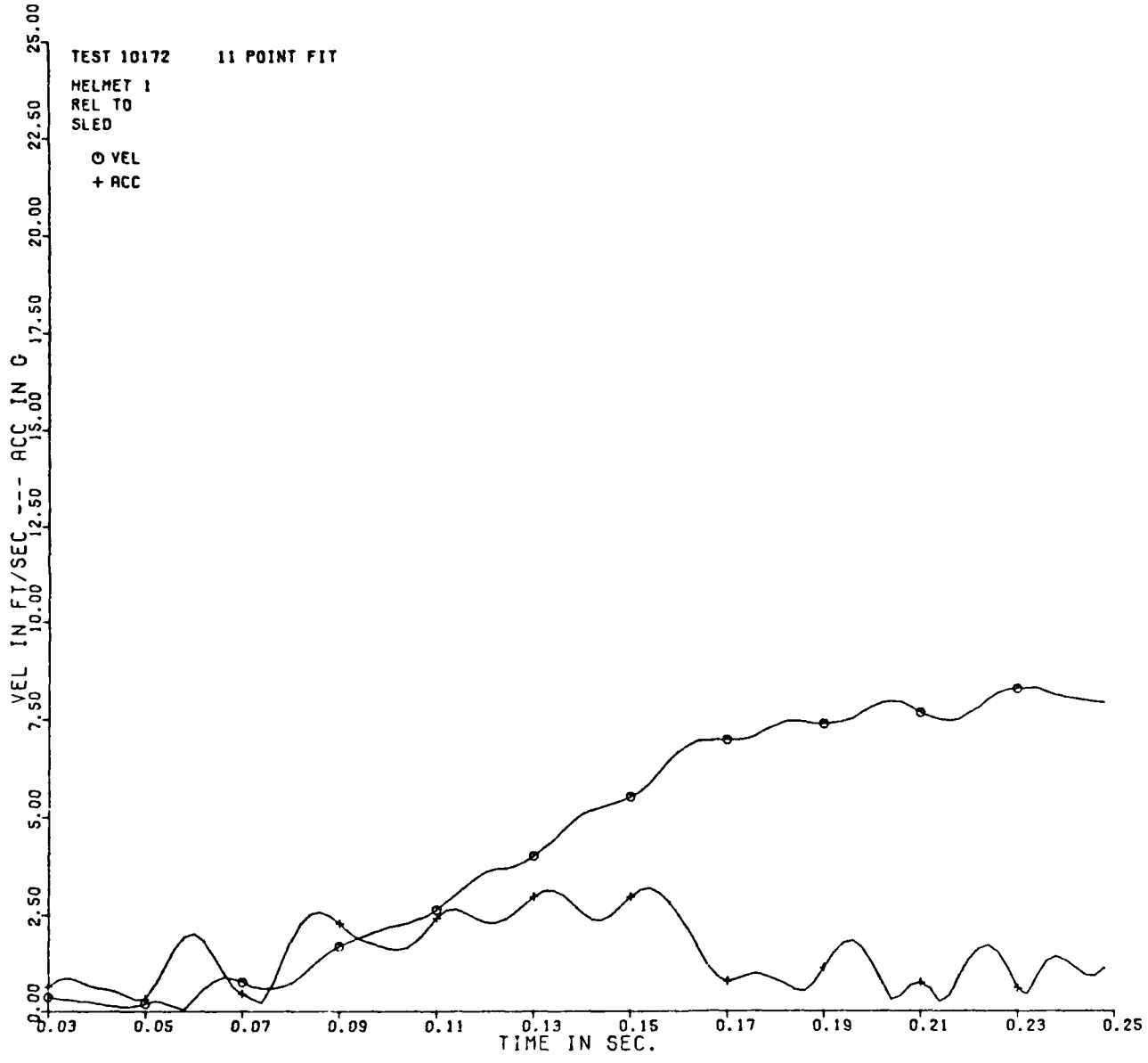
TEST 10172 11 POINT FIT
HELMET 1
REL TO
SLED
⊙ VEL
+ ACC
VEL IN FT/SEC --- ACC IN G
0.00
2.50
5.00
7.50
10.00
12.50
15.00
17.50
20.00
22.50
25.00
0.03
0.05
0.07
0.09
0.11
0.13
0.15
0.17
0.19
0.21
0.23
0.25
TIME IN SEC.

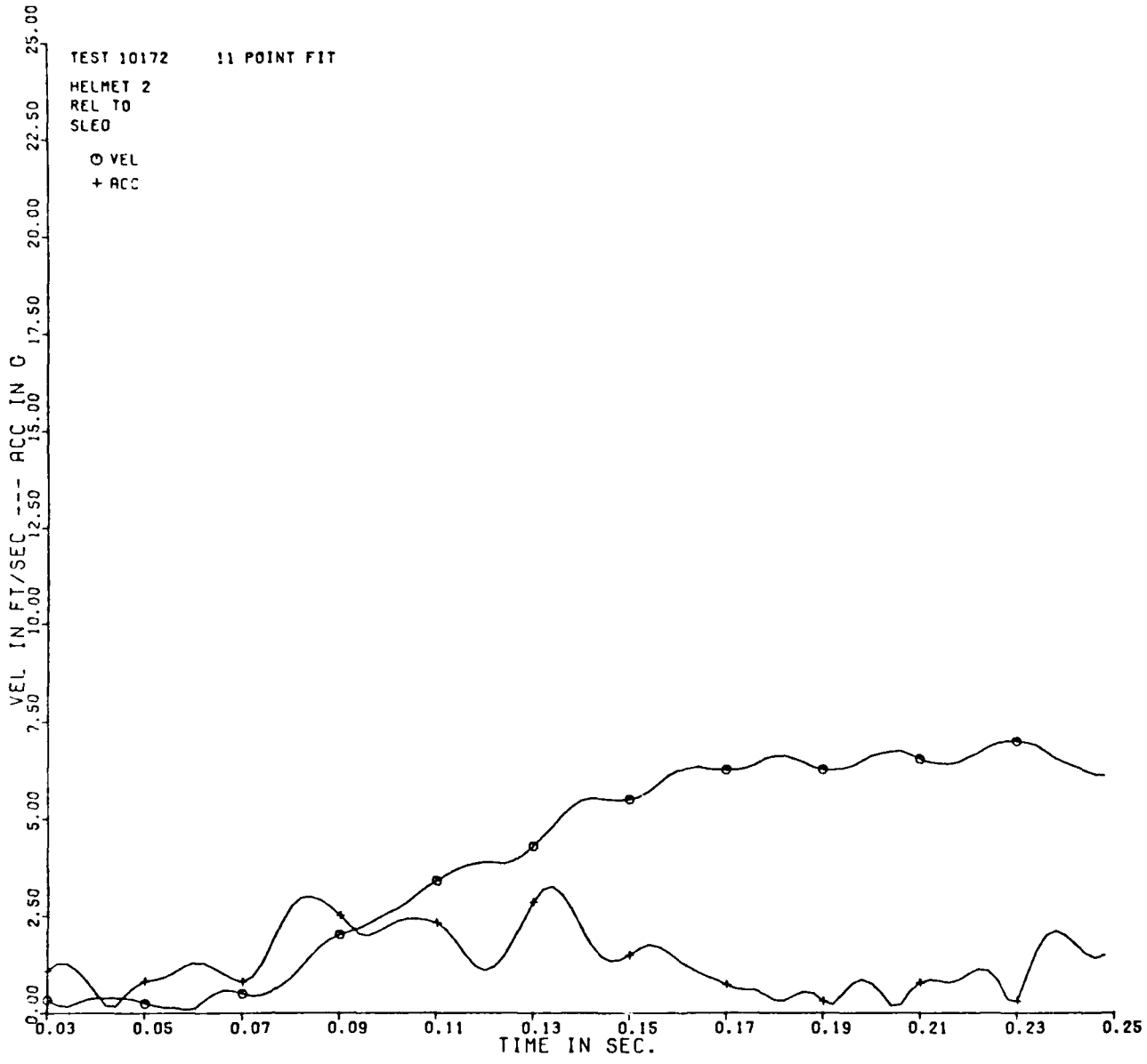
TEST 10172 11 POINT FIT
HELMET 2
REL TO
SLED
⊙ VEL
+ ACC
VEL IN FT/SEC --- ACC IN G
0.00
2.50
5.00
7.50
10.00
12.50
15.00
17.50
20.00
22.50
25.00
0.03
0.05
0.07
0.09
0.11
0.13
0.15
0.17
0.19
0.21
0.23
0.25
TIME IN SEC.

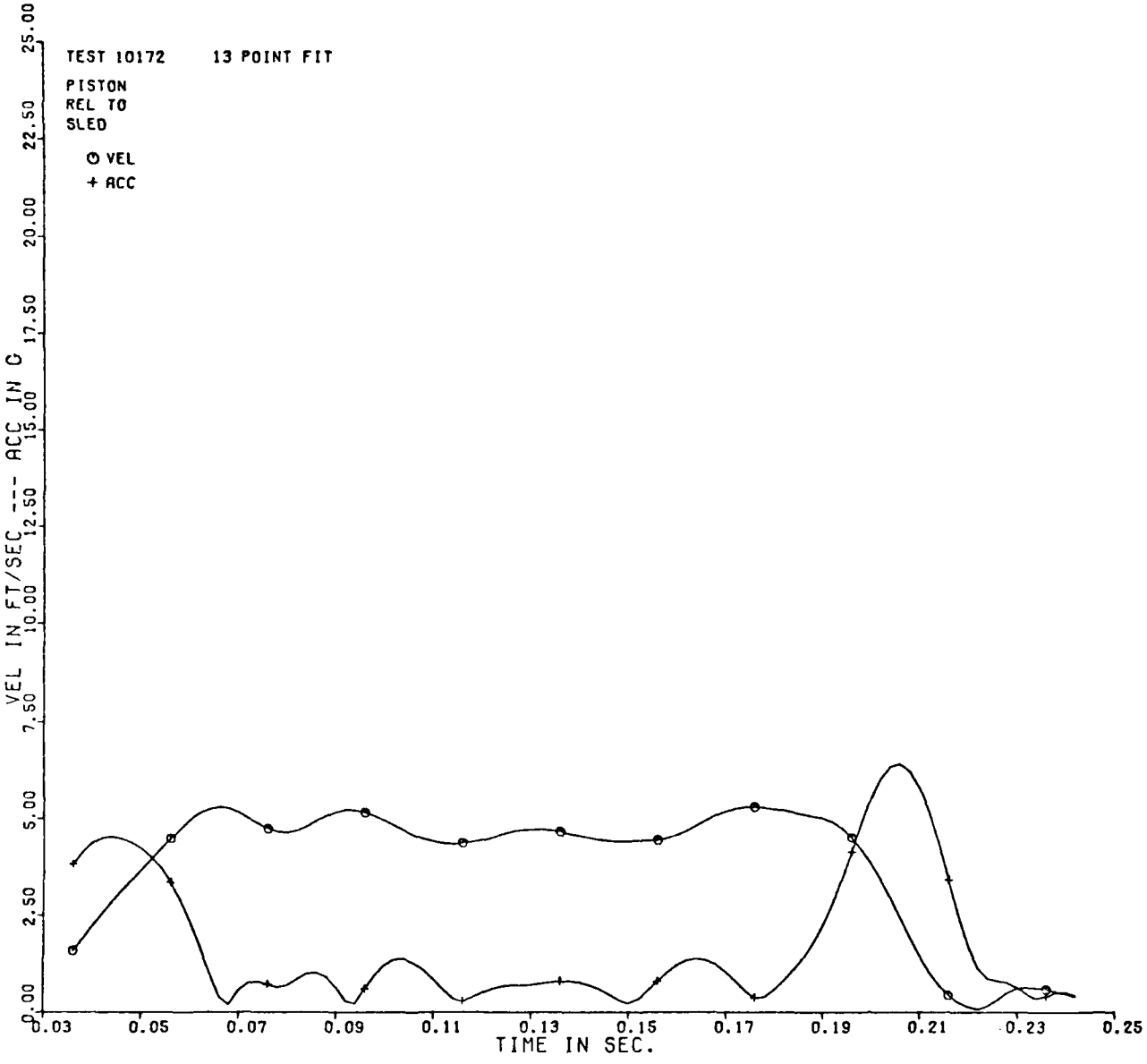
TEST 10172 13 POINT FIT
PISTON
REL TO
SLED
VEL
ACC
VEL IN FT/SEC --- ACC IN G
0.00
2.50
5.00
7.50
10.00
12.50
15.00
17.50
20.00
22.50
25.00
0.03
0.05
0.07
0.09
0.11
0.13
0.15
0.17
0.19
0.21
0.23
0.25
TIME IN SEC.

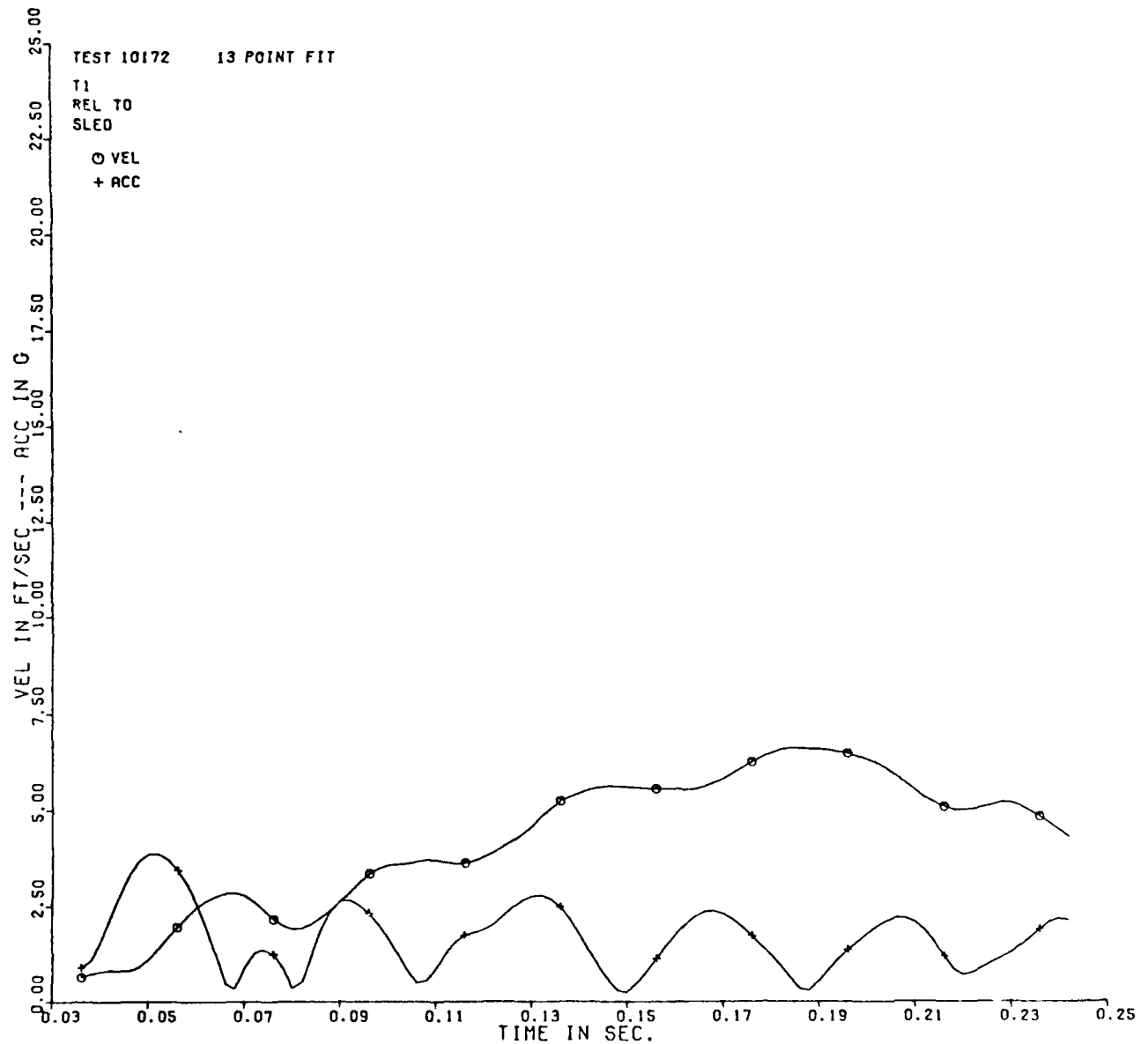
TEST 10172 13 POINT FIT
T1
REL TO
SLED
⊙ VEL
+ ACC
VEL IN FT/SEC --- ACC IN G
0.00
2.50
5.00
7.50
10.00
12.50
15.00
17.50
20.00
22.50
25.00
0.03
0.05
0.07
0.09
0.11
0.13
0.15
0.17
0.19
0.21
0.23
0.25
TIME IN SEC.

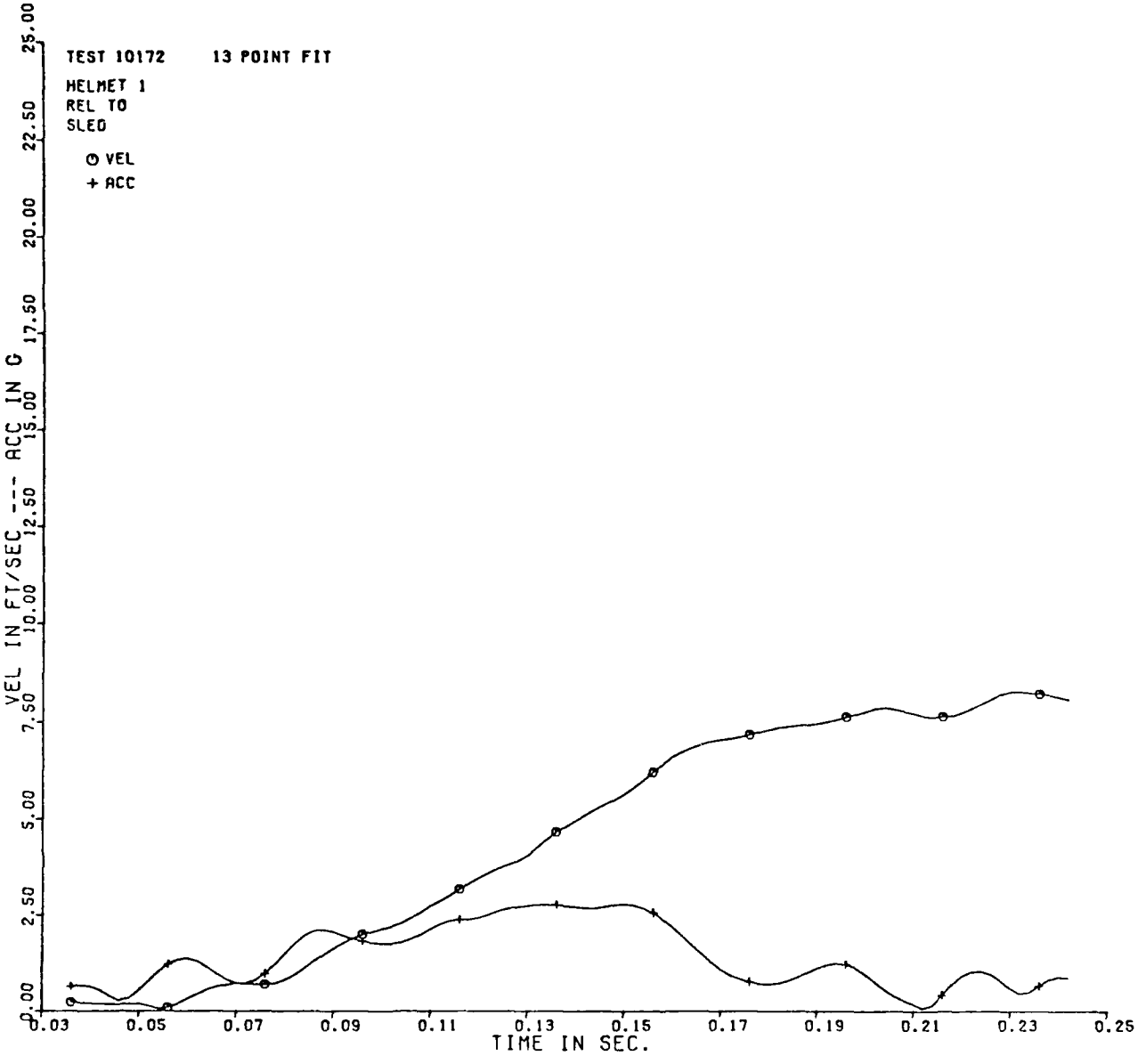
TEST 10172 13 POINT FIT
HELMET 1
REL TO
SLED
VEL
ACC
VEL IN FT/SEC --- ACC IN G
0.00
2.50
5.00
7.50
10.00
12.50
15.00
17.50
20.00
22.50
25.00
0.03
0.05
0.07
0.09
0.11
0.13
0.15
0.17
0.19
0.21
0.23
0.25
TIME IN SEC.

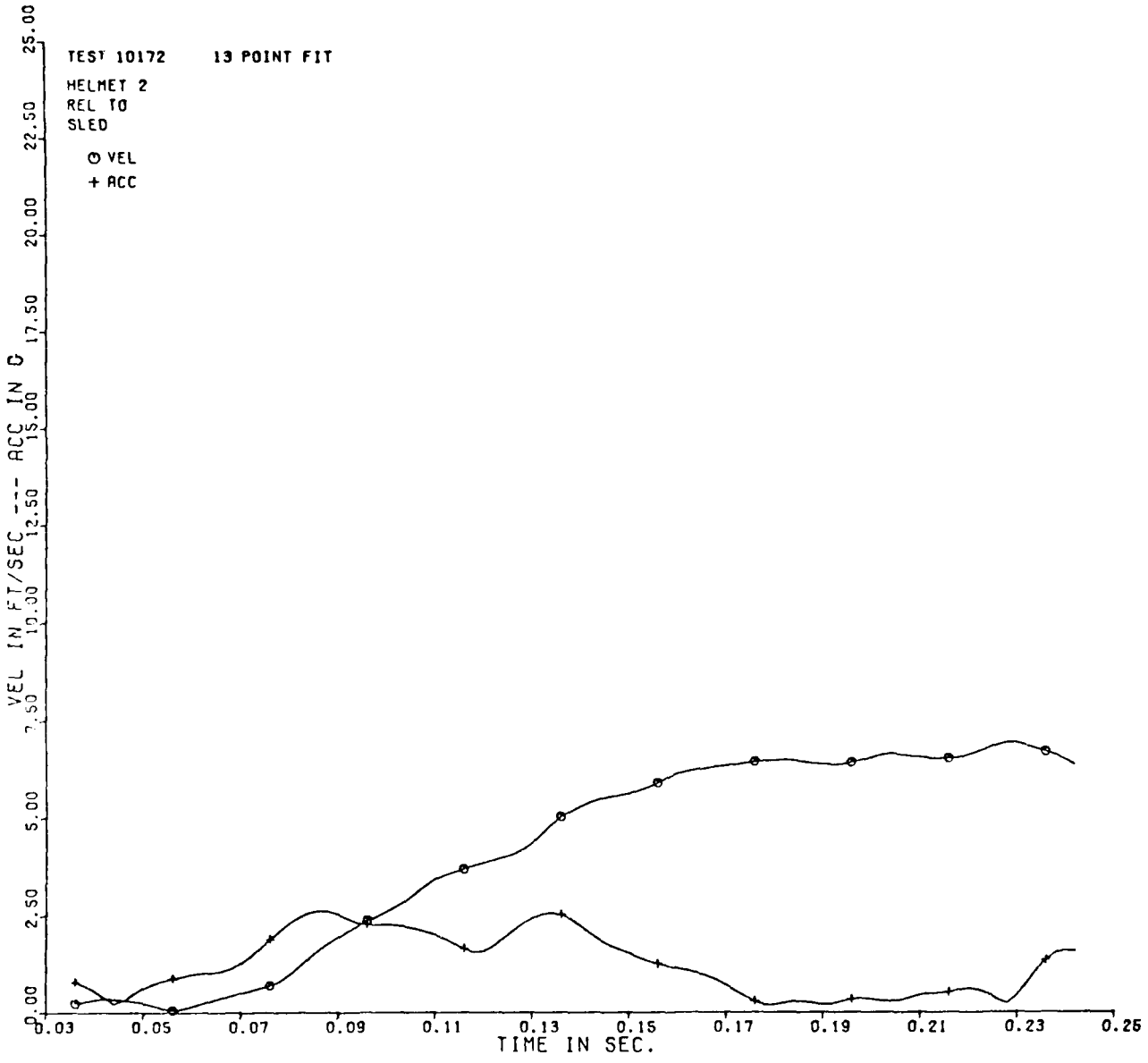
TEST 10172 13 POINT FIT
HELMET 2
REL TO
SLED
⊙ VEL
+ ACC
VEL IN FT/SEC --- ACC IN G
0.00
2.50
5.00
7.50
10.00
12.50
15.00
17.50
20.00
22.50
25.00
0.03
0.05
0.07
0.09
0.11
0.13
0.15
0.17
0.19
0.21
0.23
0.25
TIME IN SEC.

APPENDIX B

This appendix contains plots generated to compare the PZ Piston Z-axis acceleration with the same acceleration computed from photo displacement data using the quadratic fit routine with 9, 11 or 13-point fits. The PZ data are interpolated at 500 samples per second (DT=.002 seconds) for these plots. The photo acceleration data are identified as PH-9PT, PH-11PT, and PH-13PT for the 9, 11, and 13-point fits.

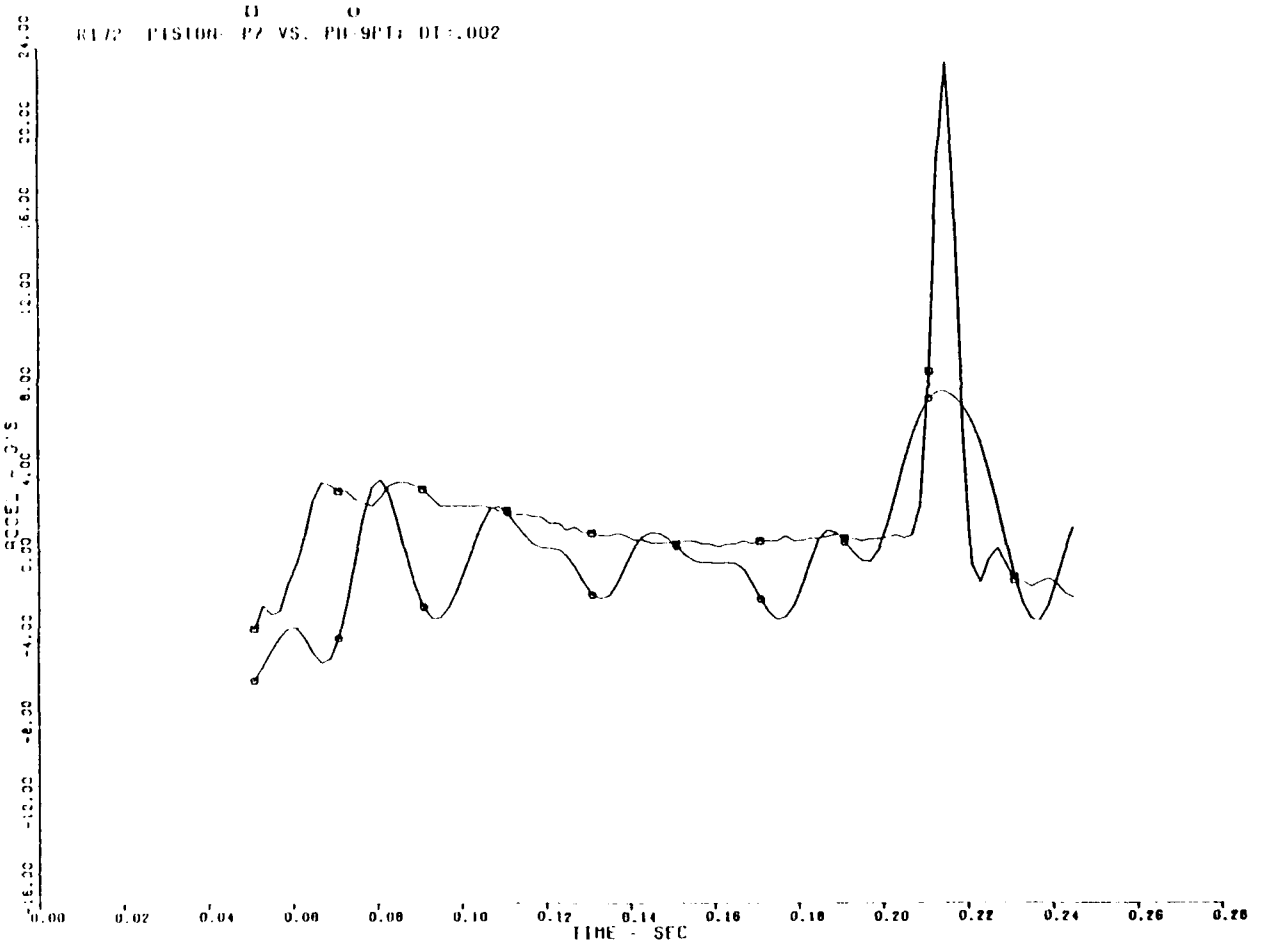
R172 PISTON PZ VS. PB-9PTS DT=.002
TIME - SEC

AD-A085 880 DAYTON UNIV OH RESEARCH INST F/G 9/2
ACCURACY OF DIGITIZED PHOTOMETRIC DATA.(U)
APR 80 P A GRAF, H T MOHLMAN F33615-76-C-0525
UNCLASSIFIED AMRL-TR-79-76 NL

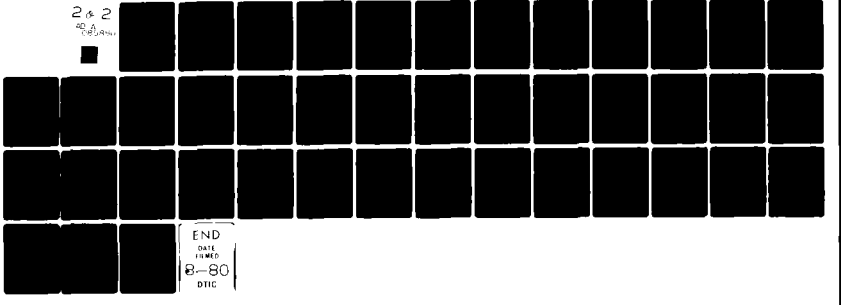

END
DATE FILMED
8-80
DTIC

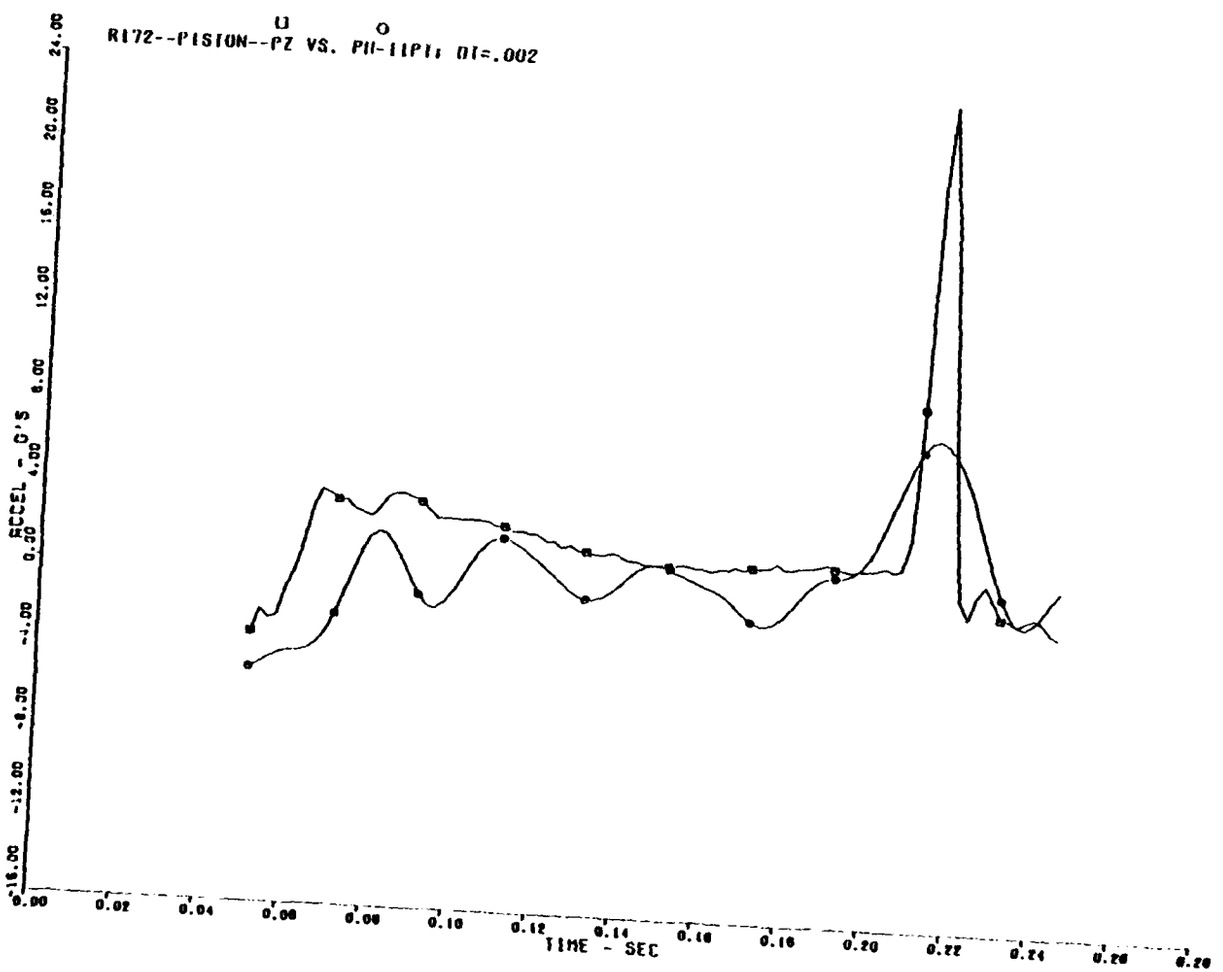
R172--PISTON--PZ VS. PH-TIPT: DT=.002
ACCEL - G'S
24.00
20.00
16.00
12.00
8.00
4.00
0.00
-4.00
-8.00
-12.00
-16.00
0.00
0.02
0.04
0.06
0.08
0.10
0.12
0.14
0.16
0.18
0.20
0.22
0.24
0.26
0.28
TIME - SEC

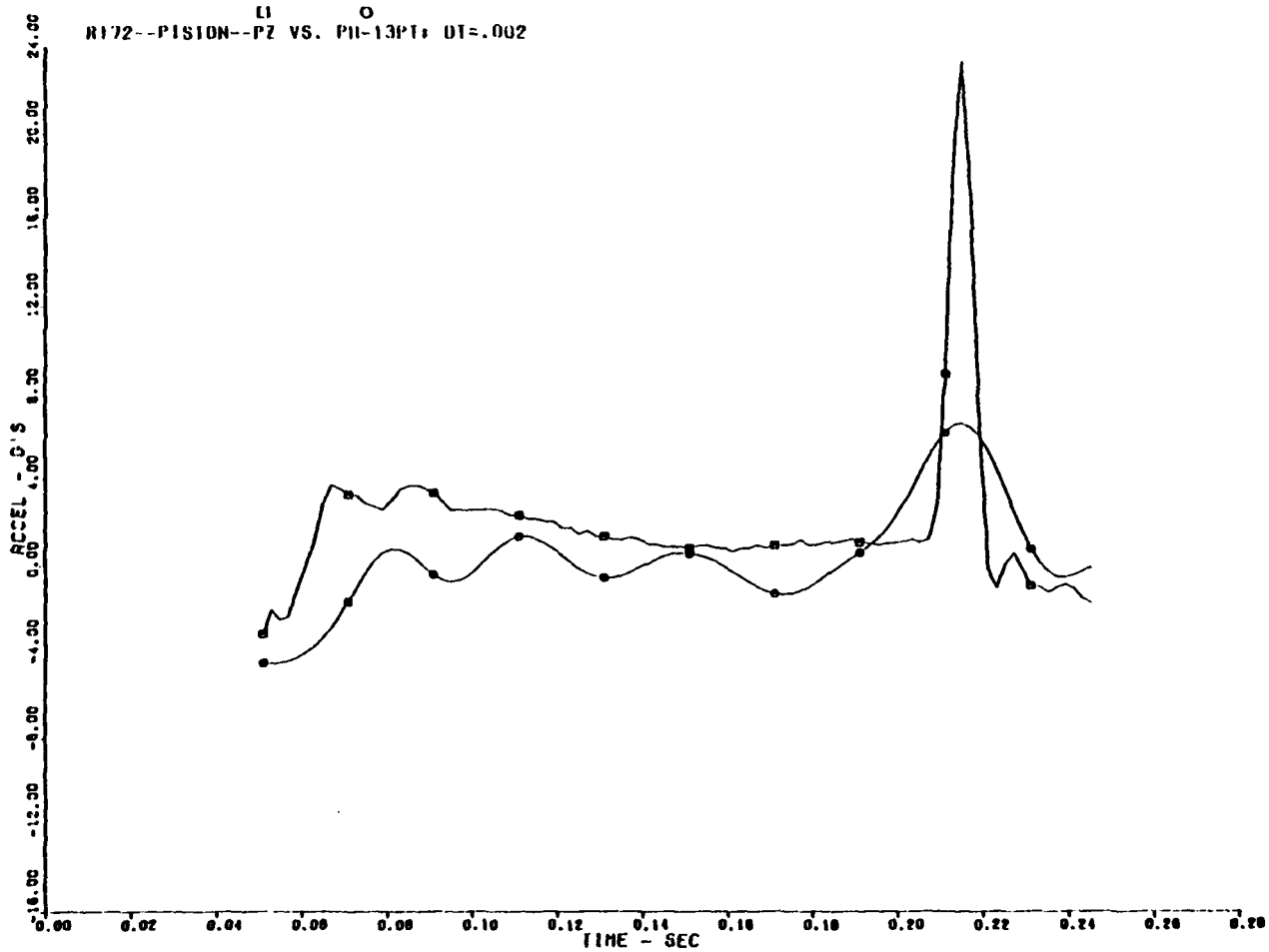
R172--PISION--PZ VS. PIS-13PTs DT=.002
ACCEL - G'S
TIME - SEC

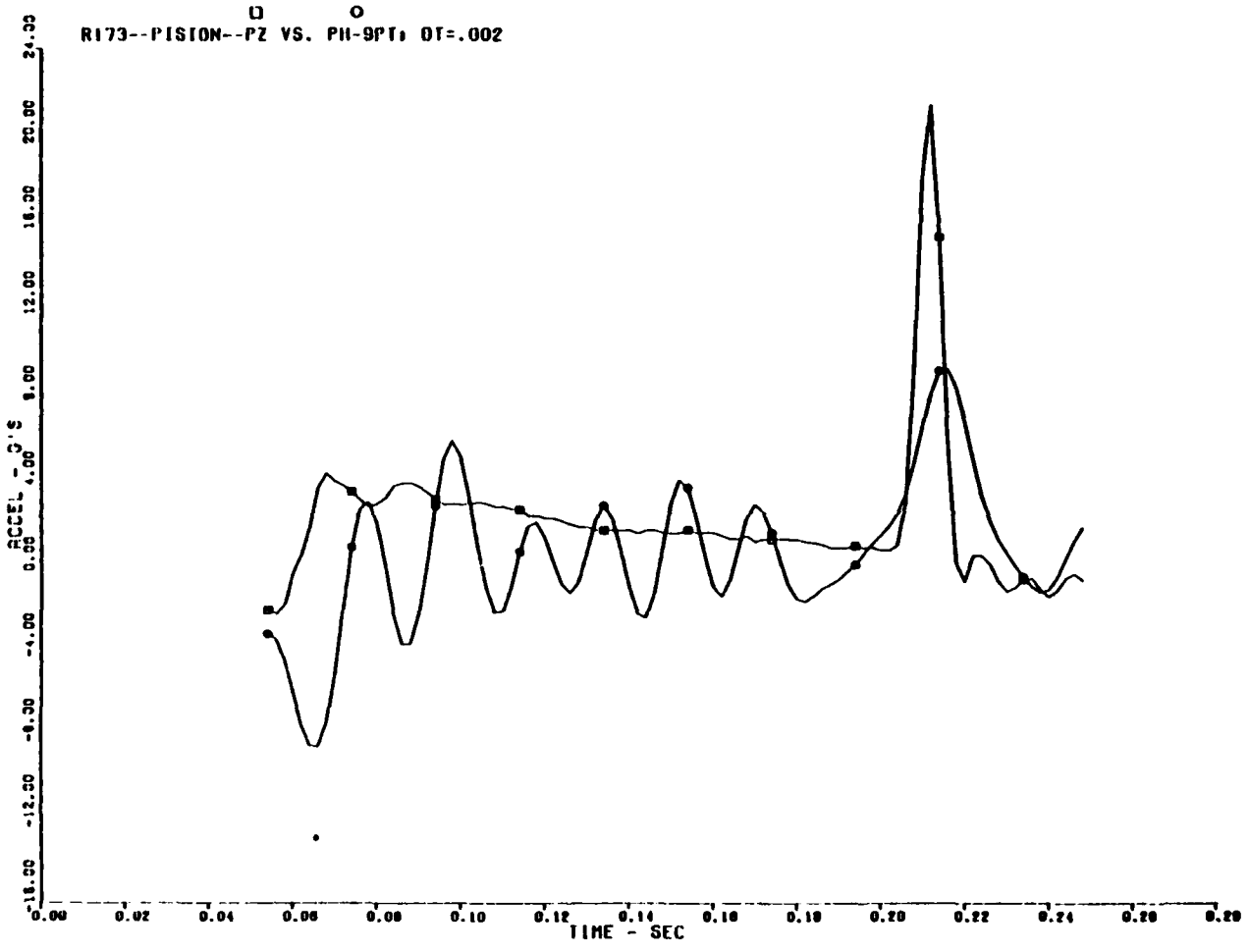
R173--PISTON--PZ VS. PH-9PTs DT=.002
ACCEL - G'S
TIME - SEC

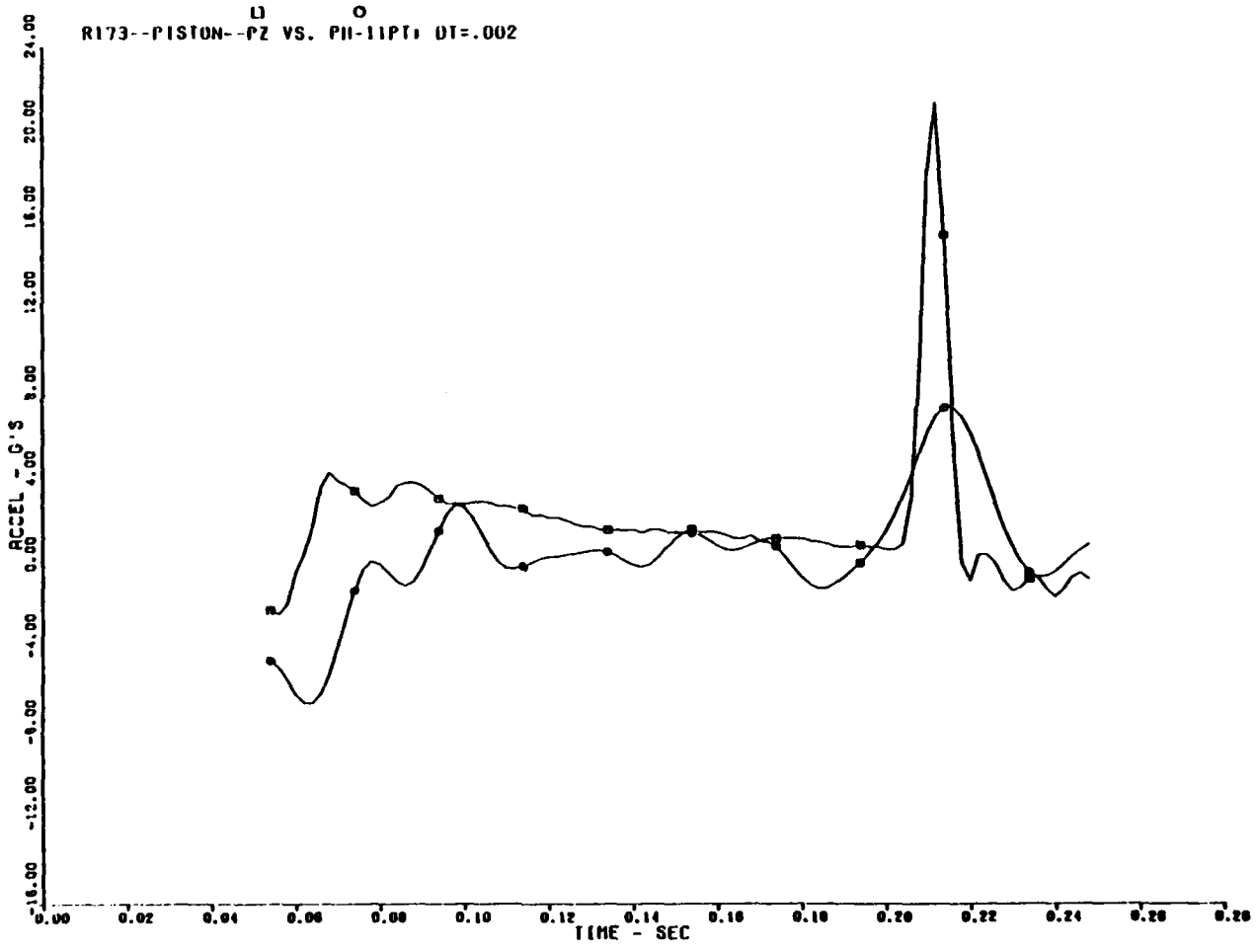
R173--PISTON--PZ VS. PH-11PT1 DT=.002
ACCEL - G'S
24.00
20.00
16.00
12.00
8.00
4.00
0.00
-4.00
-8.00
-12.00
-16.00
0.00
0.02
0.04
0.06
0.08
0.10
0.12
0.14
0.16
0.18
0.20
0.22
0.24
0.26
0.28
TIME - SEC

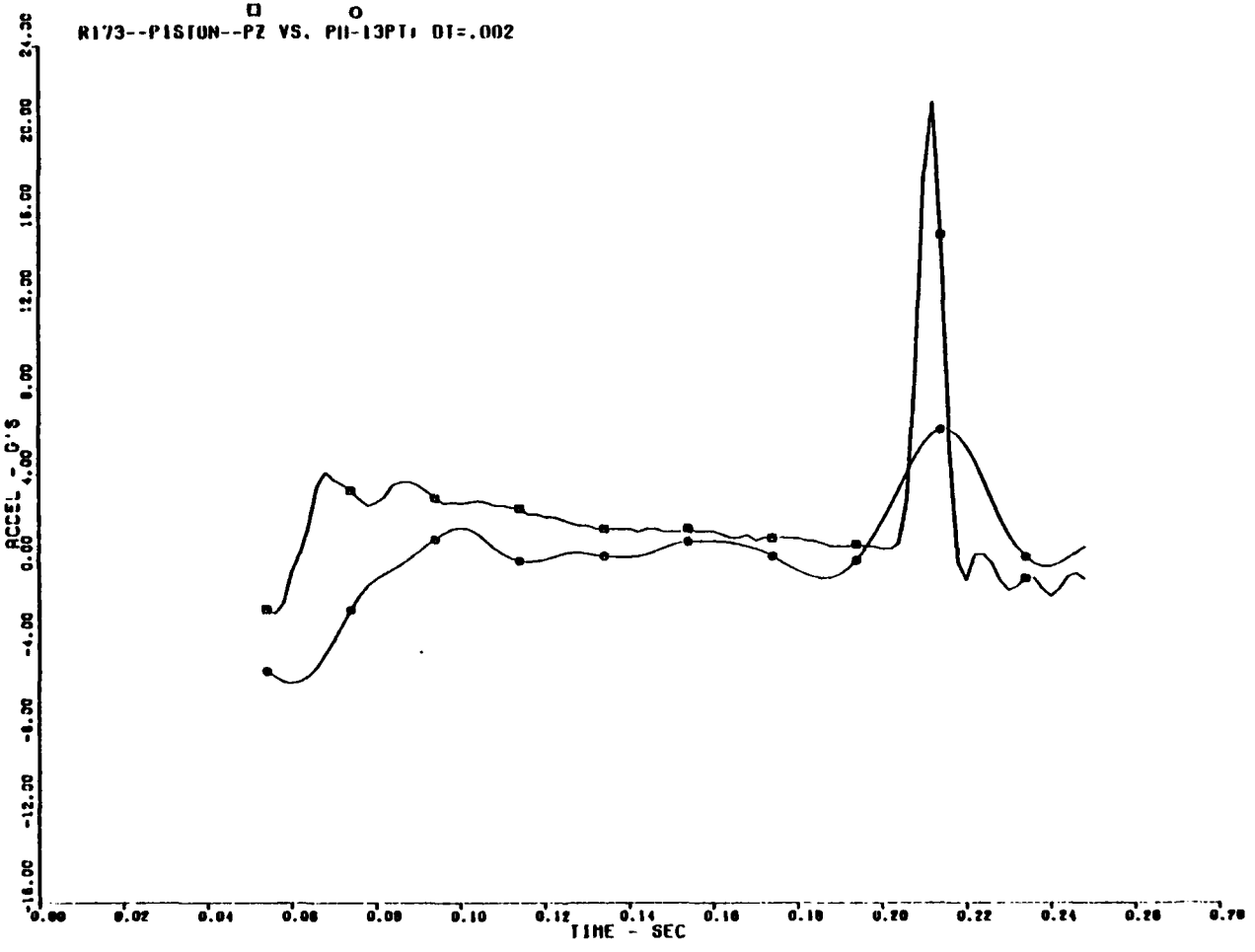
R173--PISTON--PZ VS. PII-13PT; DT=.002
ACCEL - G'S
24.00
20.00
16.00
12.00
8.00
4.00
0.00
-4.00
-8.00
-12.00
-16.00
0.00
0.02
0.04
0.06
0.08
0.10
0.12
0.14
0.16
0.18
0.20
0.22
0.24
0.26
0.28
TIME - SEC

APPENDIX C

This appendix contains piston Z-axis displacement and acceleration graphs generated to compare the photo data (PH) with the transducer displacement data (PD) and the piezo resistive damped linear accelerometer data (PZ) for tests 172 and 173. The first two displacement graphs contain plots of the PD displacement and smoothed photo displacement versus time data (PH-11PT). This PH-11PT displacement was derived using the 11-point smoothing technique. The two acceleration versus time graphs contain plots of the PZ, PD, and PH acceleration data. The PD and PH acceleration which are labeled PD-11PT and PH-11PT were derived from the PD and PH displacement using our 11-point smoothing technique. The last two displacement versus time graphs contain plots of the displacement derived from the PZ acceleration by double integration of the PZ acceleration data.

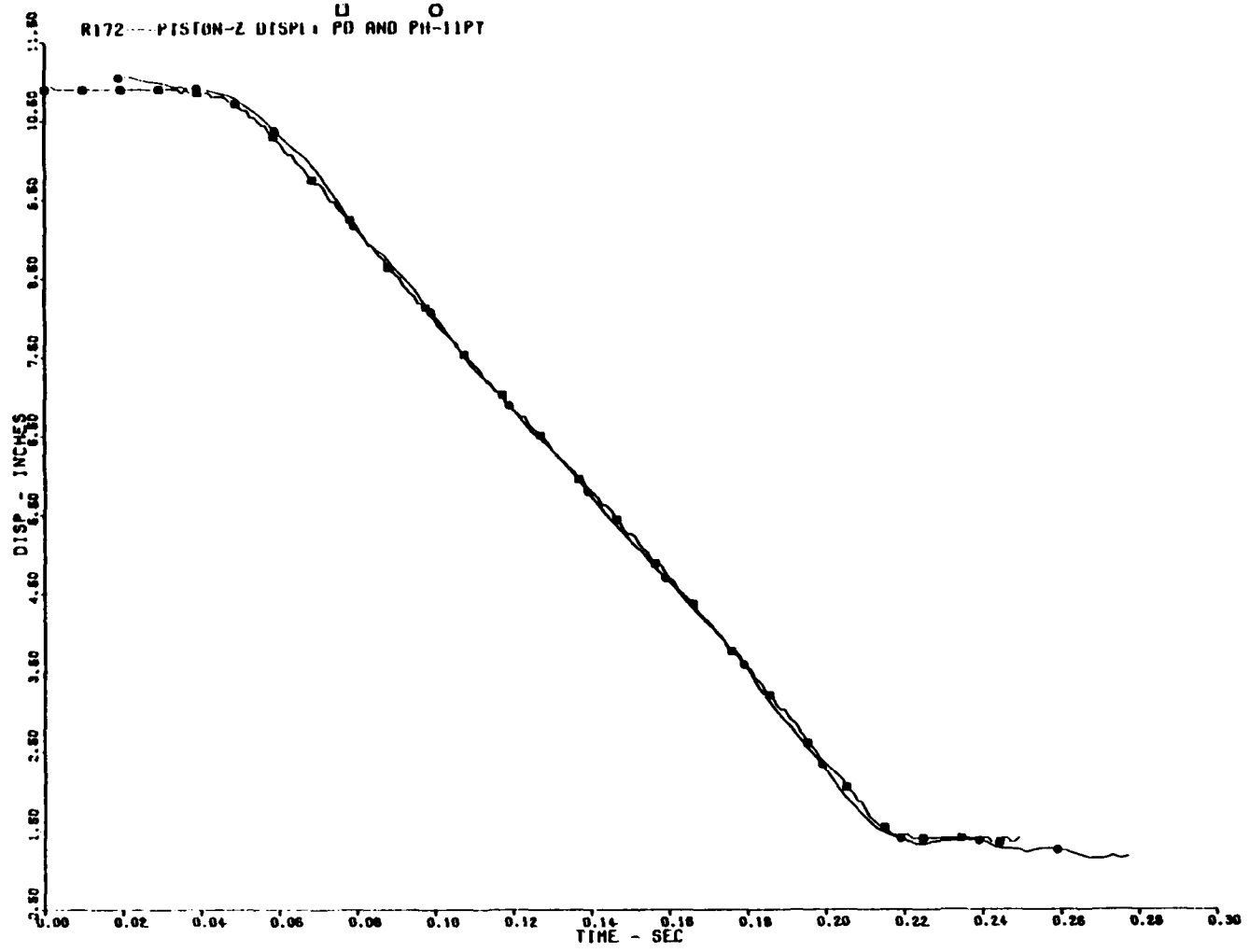
R172---PISTON-Z DISPL: PD AND PH-11PT
DISP - INCHES
TIME - SEC
0.00
0.02
0.04
0.06
0.08
0.10
0.12
0.14
0.16
0.18
0.20
0.22
0.24
0.26
0.28
0.30

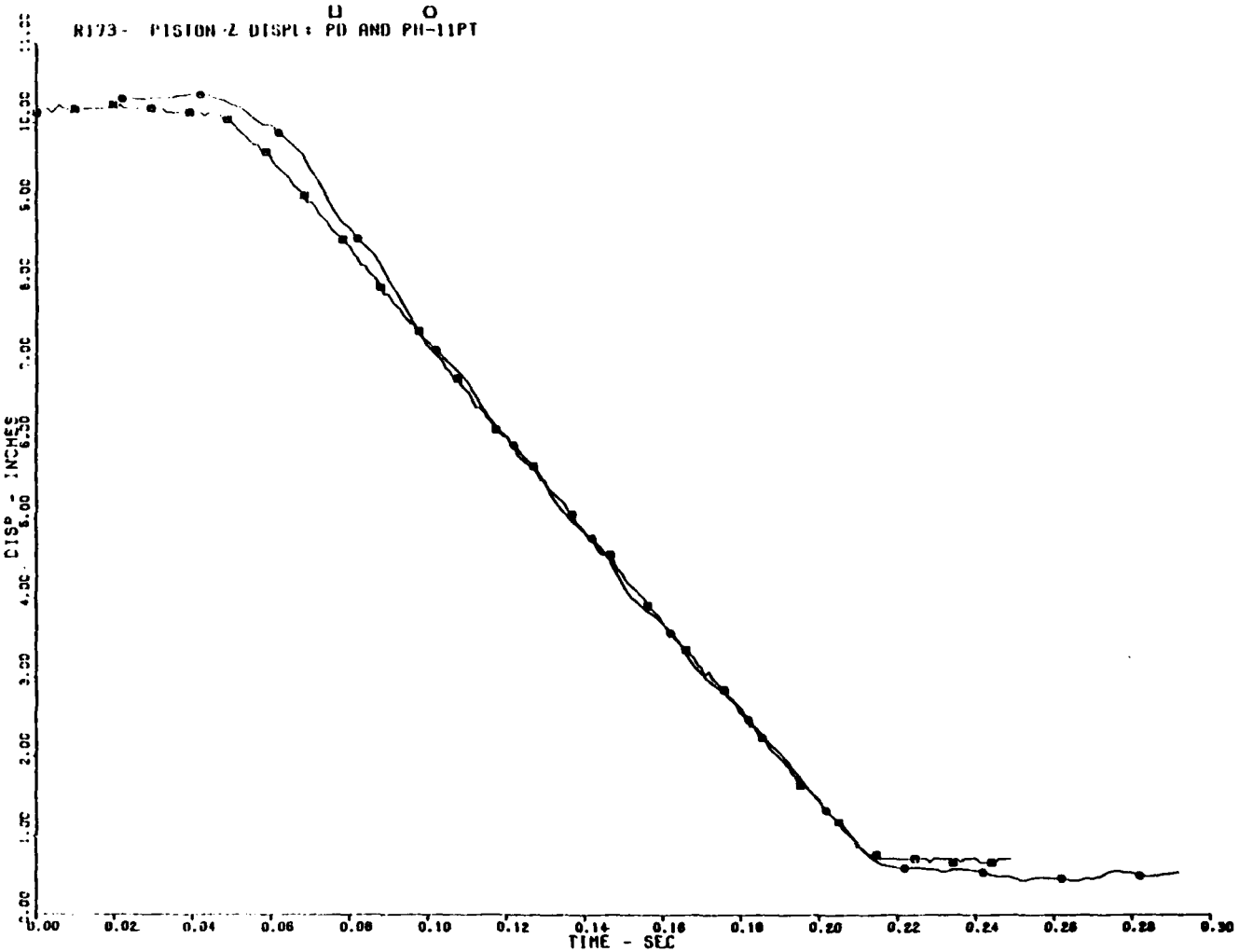
R173- PISTON-Z DISPL: PD AND PH-11PT
DISP - INCHES
TIME - SEC
0.00
0.02
0.04
0.06
0.08
0.10
0.12
0.14
0.16
0.18
0.20
0.22
0.24
0.26
0.28
0.30

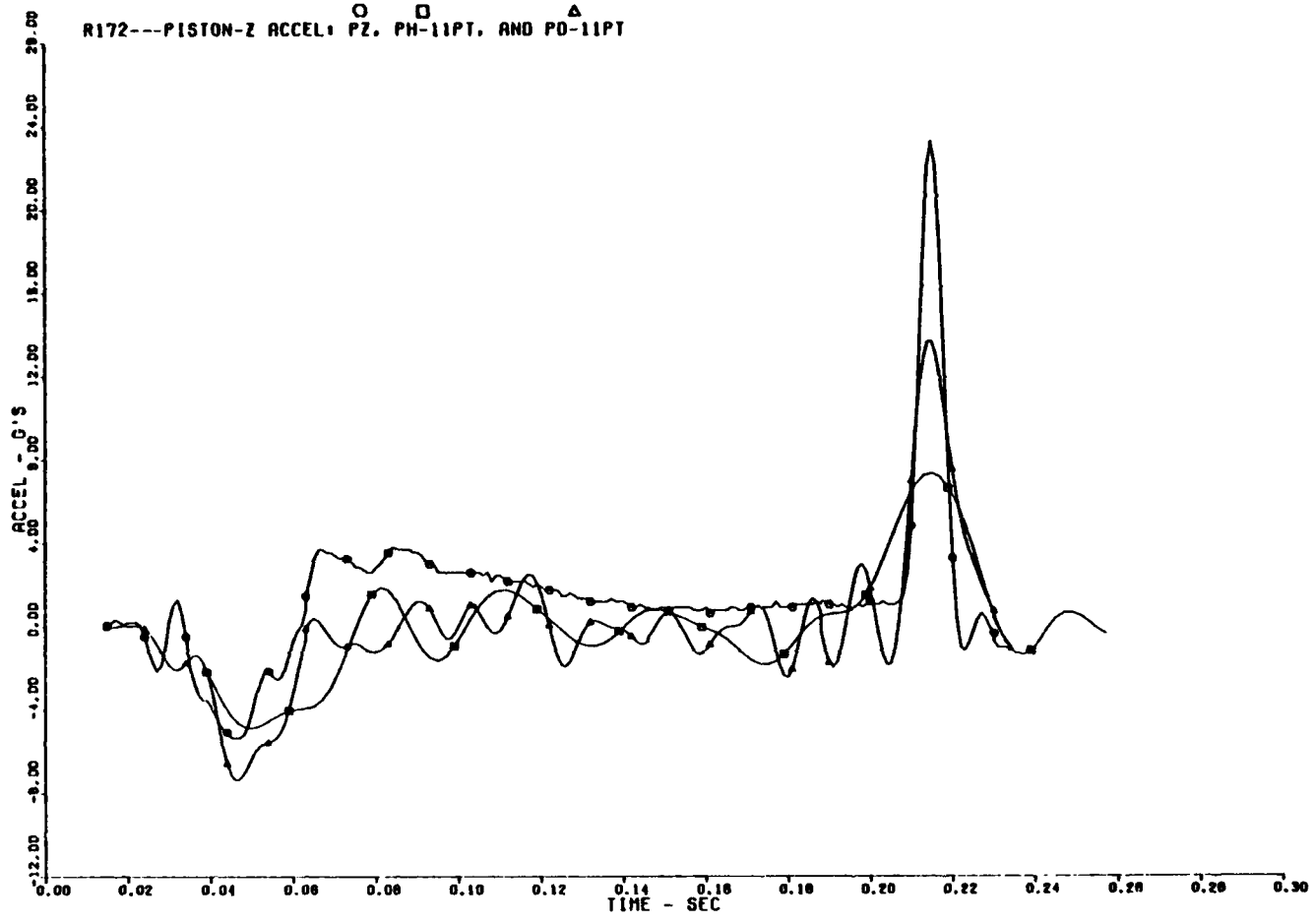
R172---PISTON-Z ACCEL: PZ, PH-11PT, AND PO-11PT
ACCEL - G'S
TIME - SEC
20.00
16.00
12.00
8.00
4.00
0.00
-4.00
-8.00
-12.00
0.00
0.02
0.04
0.06
0.08
0.10
0.12
0.14
0.16
0.18
0.20
0.22
0.24
0.26
0.28
0.30

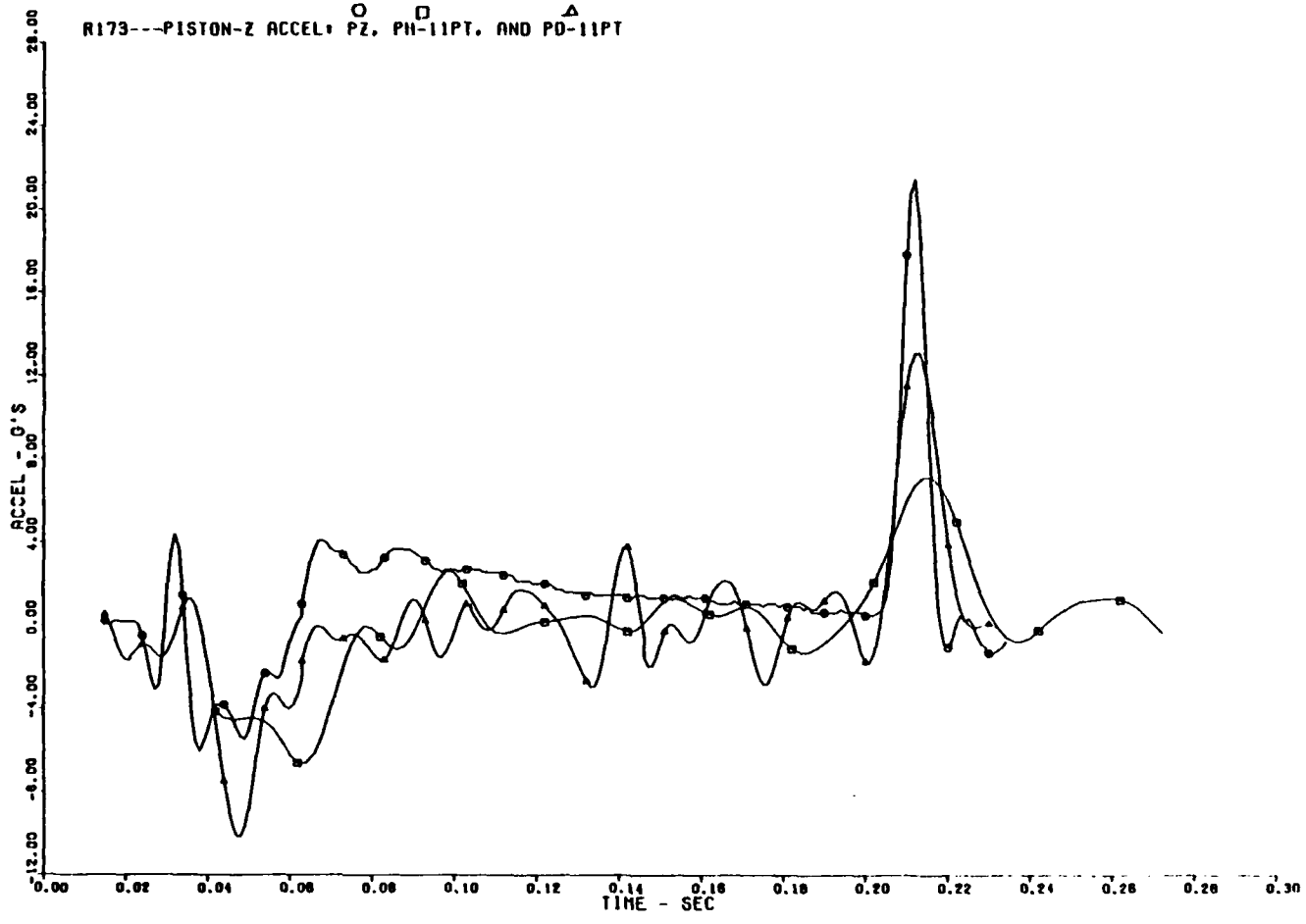
R173---PISTON-Z ACCEL: PZ, PH-11PT, AND PD-11PT
ACCEL - G'S
TIME - SEC
28.00
24.00
20.00
16.00
12.00
8.00
4.00
0.00
-4.00
-8.00
-12.00
0.00
0.02
0.04
0.06
0.08
0.10
0.12
0.14
0.16
0.18
0.20
0.22
0.24
0.26
0.28
0.30

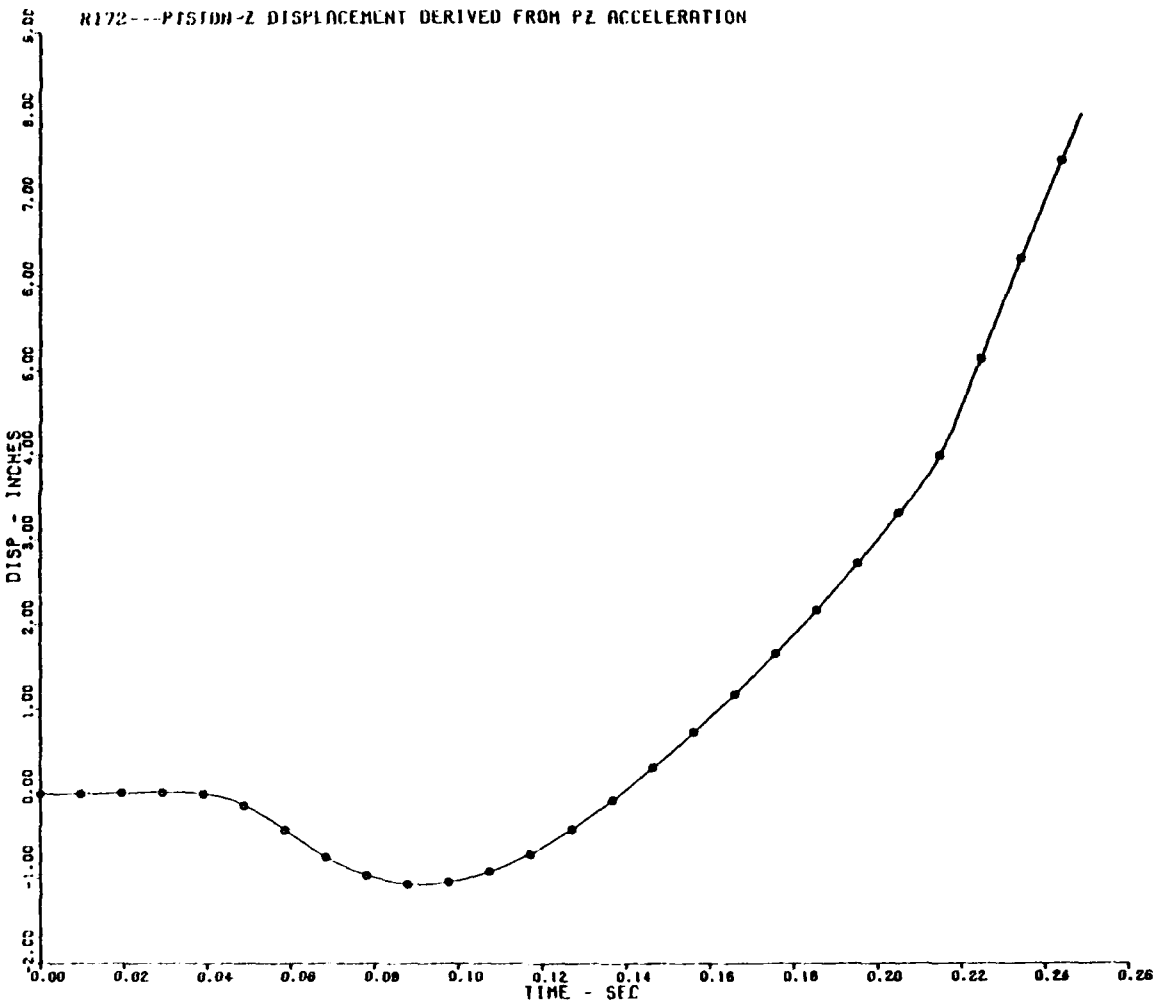
R172---PISTON-Z DISPLACEMENT DERIVED FROM PZ ACCELERATION
DISP - INCHES
TIME - SEC
-2.00
-1.00
0.00
1.00
2.00
3.00
4.00
5.00
6.00
7.00
8.00
0.00
0.02
0.04
0.06
0.08
0.10
0.12
0.14
0.16
0.18
0.20
0.22
0.24
0.26

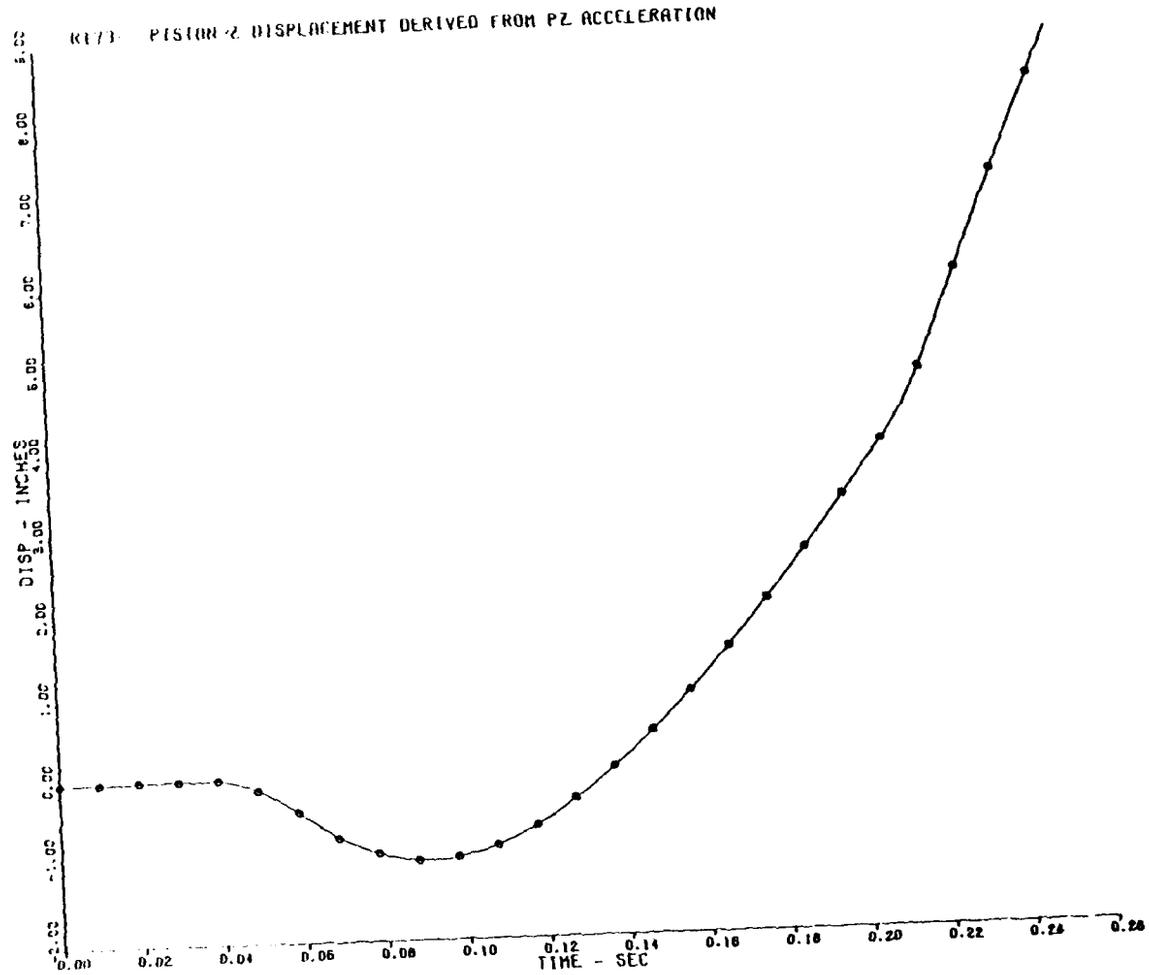
RUN 3 PISTON 2 DISPLACEMENT DERIVED FROM PZ ACCELERATION
DISP - INCHES
TIME - SEC
0.00
0.02
0.04
0.06
0.08
0.10
0.12
0.14
0.16
0.18
0.20
0.22
0.24
0.26

APPENDIX D

The plots in this appendix compare 11-point fit displacement, velocity, and acceleration data with measured acceleration and derived velocity and displacement data. The displacement used as input to the 11-point fit was derived from the measured acceleration by double integration of the measured acceleration; thus, we know what the final acceleration should be and can accurately evaluate the effectiveness of the 11-point smoothing. The measured acceleration data are labeled as "original" data on the plots, while the derived velocity and displacement data are identified as "integrated" data.

The 172 PZ and 173 PZ data are piston Z-axis acceleration data measured with a Piezo resistive accelerometer and digitized at 1024 samples per second (DT=.0009766 seconds per sample). The 172 HX and 172 HZ data are X-axis and Z-axis acceleration data measured with a Piezo resistive accelerometer attached to the roof of the subjects mouth. All these data were also interpolated at 500 samples per second (DT=.002 seconds per sample) to evaluate the 11-point smoothing at this standard sampling rate.

The 3-point quadratic fit does not smooth the data; it is used only as a convenient method to compute velocity and acceleration from raw displacement data. The 3-point fit of the PZ acceleration data are presented here to determine the effect of the integration routine on the recomputed acceleration data. The plots show that the integration routine used to compute the displacement from the given PZ acceleration degrades the peak acceleration less than 1 g. Thus, the differences between the original and 11-point data are caused by the 11-point smoothing technique.

Some of the acceleration and displacement plots contain σ and r values where σ is the standard deviation about the mean difference between the two curves and r is the correlation coefficient which is a measure of how well the smoothed curve follows the original data points.

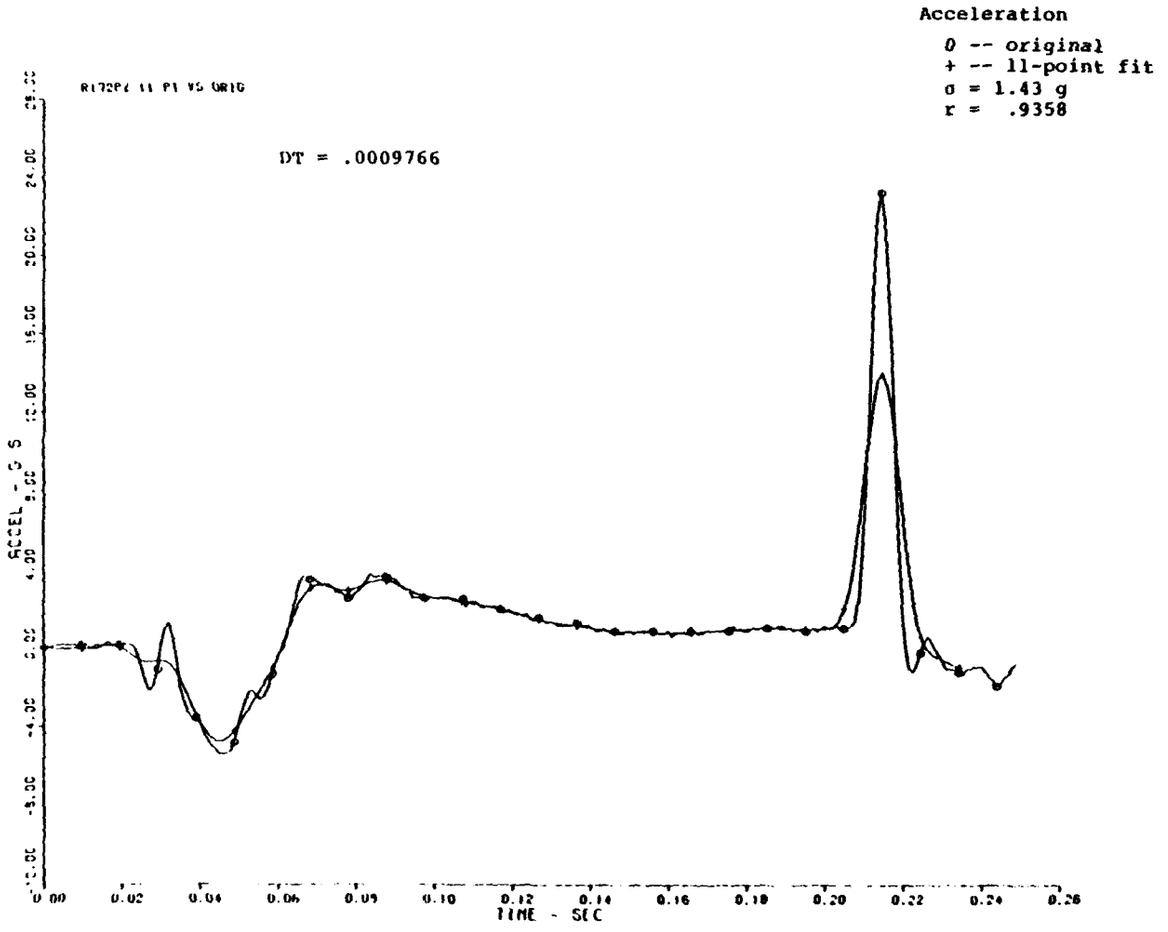
Acceleration
0 -- original
+ -- 11-point fit
σ = 1.43 g
r = .9358
DT = .0009766
ACCEL - G S
TIME - SEC
0.00
0.02
0.04
0.06
0.08
0.10
0.12
0.14
0.16
0.18
0.20
0.22
0.24
0.26

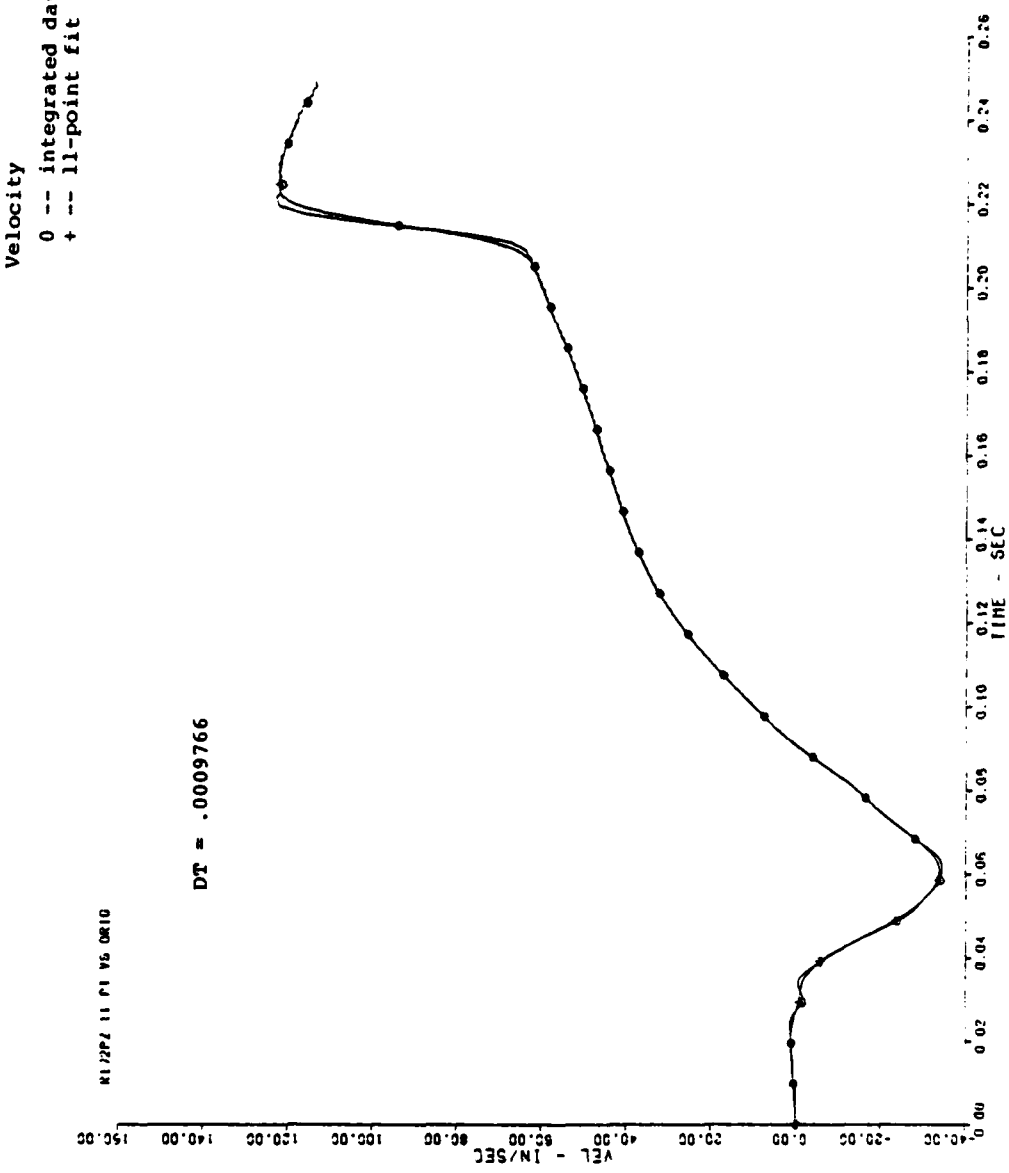
Velocity
0 -- integrated data
+ -- 11-point fit
DT = .0009766
VEL - IN/SEC
TIME - SEC

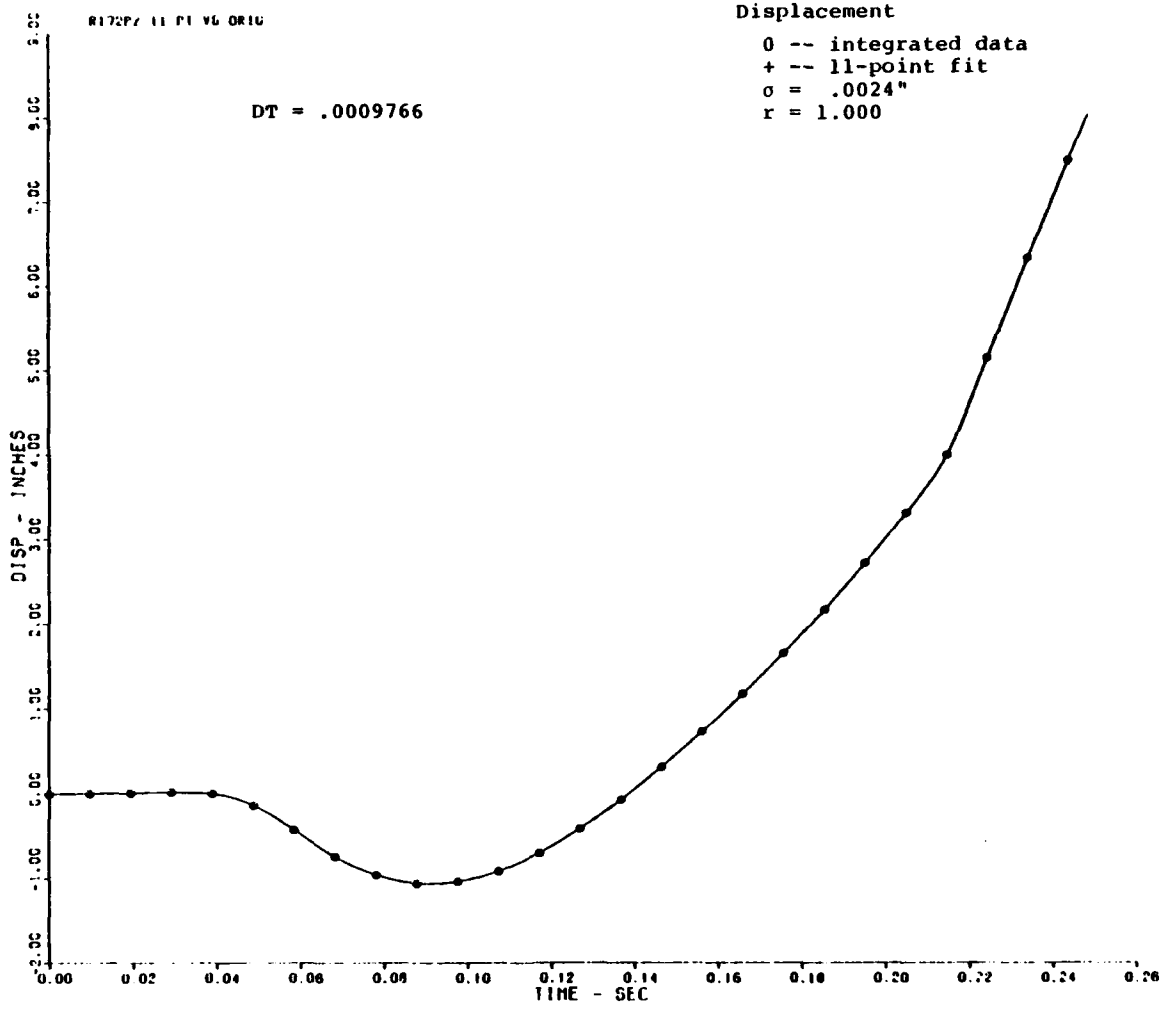
Displacement
0 -- integrated data
+ -- 11-point fit
σ = .0024"
r = 1.000
DT = .0009766
DISP - INCHES
TIME - SEC
0.00
0.02
0.04
0.06
0.08
0.10
0.12
0.14
0.16
0.18
0.20
0.22
0.24
0.26

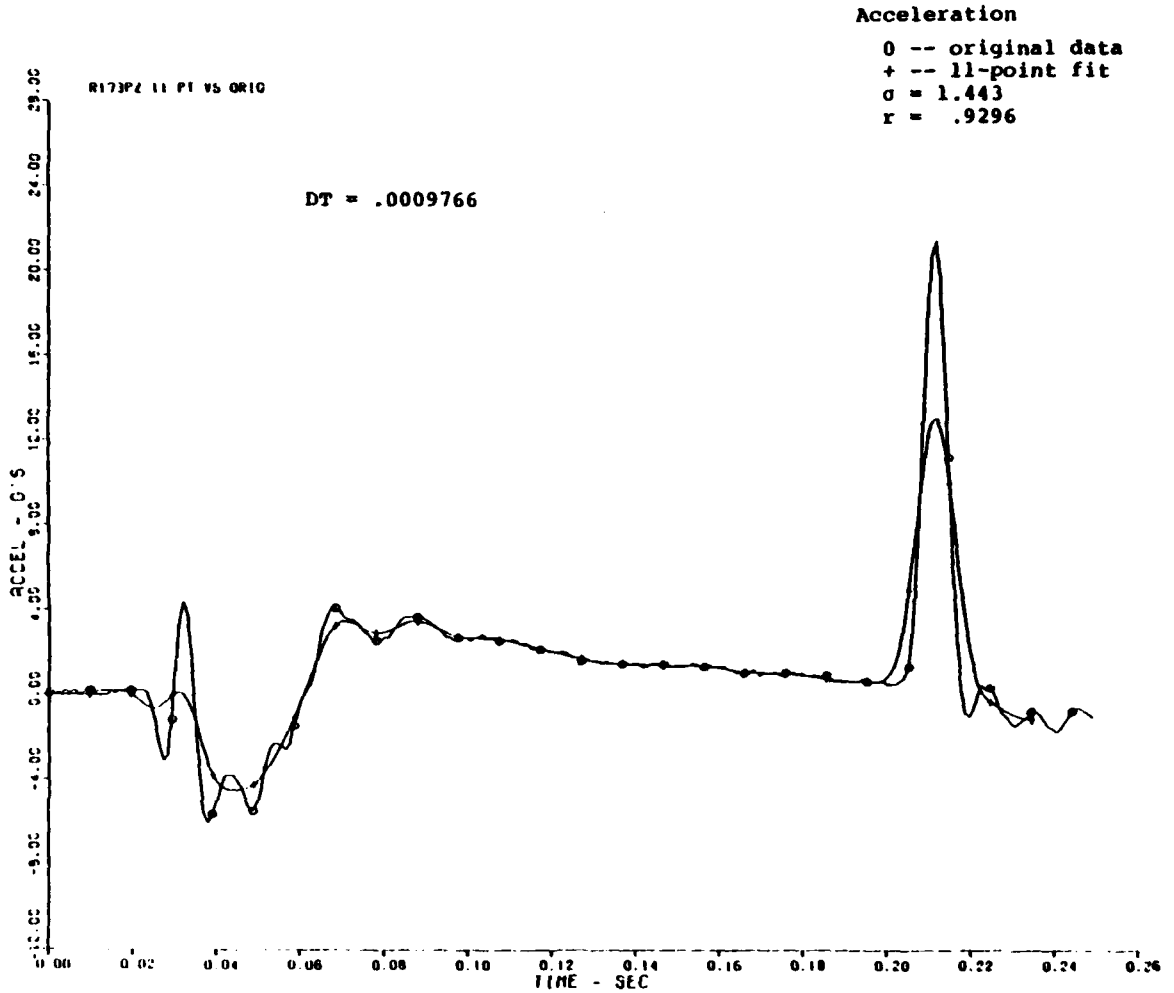
Acceleration
0 -- original data
+ -- 11-point fit
σ = 1.443
r = .9296
DT = .0009766
ACCEL - G'S
TIME - SEC
0.00
0.02
0.04
0.06
0.08
0.10
0.12
0.14
0.16
0.18
0.20
0.22
0.24
0.26

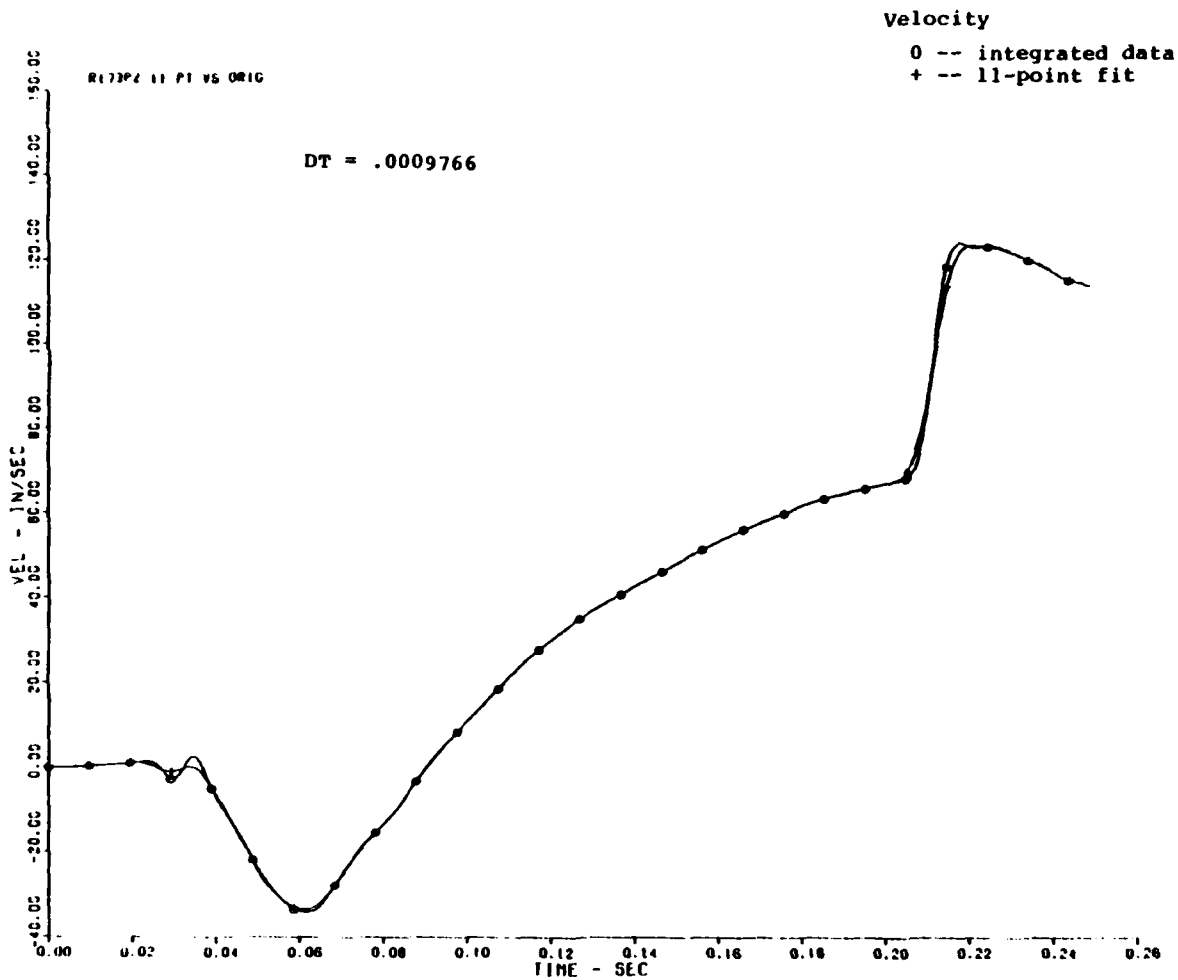
Velocity
0 -- integrated data
+ -- 11-point fit
DT = .0009766
VEL - IN/SEC
TIME - SEC
0.00
0.02
0.04
0.06
0.08
0.10
0.12
0.14
0.16
0.18
0.20
0.22
0.24
0.26

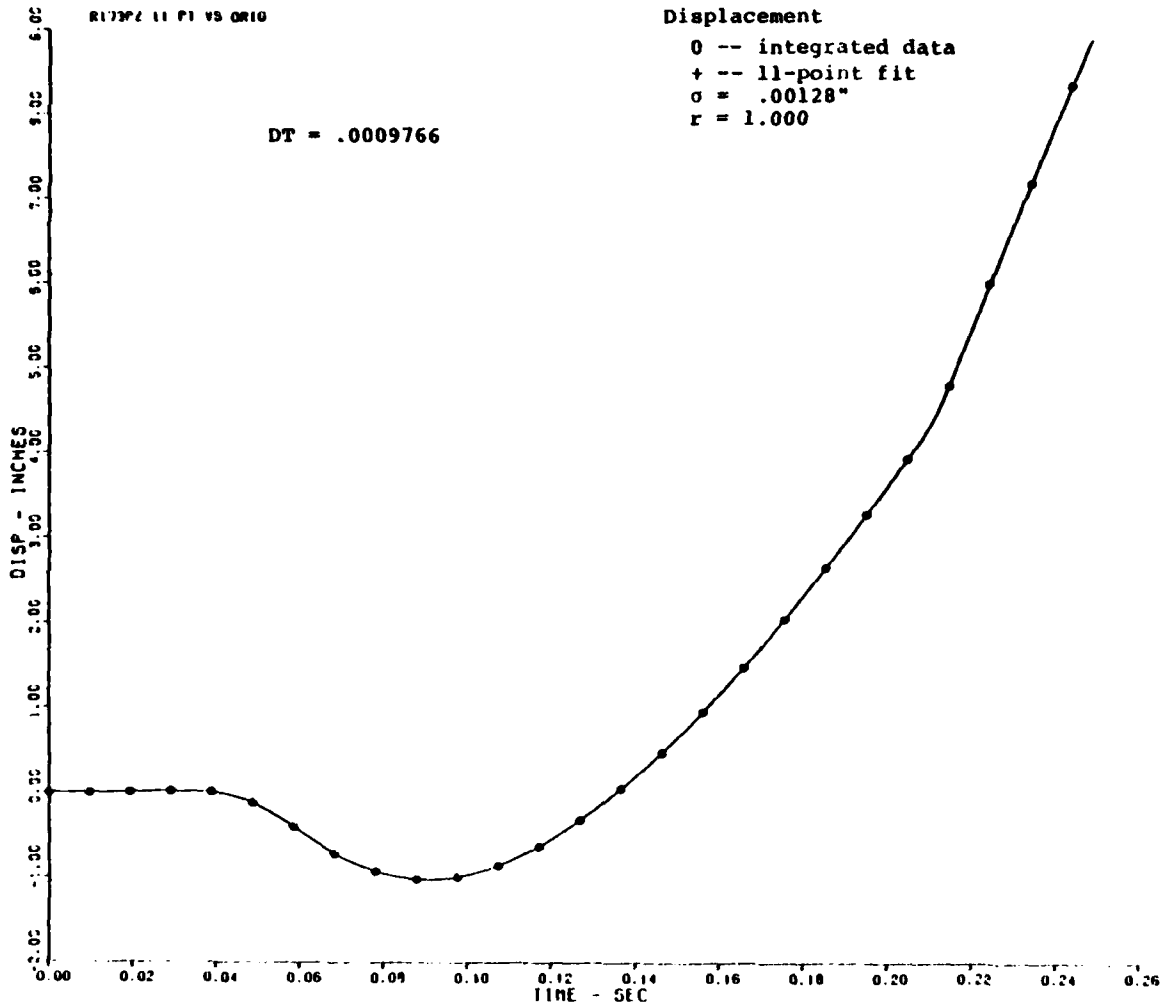
Displacement
0 -- integrated data
+ -- 11-point fit
σ = .00128"
r = 1.000
DT = .0009766
DISP - INCHES
TIME - SEC
0.00
0.02
0.04
0.06
0.08
0.10
0.12
0.14
0.16
0.18
0.20
0.22
0.24
0.26

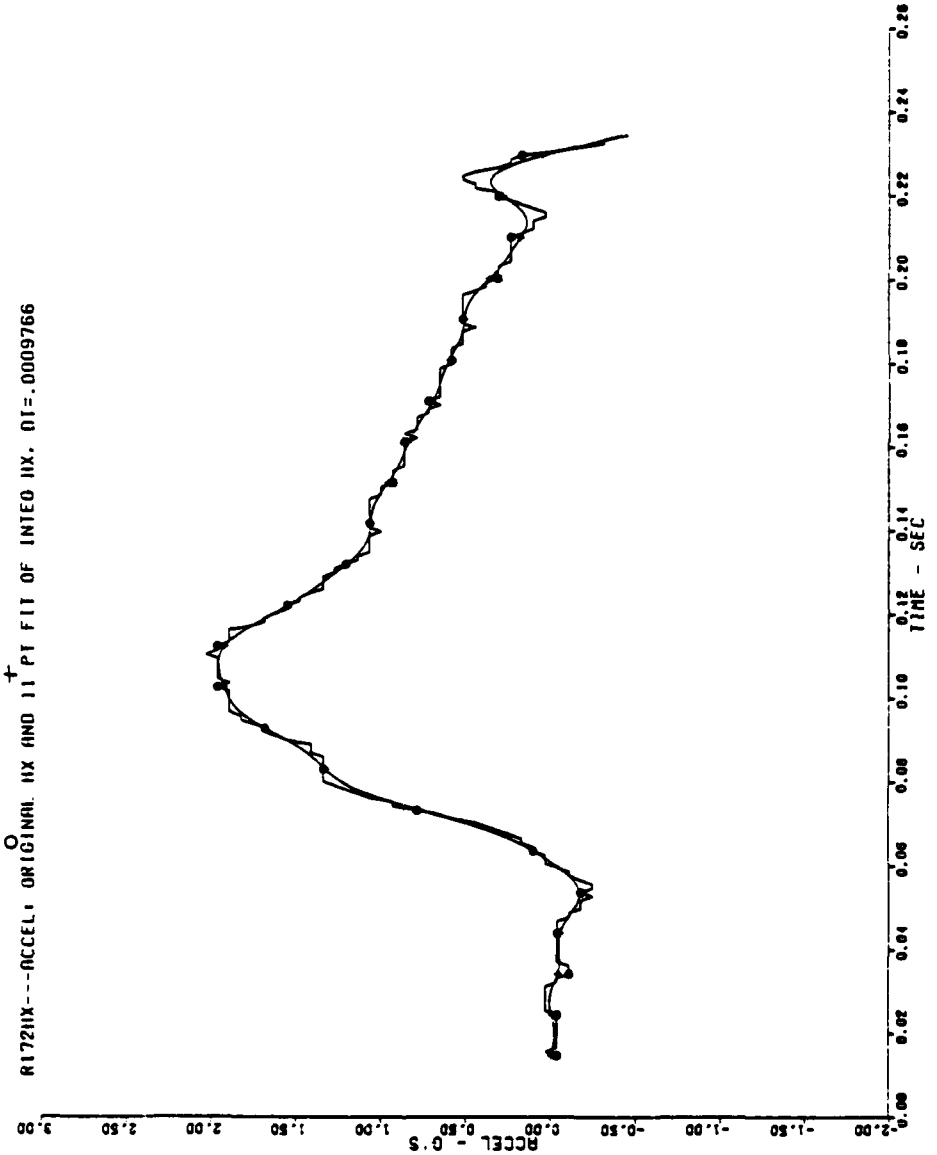
R172HX---ACCEL: ORIGINAL HX AND 11 PT FIT OF INTEG HX. DT=.0009766
ACCEL - G'S
TIME - SEC

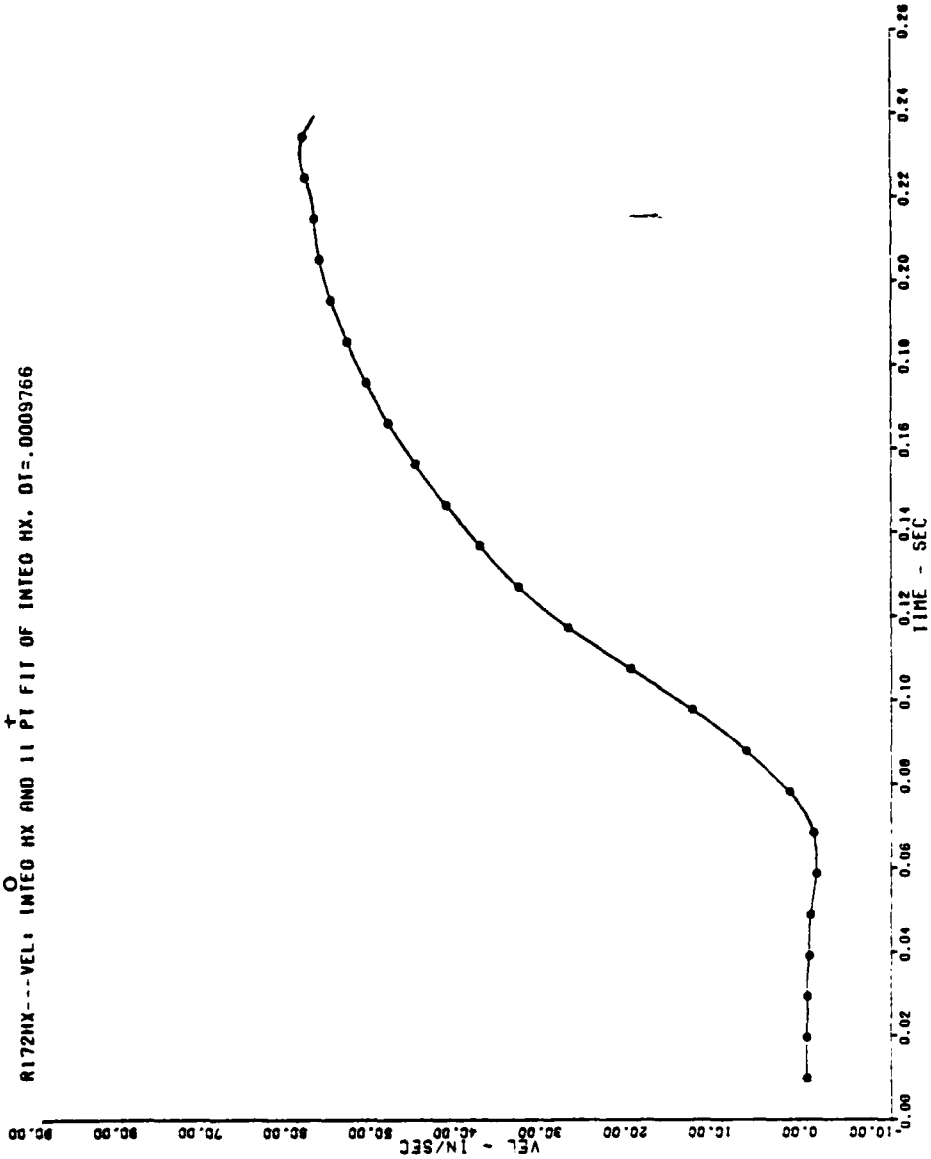
R172HX---VEL. INTEG HX AND II PT FIT OF INTEG HX. DT=.0009766
VEL. - IN/SEC
TIME - SEC
-10.00
0.00
10.00
20.00
30.00
40.00
50.00
60.00
70.00
80.00
90.00
0.00
0.02
0.04
0.06
0.08
0.10
0.12
0.14
0.16
0.18
0.20
0.22
0.24
0.26

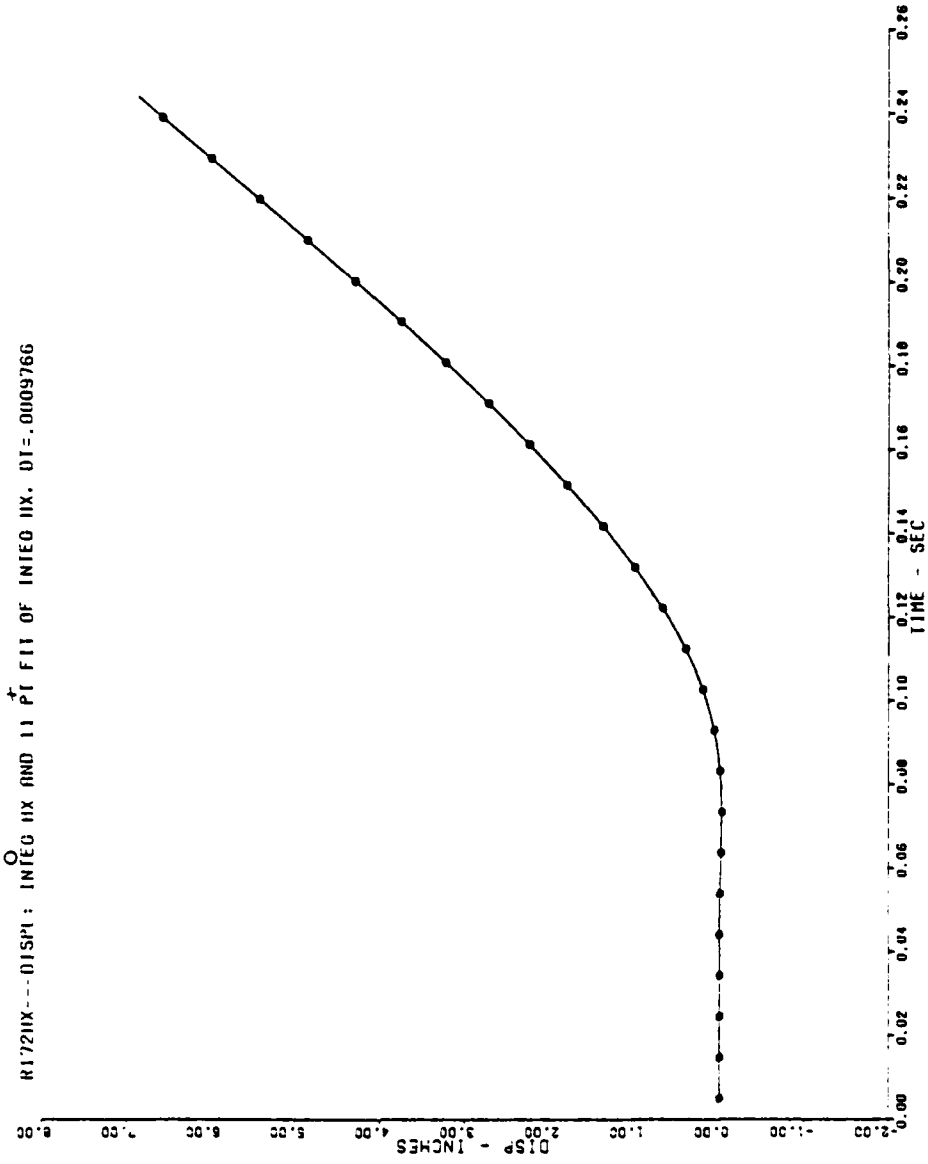
R1721IX---DISPL: INTEG IIX AND II PT FIT OF INTEG IIX. DT=.0009766
DISP - INCHES
TIME - SEC
-2.00
-1.00
0.00
1.00
2.00
3.00
4.00
5.00
6.00
0.00
0.02
0.04
0.06
0.08
0.10
0.12
0.14
0.16
0.18
0.20
0.22
0.24
0.26

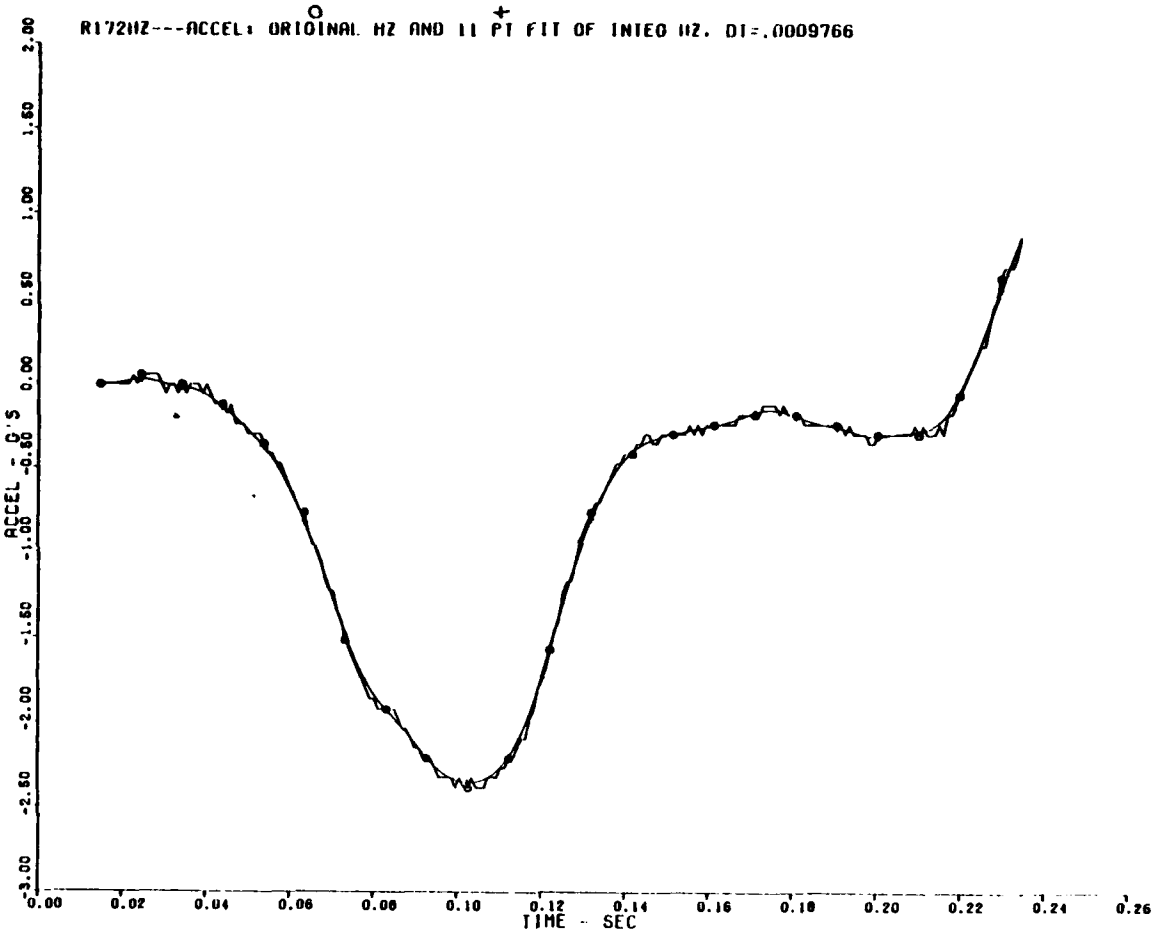
R172HZ---ACCEL: ORIGINAL HZ AND 11 PT FIT OF INTEG HZ. DT=.0009766
ACCEL - G'S
2.00
1.50
1.00
0.50
0.00
-0.50
-1.00
-1.50
-2.00
-2.50
-3.00
0.00
0.02
0.04
0.06
0.08
0.10
0.12
0.14
0.16
0.18
0.20
0.22
0.24
0.26
TIME - SEC

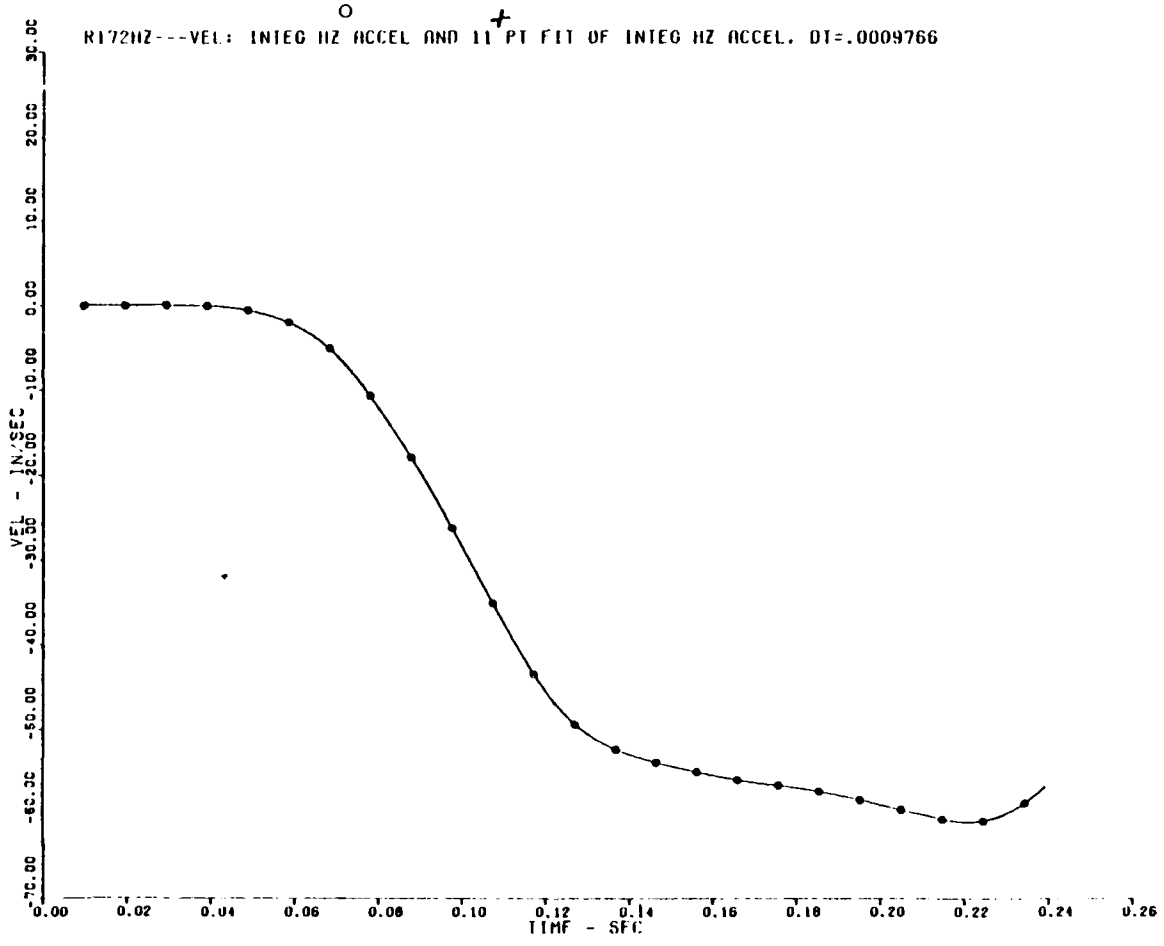
R172NZ---VEL: INTEG HZ ACCEL AND 11 PT FIT OF INTEG HZ ACCEL. DT=.0009766
VEL - IN/SEC
30.00
20.00
10.00
0.00
-10.00
-20.00
-30.00
-40.00
-50.00
-60.00
-70.00
0.00
0.02
0.04
0.06
0.08
0.10
0.12
0.14
0.16
0.18
0.20
0.22
0.24
0.26
TIME - SEC

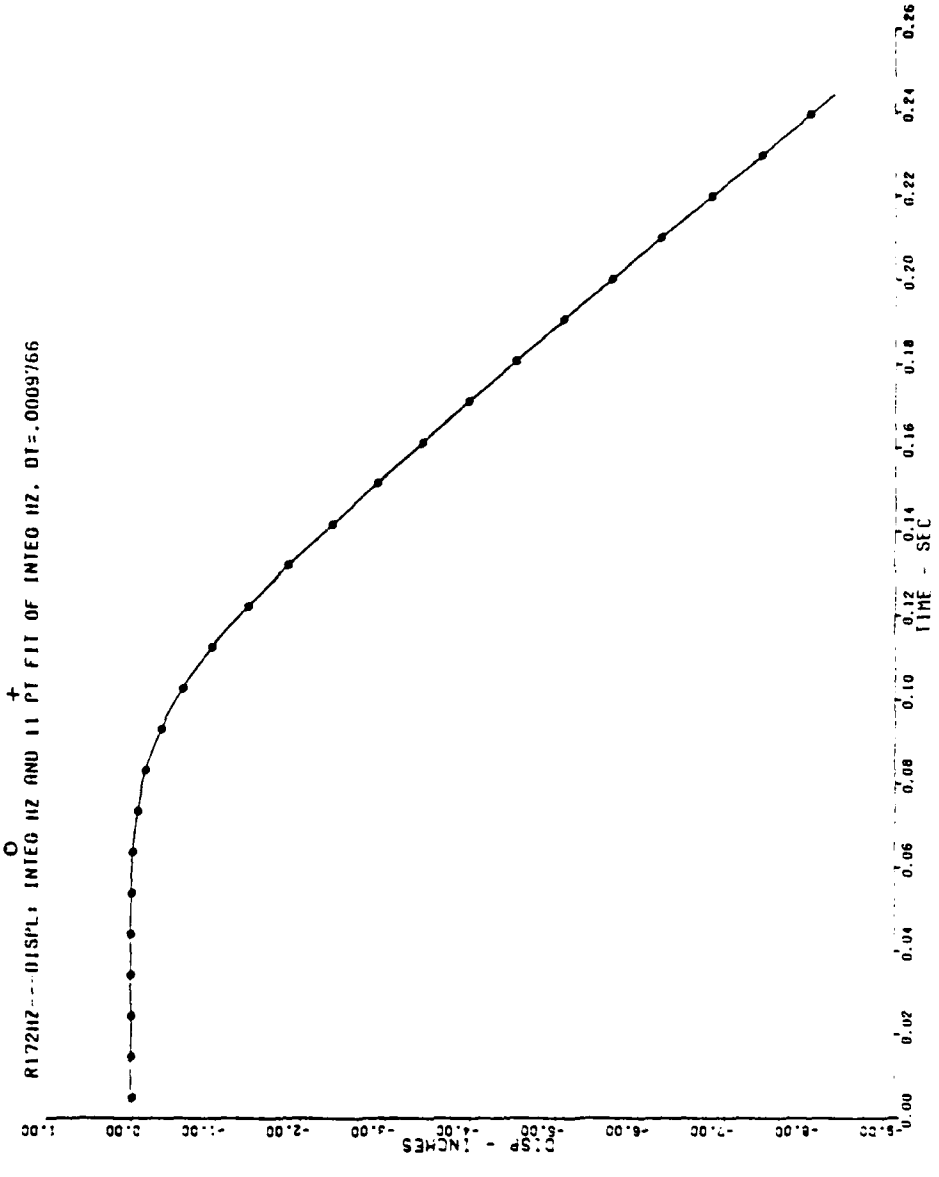
O
R172HZ---DISPL, INTEG HZ AND 11 PT FIT OF INTEG HZ, DT=.0009766
+
DISP - INCHES
TIME - SEC
0.00
0.02
0.04
0.06
0.08
0.10
0.12
0.14
0.16
0.18
0.20
0.22
0.24
0.26
-8.00
-7.00
-6.00
-5.00
-4.00
-3.00
-2.00
-1.00
0.00
1.00

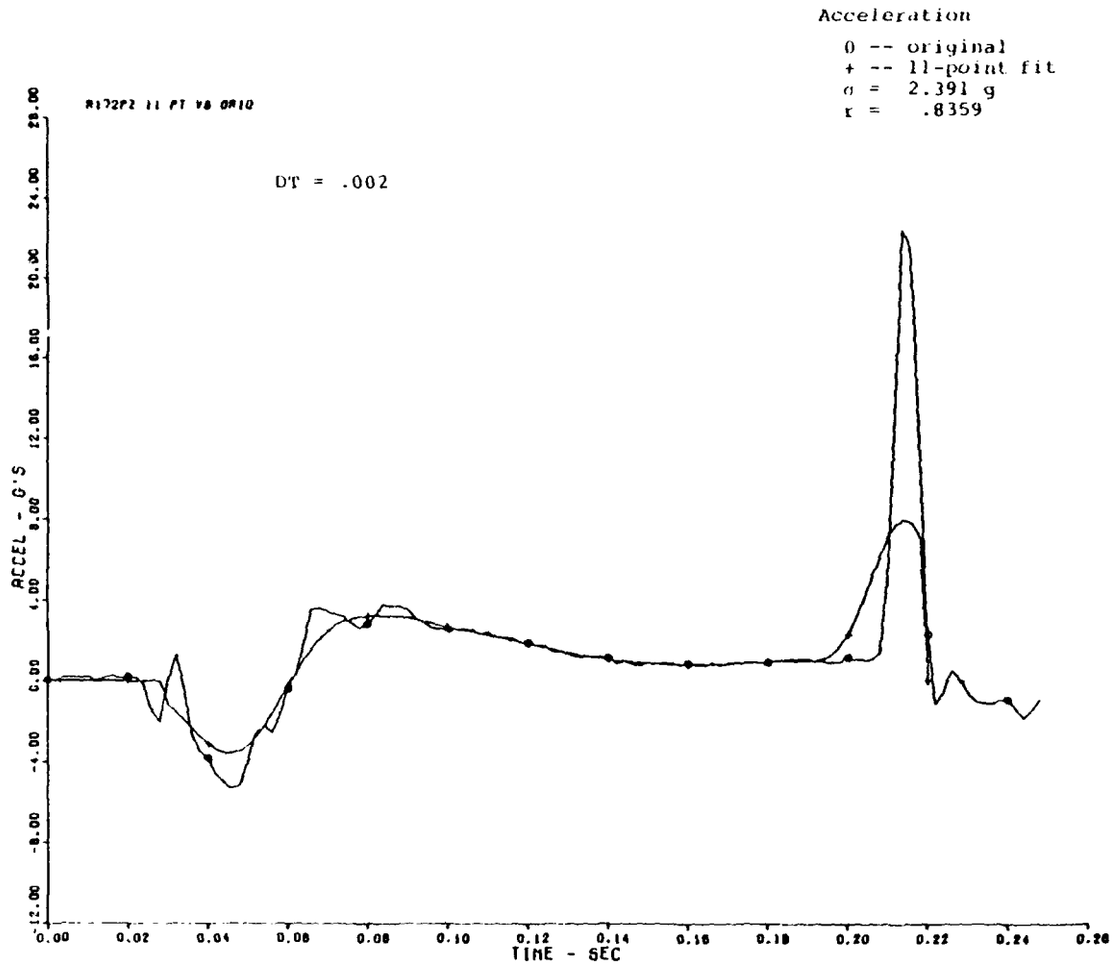
Acceleration
0 -- original
+ -- 11-point fit
σ = 2.391 g
r = .8359
R172P2 11 PT V8 OR10
DT = .002
ACCEL - G'S
TIME - SEC
28.00
24.00
20.00
16.00
12.00
8.00
4.00
0.00
-4.00
-8.00
-12.00
0.00
0.02
0.04
0.06
0.08
0.10
0.12
0.14
0.16
0.18
0.20
0.22
0.24
0.26

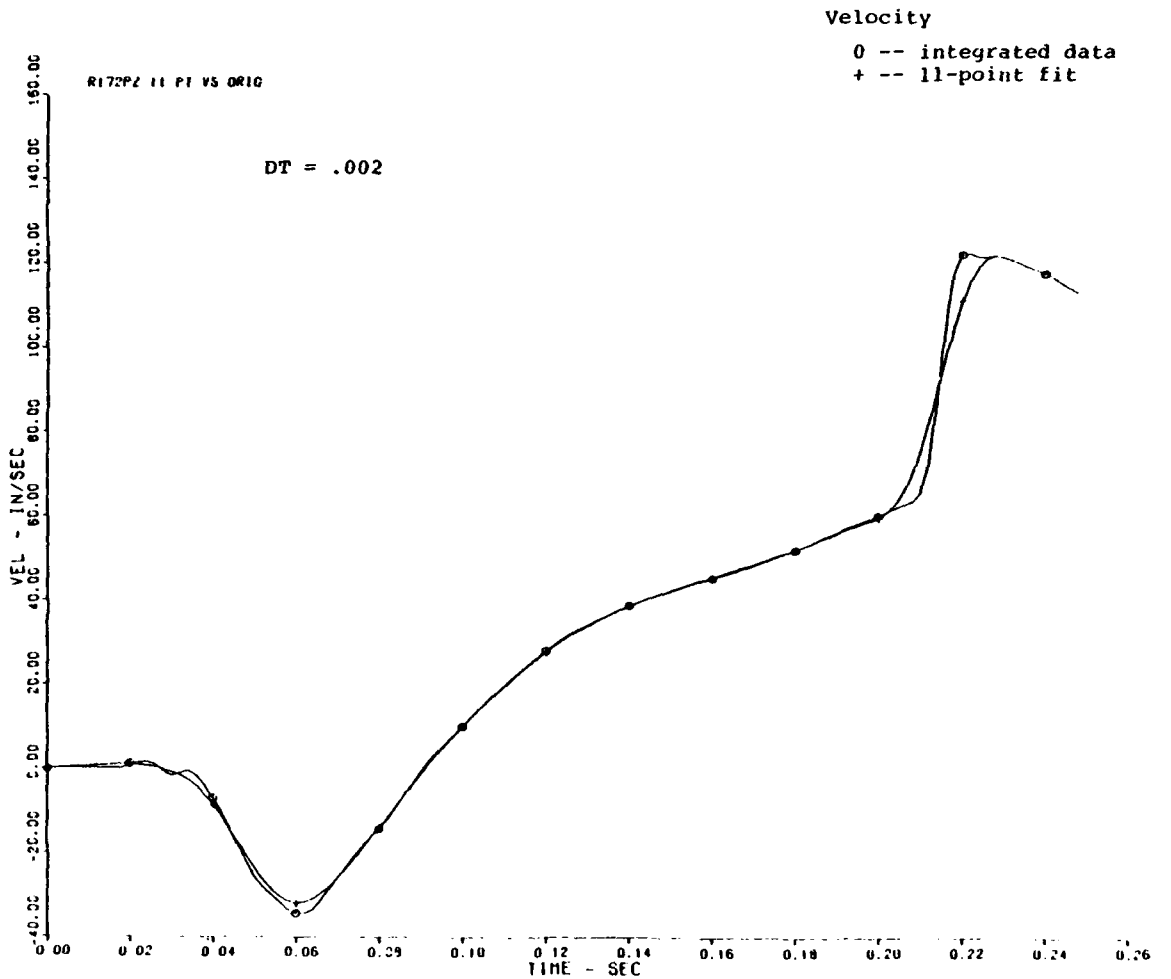
Velocity
0 -- integrated data
+ -- 11-point fit
R172P2 11 PT VS ORIG
DT = .002
VEL - IN/SEC
TIME - SEC
0.00
0.02
0.04
0.06
0.08
0.10
0.12
0.14
0.16
0.18
0.20
0.22
0.24
0.26

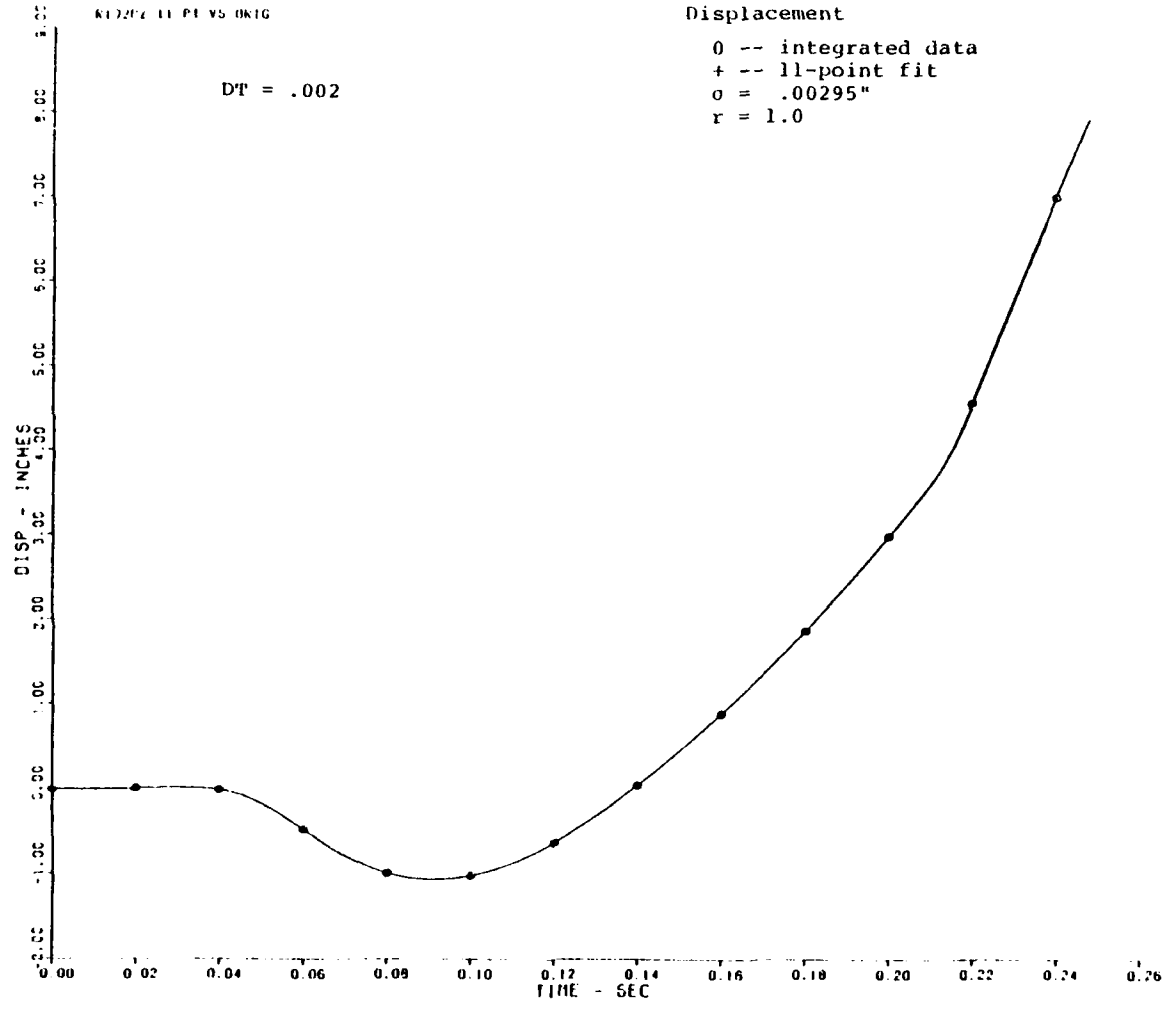
DT = .002
Displacement
0 -- integrated data
+ -- 11-point fit
σ = .00295"
r = 1.0
DISP - INCHES
TIME - SEC
0.00
0.02
0.04
0.06
0.08
0.10
0.12
0.14
0.16
0.18
0.20
0.22
0.24
0.26

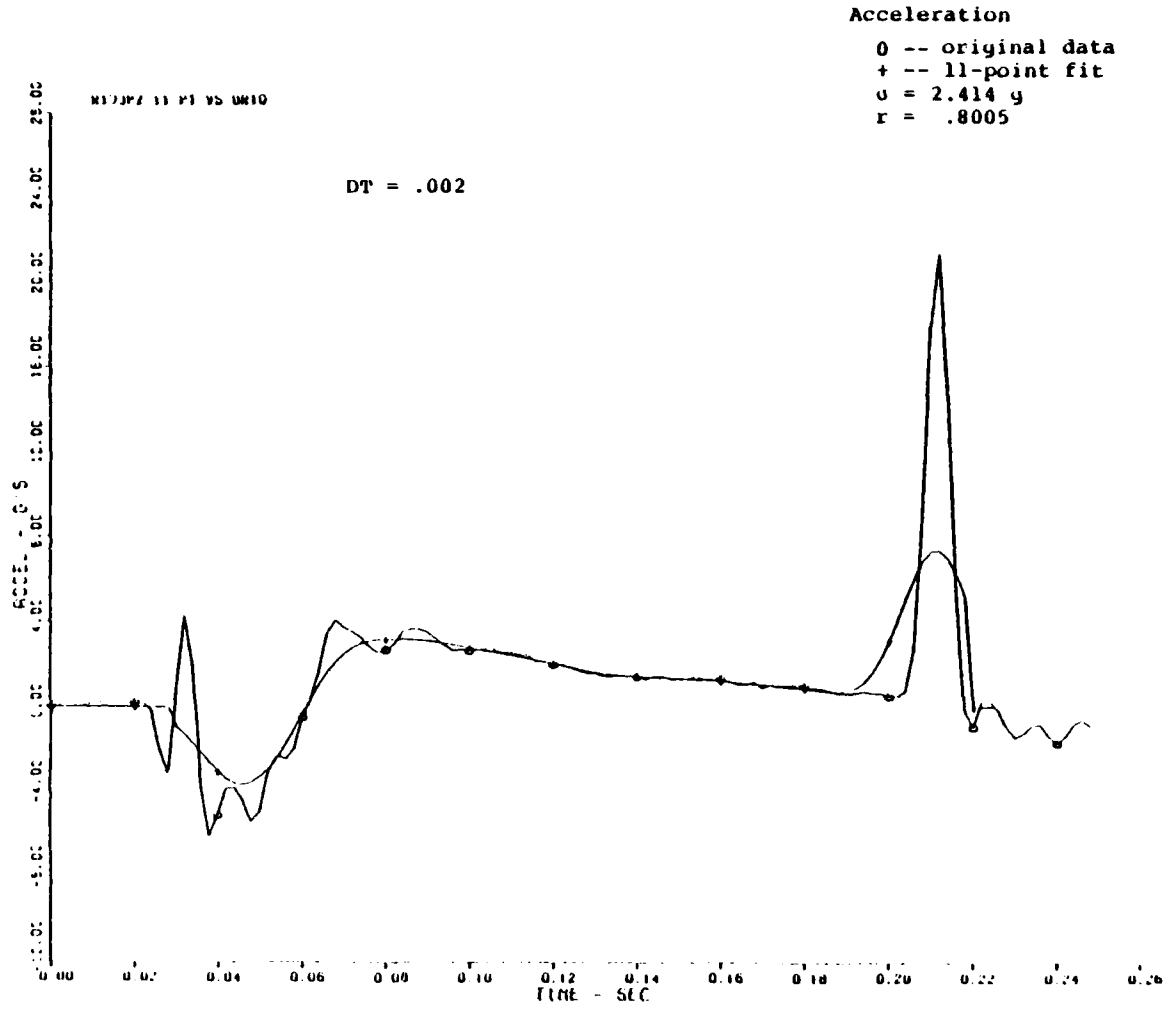
Acceleration
0 -- original data
+ -- 11-point fit
σ = 2.414 g
r = .8005
DT = .002
TIME - SEC

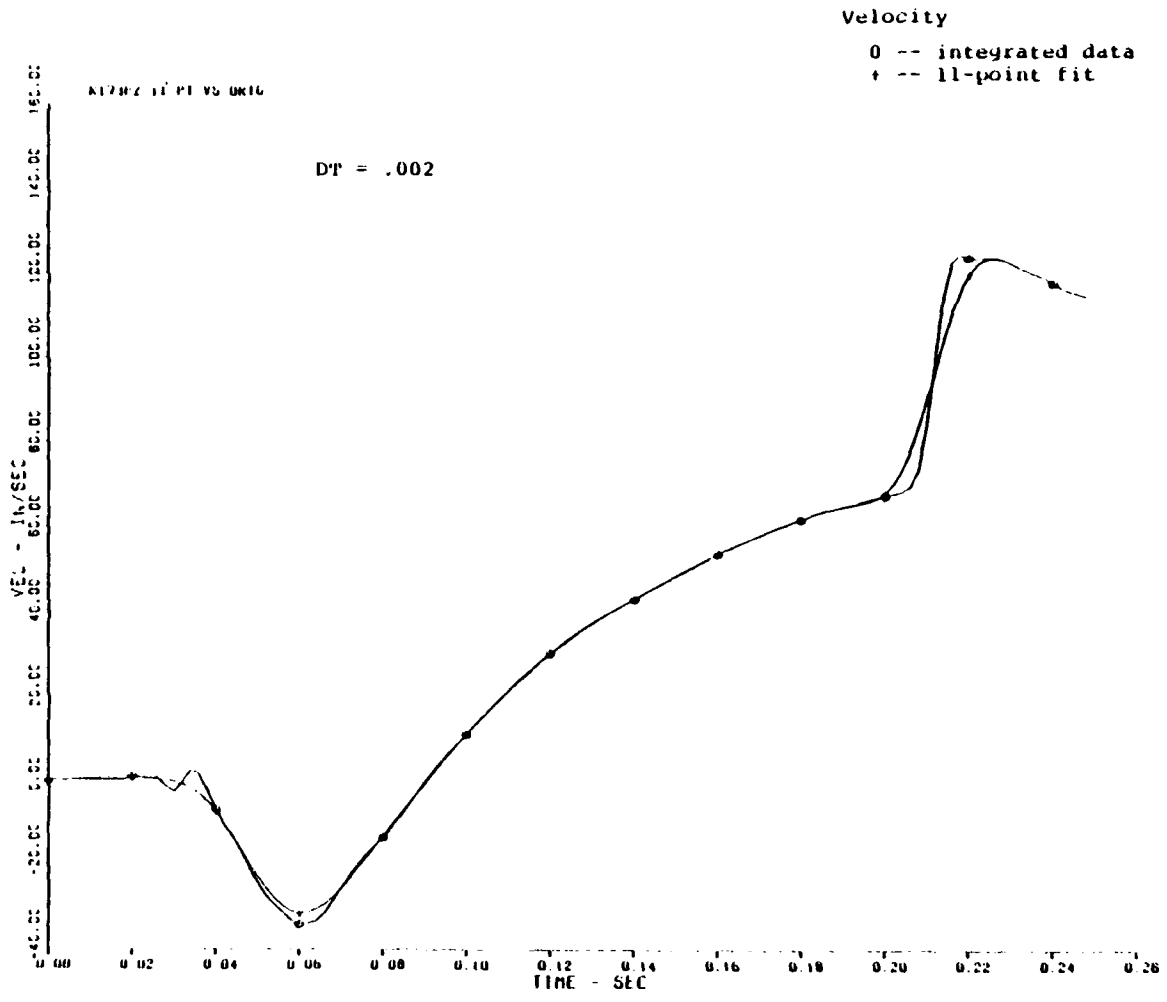
Velocity
0 -- integrated data
+ -- 11-point fit
DT = .002
VEL - IN/SEC
TIME - SEC

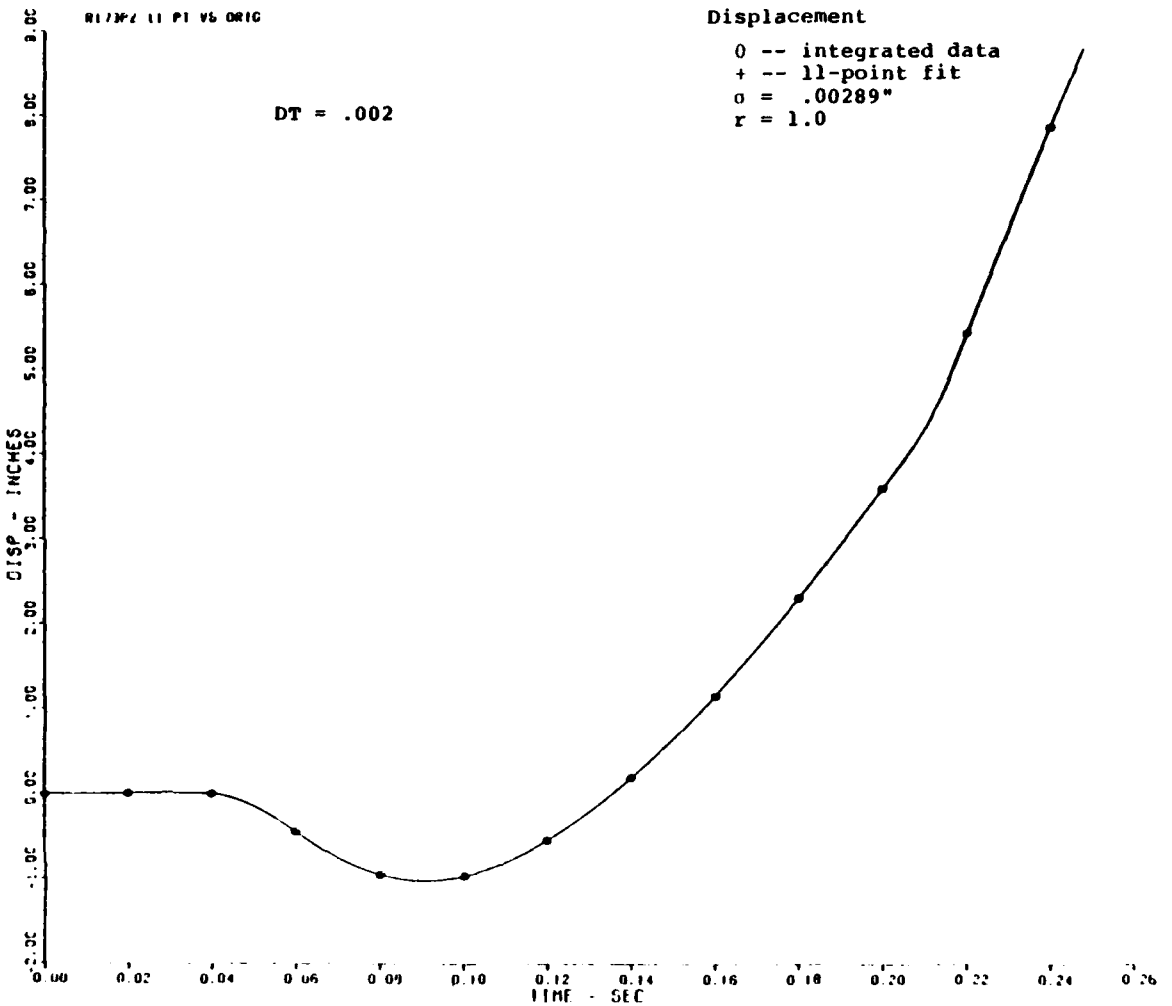
Displacement
0 -- integrated data
+ -- 11-point fit
σ = .00289"
r = 1.0
DT = .002
DISP - INCHES
TIME - SEC
0.00
0.02
0.04
0.06
0.08
0.10
0.12
0.14
0.16
0.18
0.20
0.22
0.24
0.26

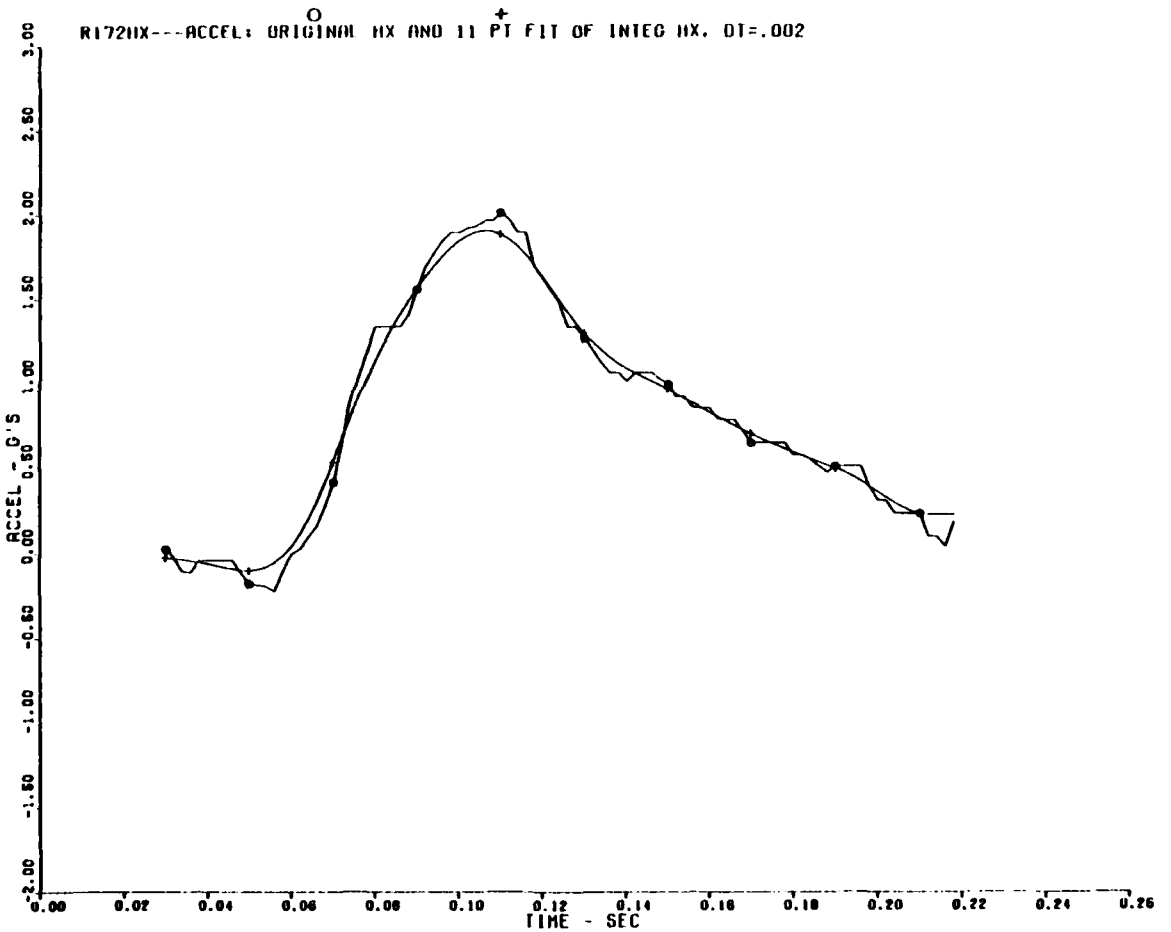
O
+
R172HX---ACCEL: ORIGINAL HX AND 11 PT FIT OF INTEG HX, DT=.002
ACCEL - G'S
3.00
2.50
2.00
1.50
1.00
0.50
0.00
-0.50
-1.00
-1.50
-2.00
0.00
0.02
0.04
0.06
0.08
0.10
0.12
0.14
0.16
0.18
0.20
0.22
0.24
0.26
TIME - SEC

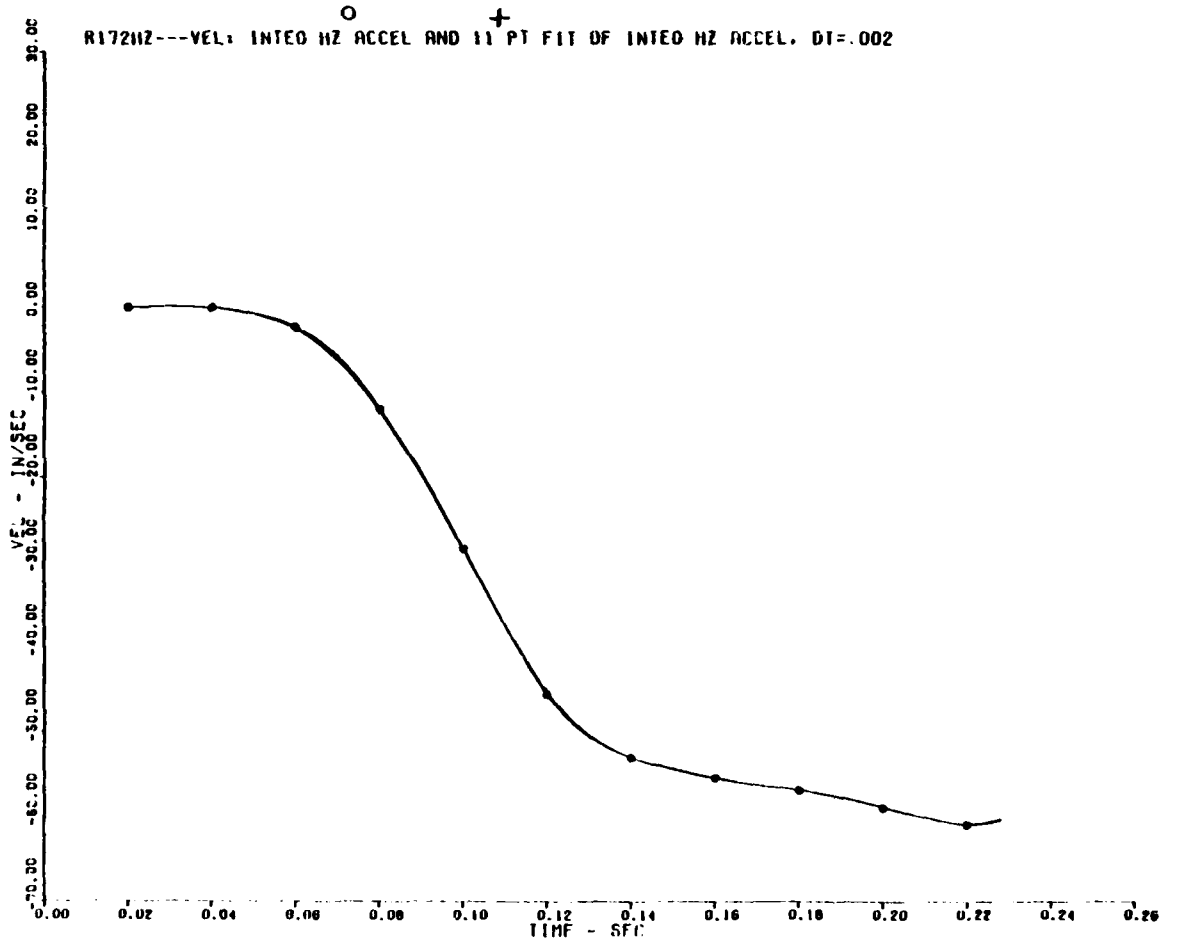
R172HZ---VEL: INTEG HZ ACCEL AND 11 PT FIT OF INTEG HZ ACCEL. DT=.002
VEL - IN/SEC
TIME - SEC
0.00
0.02
0.04
0.06
0.08
0.10
0.12
0.14
0.16
0.18
0.20
0.22
0.24
0.26

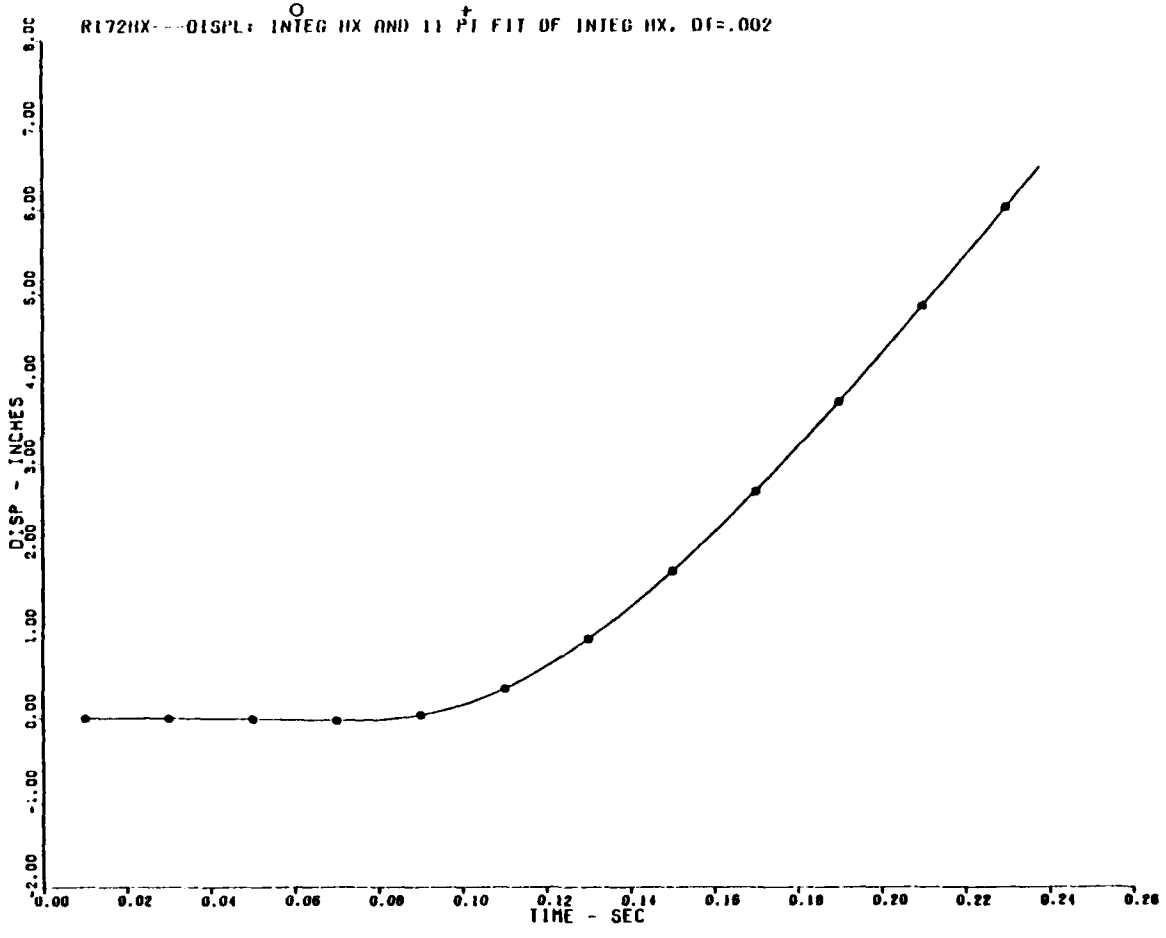
R172HX---DISPL: INTEG HX AND 11 PT FIT OF INTEG HX, DT=.002
DISP - INCHES
TIME - SEC
8.00
7.00
6.00
5.00
4.00
3.00
2.00
1.00
0.00
-1.00
-2.00
0.00
0.02
0.04
0.06
0.08
0.10
0.12
0.14
0.16
0.18
0.20
0.22
0.24
0.26

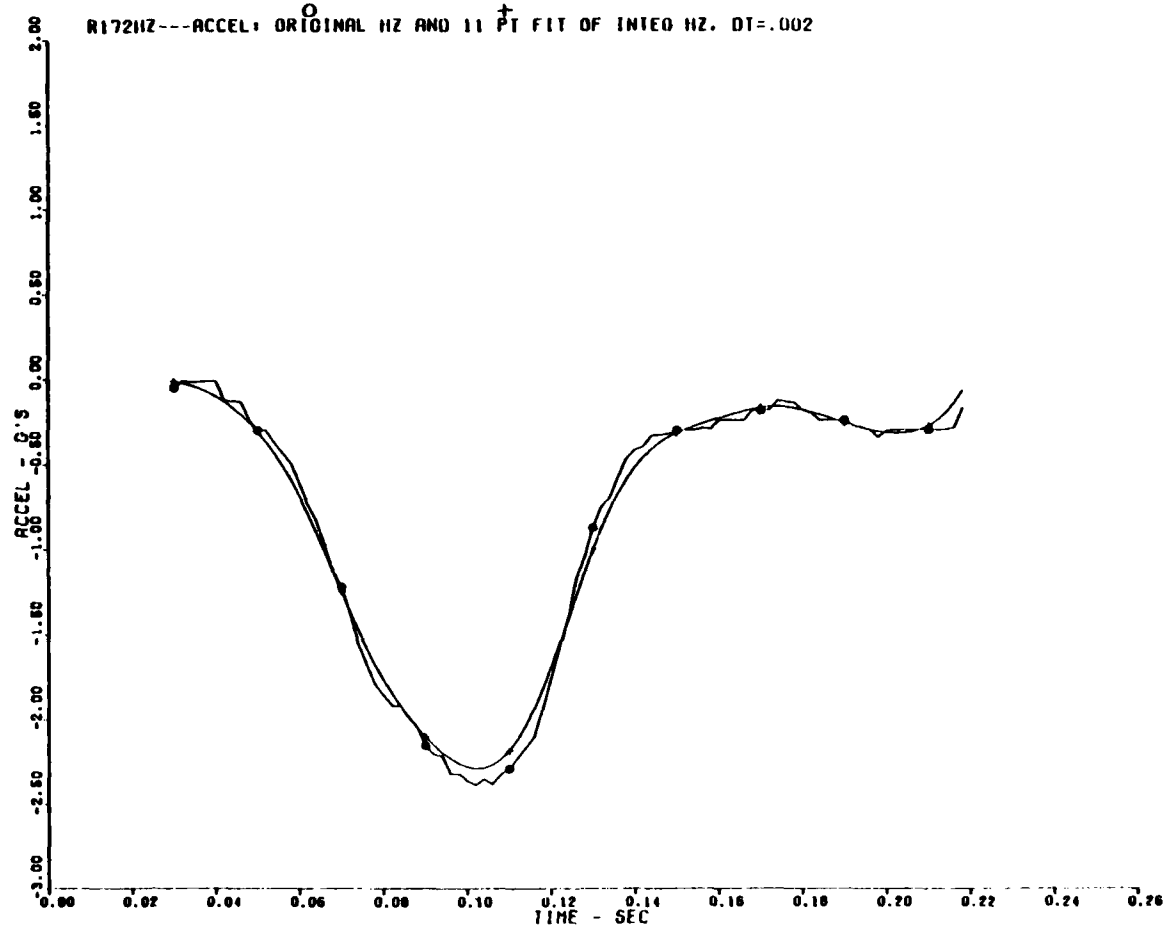
R172HZ---ACCEL: ORIGINAL HZ AND 11 PT FIT OF INTEG HZ. DT=.002
ACCEL - G'S
TIME - SEC
2.00
1.50
1.00
0.50
0.00
-0.50
-1.00
-1.50
-2.00
-2.50
-3.00
0.00
0.02
0.04
0.06
0.08
0.10
0.12
0.14
0.16
0.18
0.20
0.22
0.24
0.26

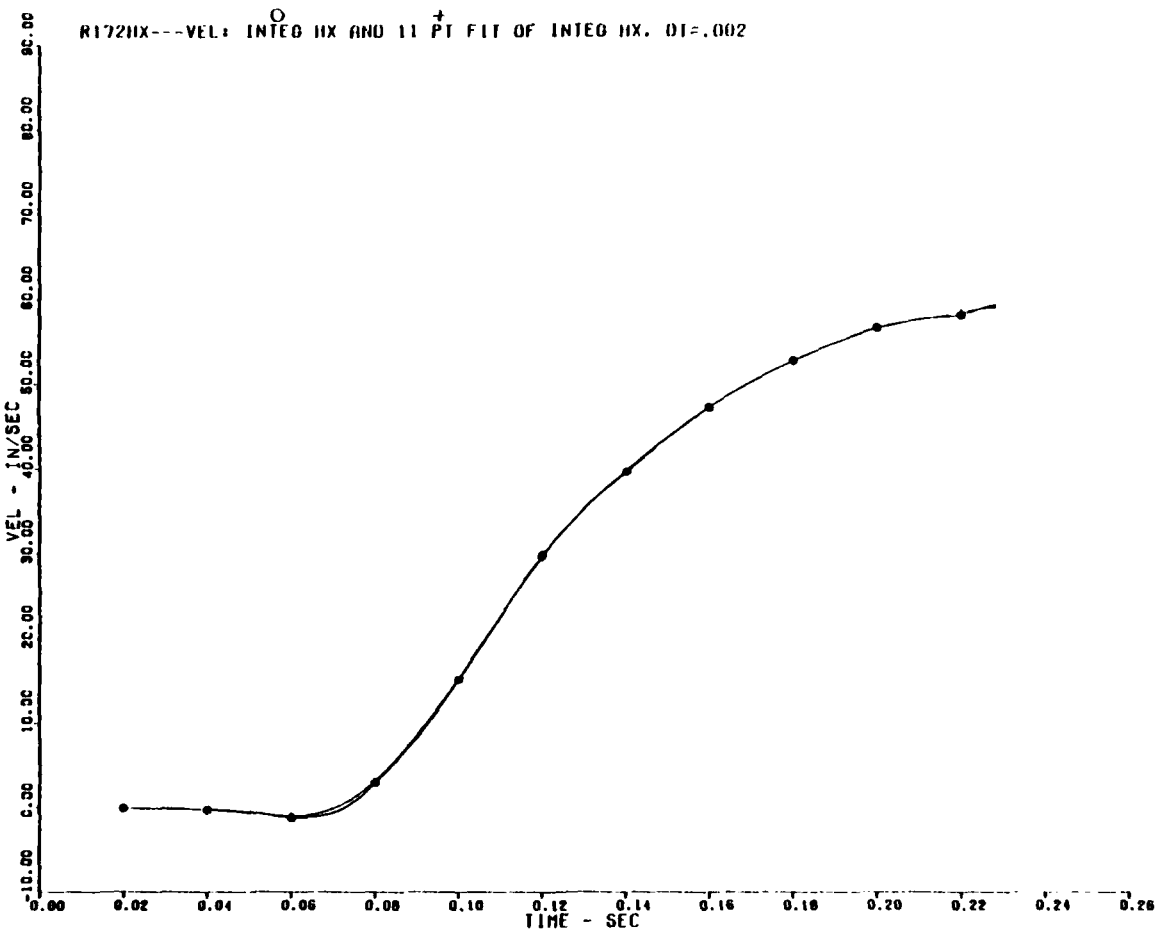
R172HX---VEL: INTEG HX AND 11 PT FIT OF INTEG HX. DT=.002
VEL - IN/SEC
-10.00
0.00
10.00
20.00
30.00
40.00
50.00
60.00
70.00
80.00
90.00
0.00
0.02
0.04
0.06
0.08
0.10
0.12
0.14
0.16
0.18
0.20
0.22
0.24
0.26
TIME - SEC

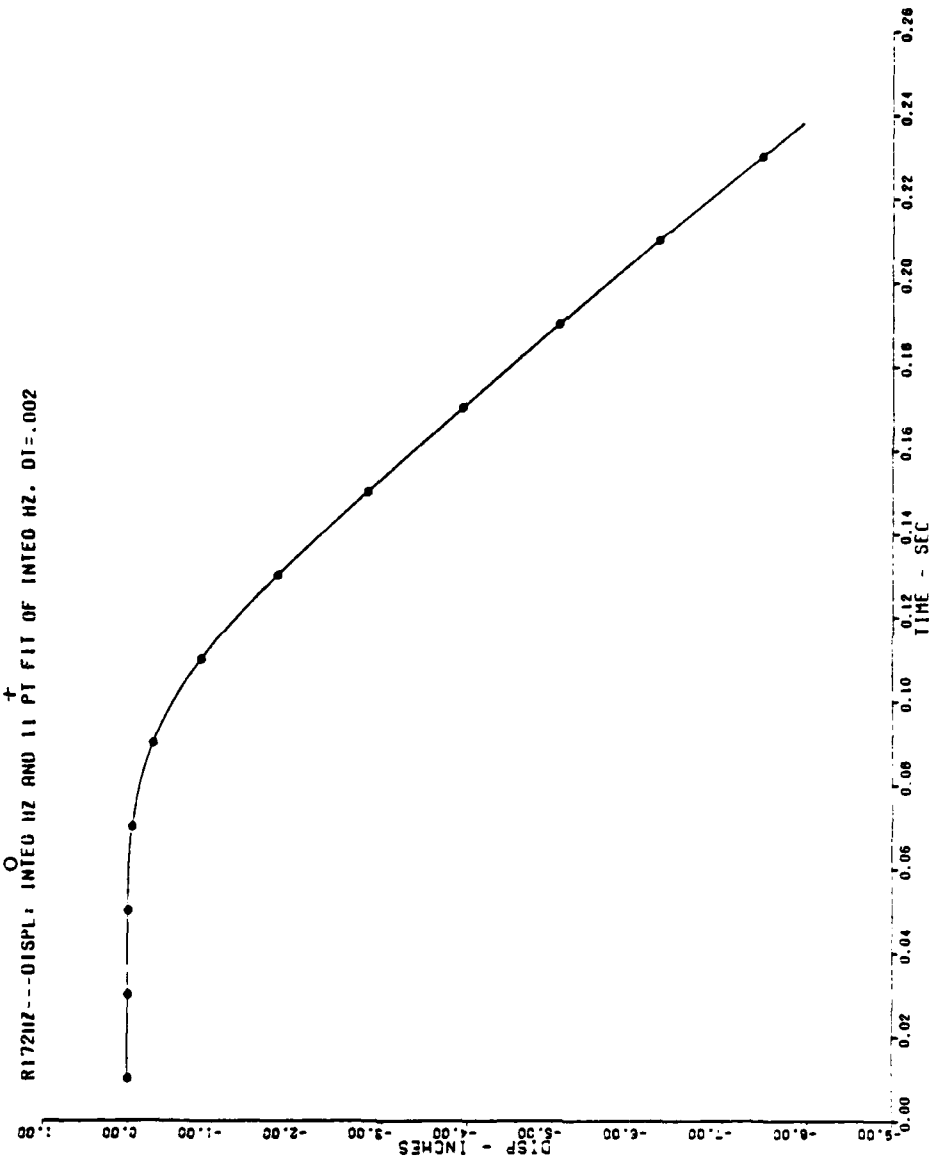
R1721HZ---DISPL: INTEG HZ AND 11 PT FIT OF INTEG HZ. DT=.002
O
+
DISP - INCHES
TIME - SEC
1.00
0.00
-1.00
-2.00
-3.00
-4.00
-5.00
-6.00
-7.00
-8.00
0.00
0.02
0.04
0.06
0.08
0.10
0.12
0.14
0.16
0.18
0.20
0.22
0.24
0.26

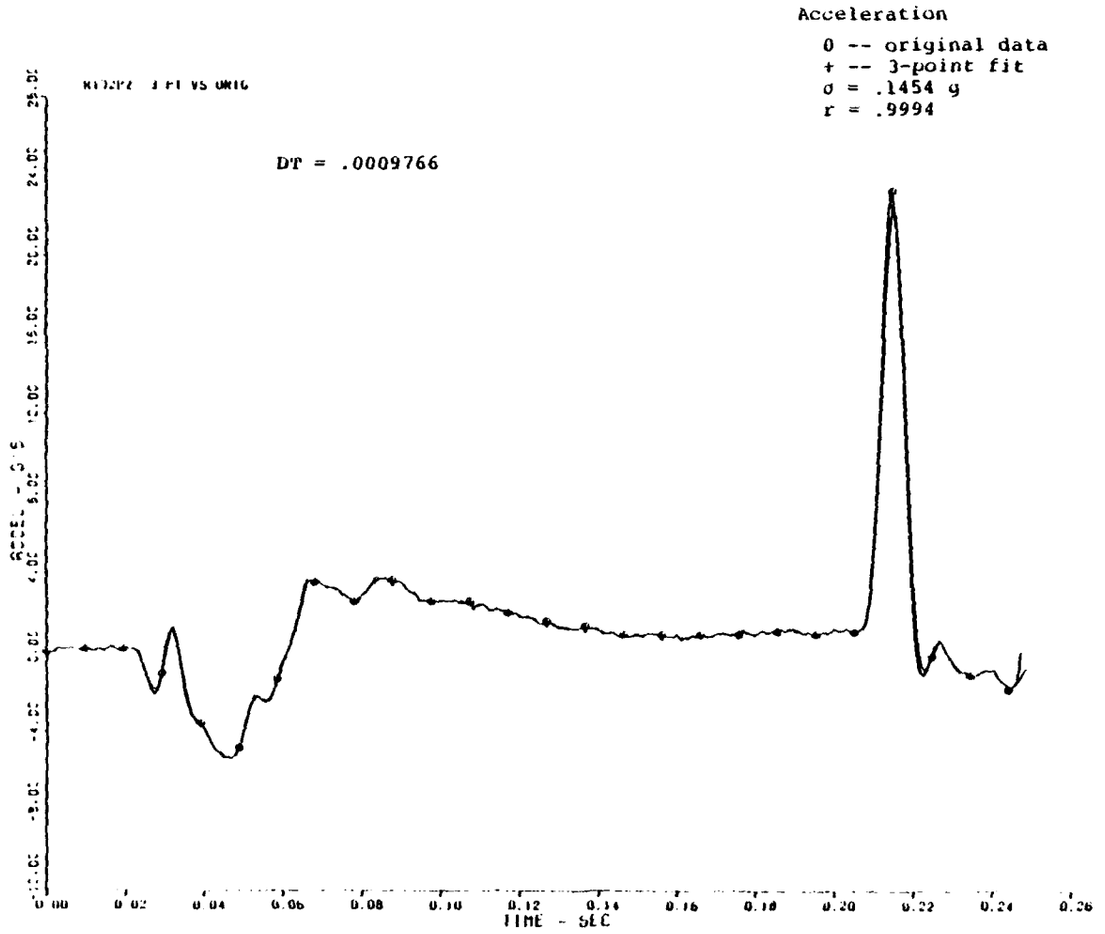
Acceleration
0 -- original data
+ -- 3-point fit
σ = .1454 g
r = .9994
DT = .0009766
TIME - SEC

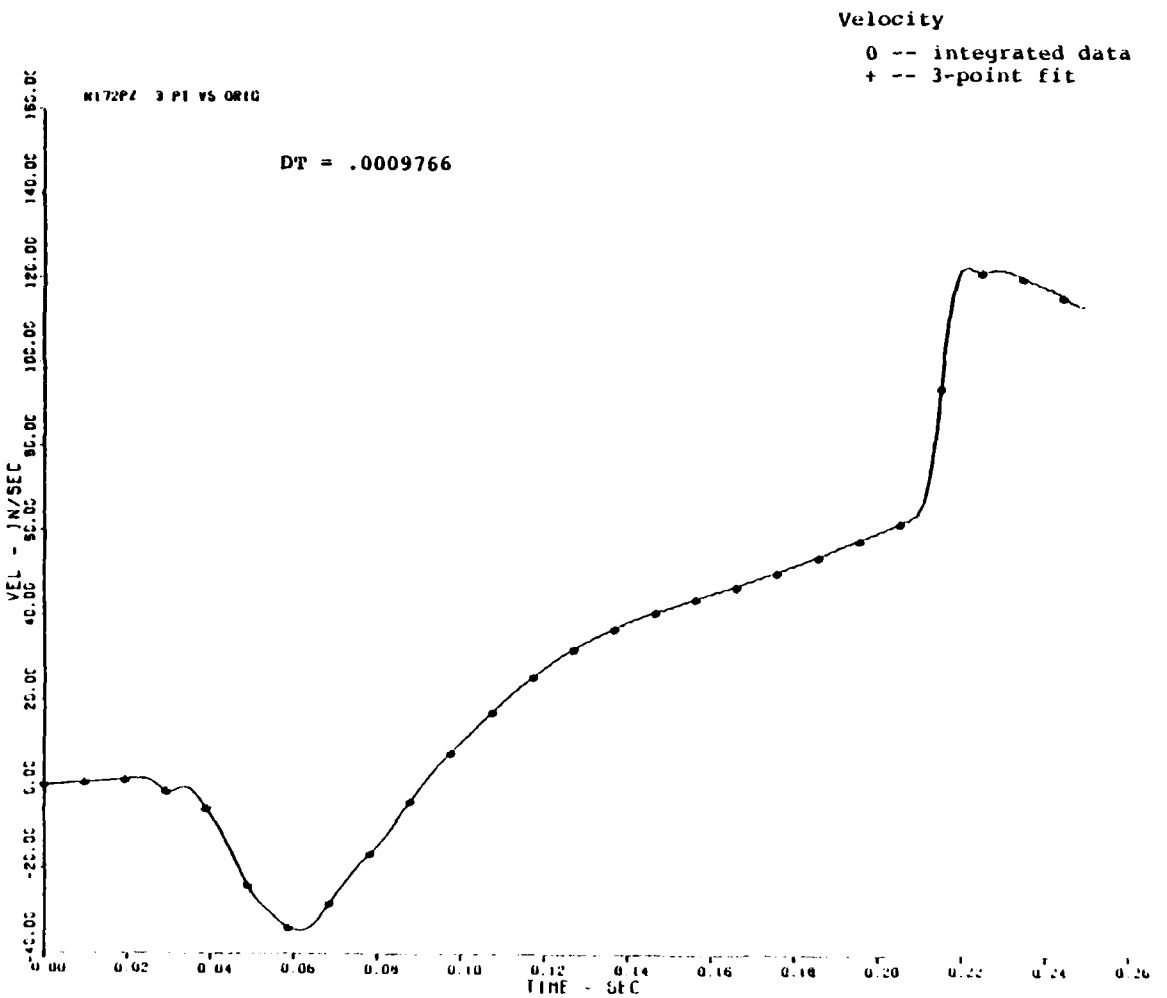
Velocity
0 -- integrated data
+ -- 3-point fit
DT = .0009766
VEL - IN/SEC
TIME - SEC

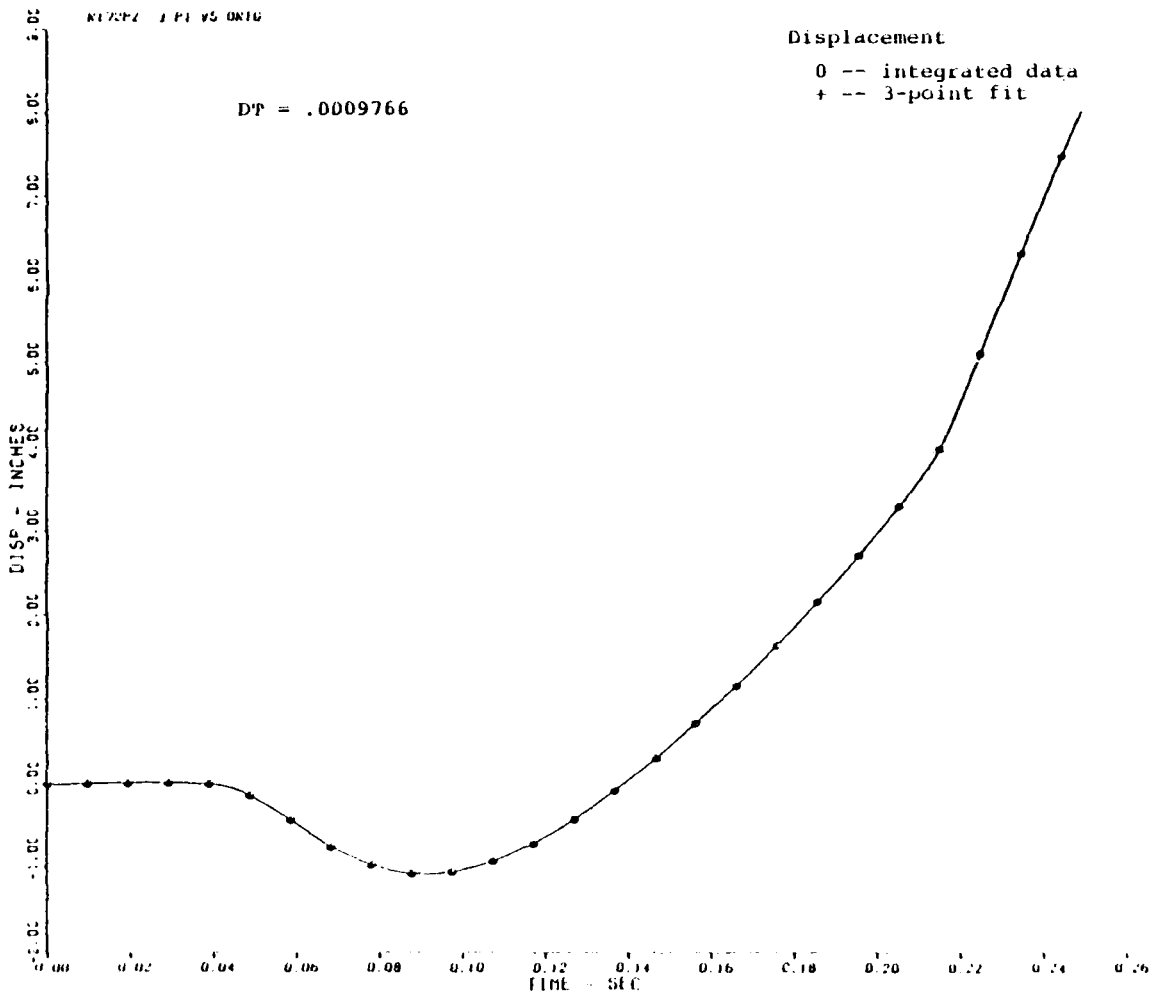
Displacement
0 -- integrated data
+ -- 3-point fit
DT = .0009766
DISP - INCHES
TIME - SEC

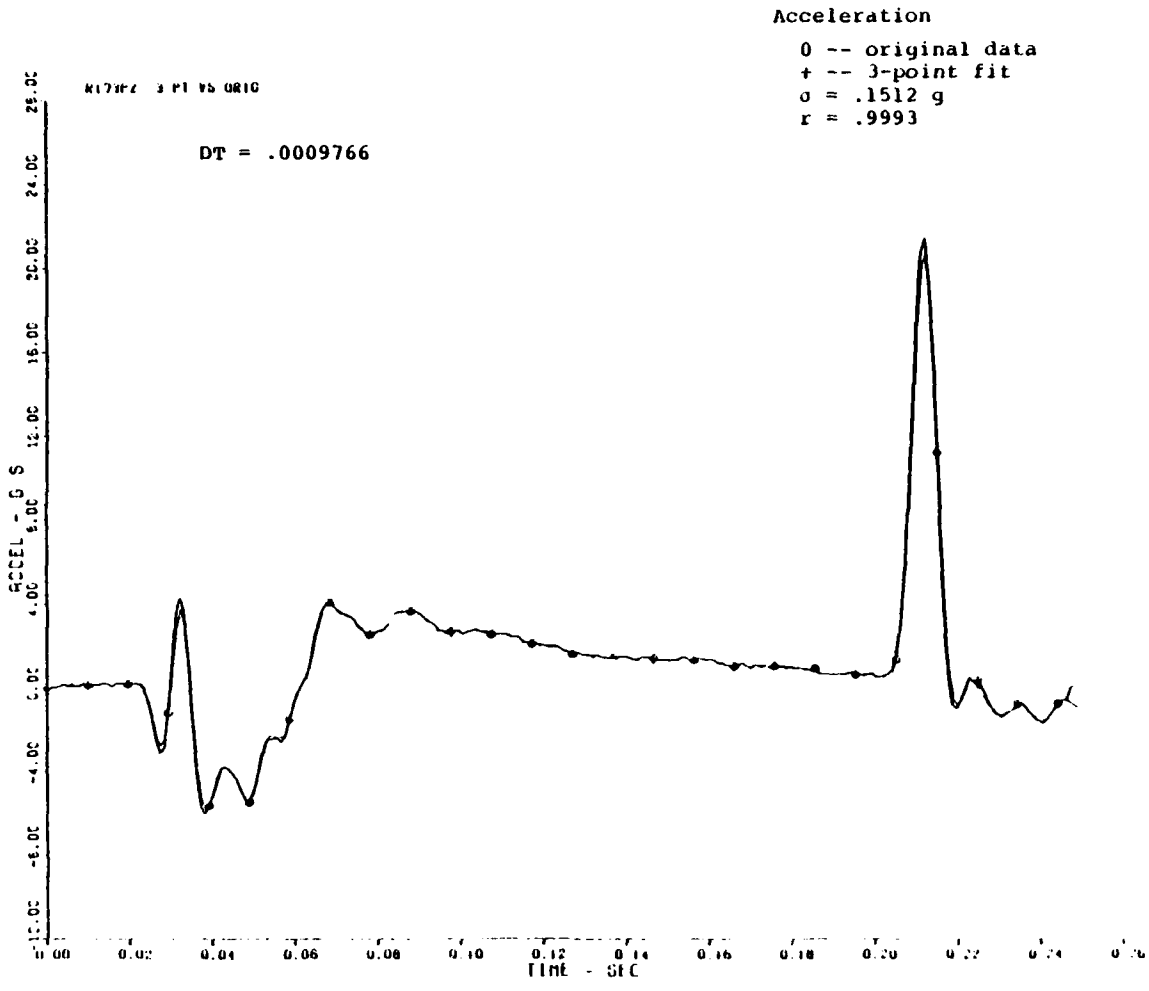
Acceleration
0 -- original data
+ -- 3-point fit
σ = .1512 g
r = .9993
DT = .0009766
ACCEL - G S
TIME - SEC

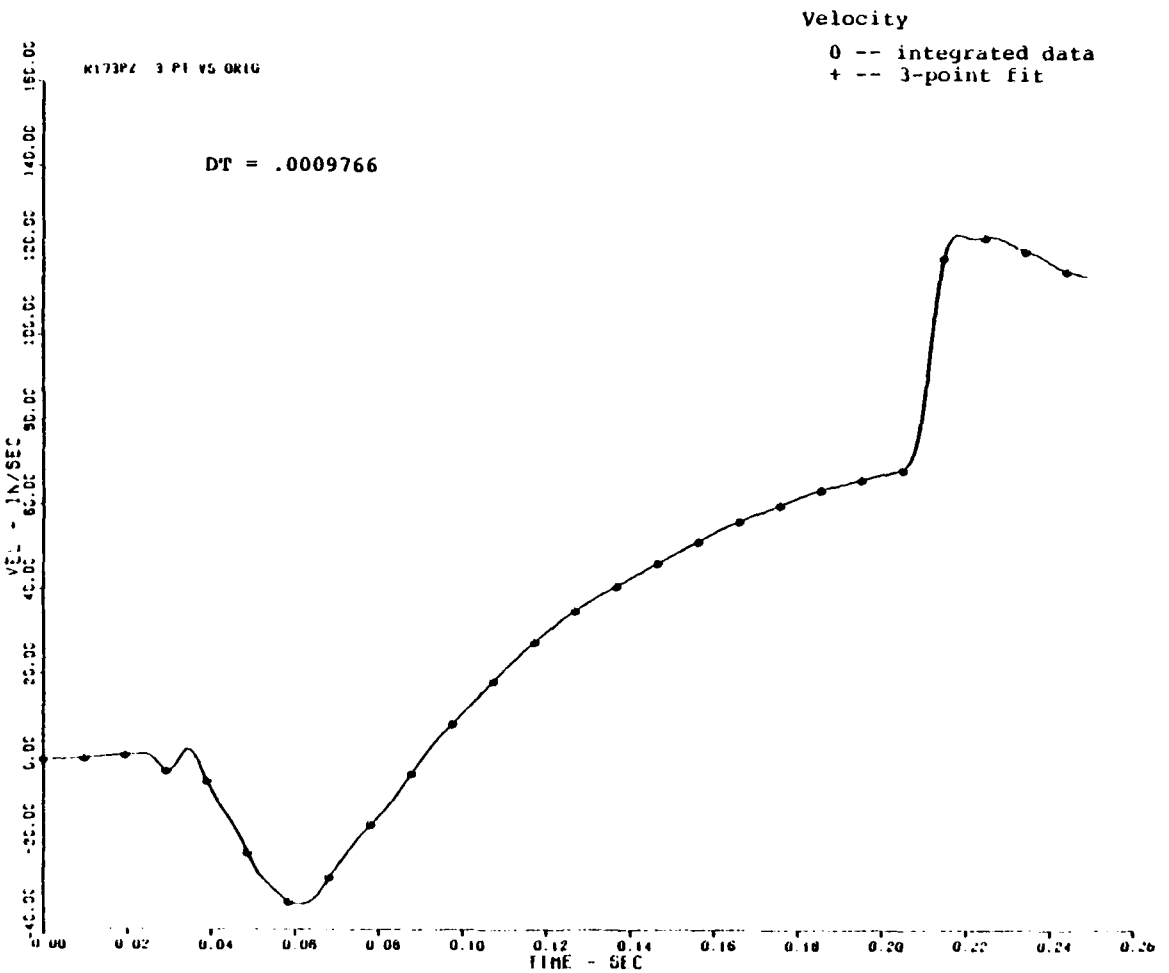
Velocity
0 -- integrated data
+ -- 3-point fit
K173PZ 3 PT VS ORIG
DT = .0009766
VEL - IN/SEC
TIME - SEC

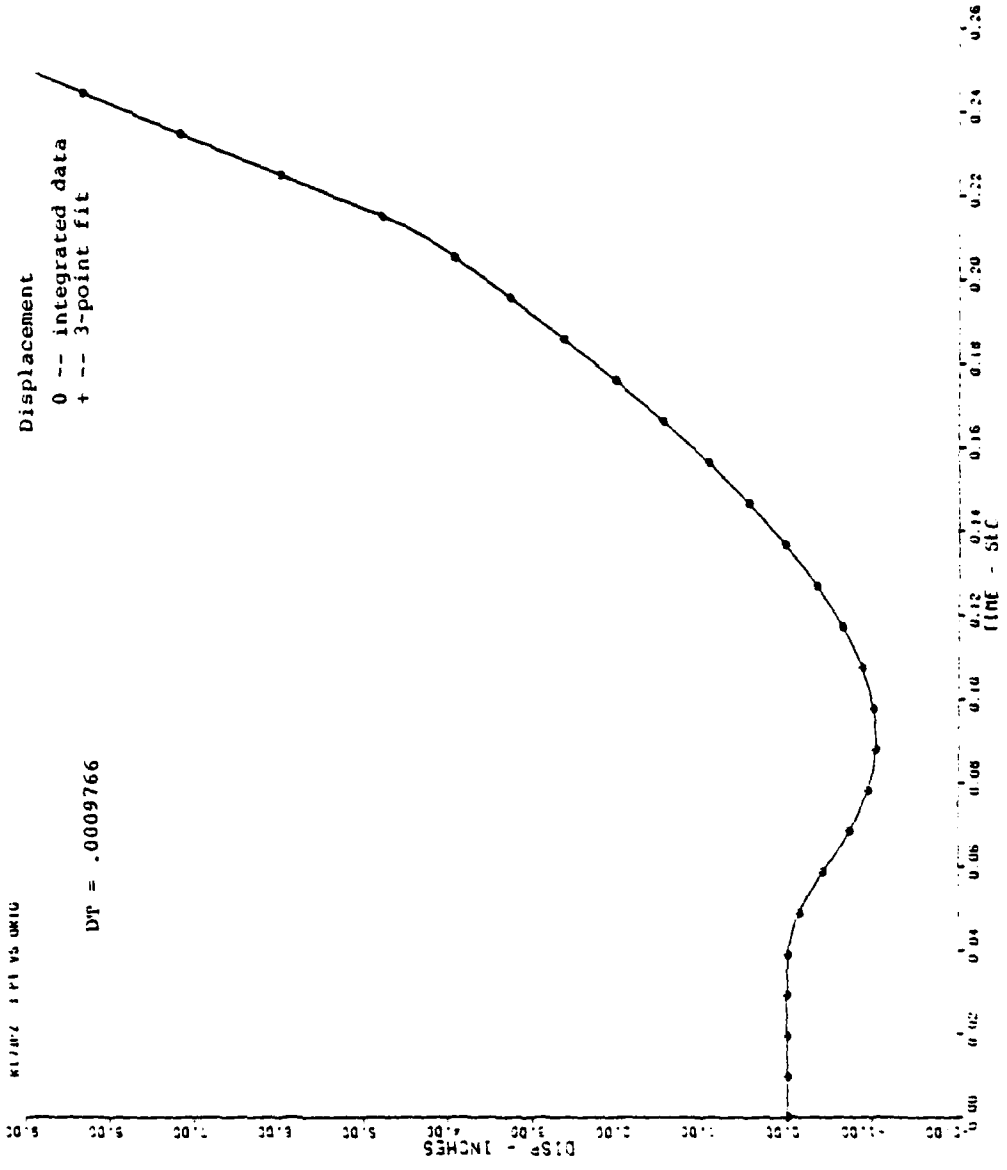

*U.S.Government Printing Office: 1980 — 657-084/632